Heavy element nucleosynthesis in neutron star mergers and its electromagnetic signatures

Gabriel Martínez-Pinedo

GWsNS-2023: Gravitational Waves from Neutron Stars
Centre Paul Langevin, Aussois, France
June 5-9, 2023

ERC AdG KILONOVA

R-process review

REVIEWS OF MODERN PHYSICS, VOLUME 93, JANUARY–MARCH 2021

Origin of the heaviest elements: The rapid neutron-capture process

John J. Cowan*

HLD Department of Physics and Astronomy, University of Oklahoma, 440 West Brooks Street, Norman, Oklahoma 73019, USA

Christopher Sneden†

Department of Astronomy, University of Texas, 2515 Speedway, Austin, Texas 78712-1205, USA

James E. Lawler‡

Physics Department, University of Wisconsin–Madison, 1150 University Avenue, Madison, Wisconsin 53706-1390, USA

Ani Aprahamian§ and Michael Wiescher¶

Department of Physics and Joint Institute for Nuclear Astrophysics, University of Notre Dame, 225 Nieuwland Science Hall, Notre Dame, Indiana 46556, USA

Karlheinz Langanke**

GSI Helmholtzzentrum für Schwerionenforschung, Planckstraße 1, 64291 Darmstadt, Germany and Institut für Kernphysik (Theoriezentrum), Fachbereich Physik, Technische Universität Darmstadt, Schlossgartenstraße 2, 64298 Darmstadt, Germany

Gabriel Martínez-Pinedo††

GSI Helmholtzzentrum für Schwerionenforschung, Planckstraße 1, 64291 Darmstadt, Germany; Institut für Kernphysik (Theoriezentrum), Fachbereich Physik, Technische Universität Darmstadt, Schlossgartenstraße 2, 64298 Darmstadt, Germany; and Helmholtz Forschungsakademie Hessen für FAIR, GSI Helmholtzzentrum für Schwerionenforschung, Planckstraße 1, 64291 Darmstadt, Germany

Friedrich-Karl Thielemann‡‡

Department of Physics, University of Basel, Klingelbergstrasse 82, 4056 Basel, Switzerland and GSI Helmholtzzentrum für Schwerionenforschung, Planckstraße 1, 64291 Darmstadt, Germany

Solar system abundances

Solar photosphere and meteorites:
chemical signature of gas cloud where the Sun formed

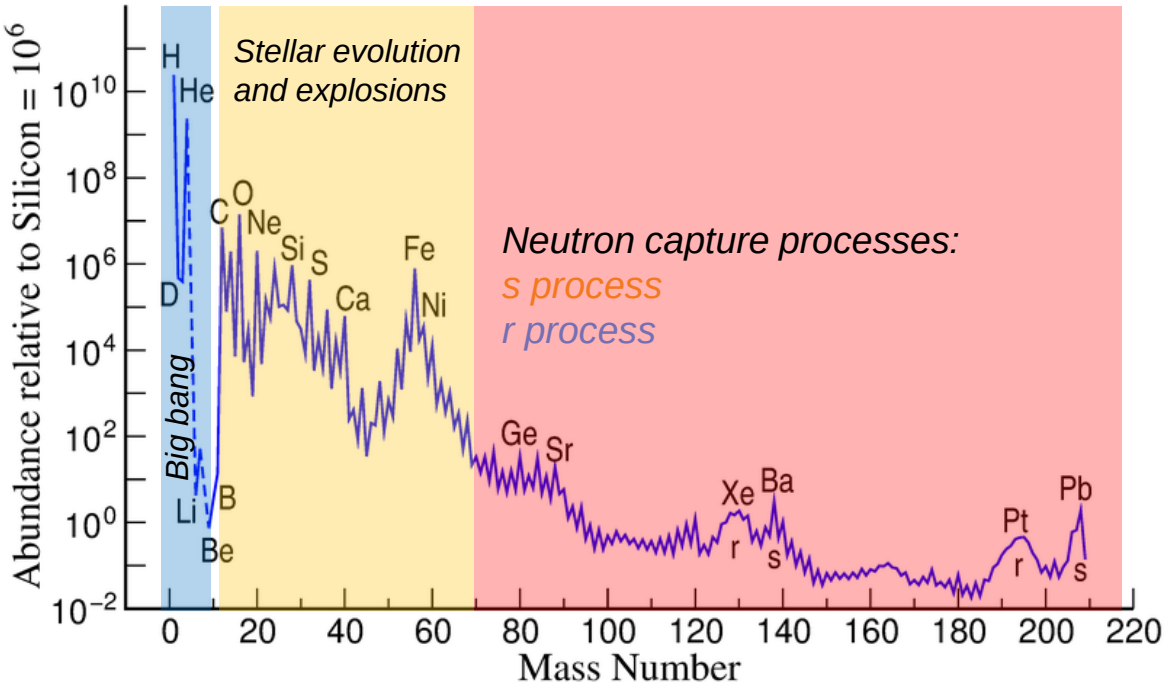

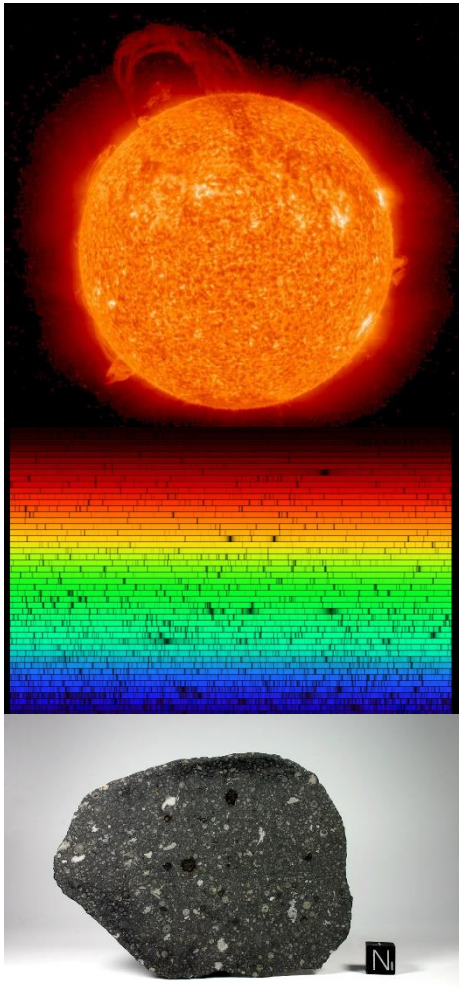

Signatures of nuclear structure and nuclear stability
Contributions of different nucleosynthesis processes

Nucleosynthesis processes

Fusion reactions during stellar evolution produce elements up to Iron

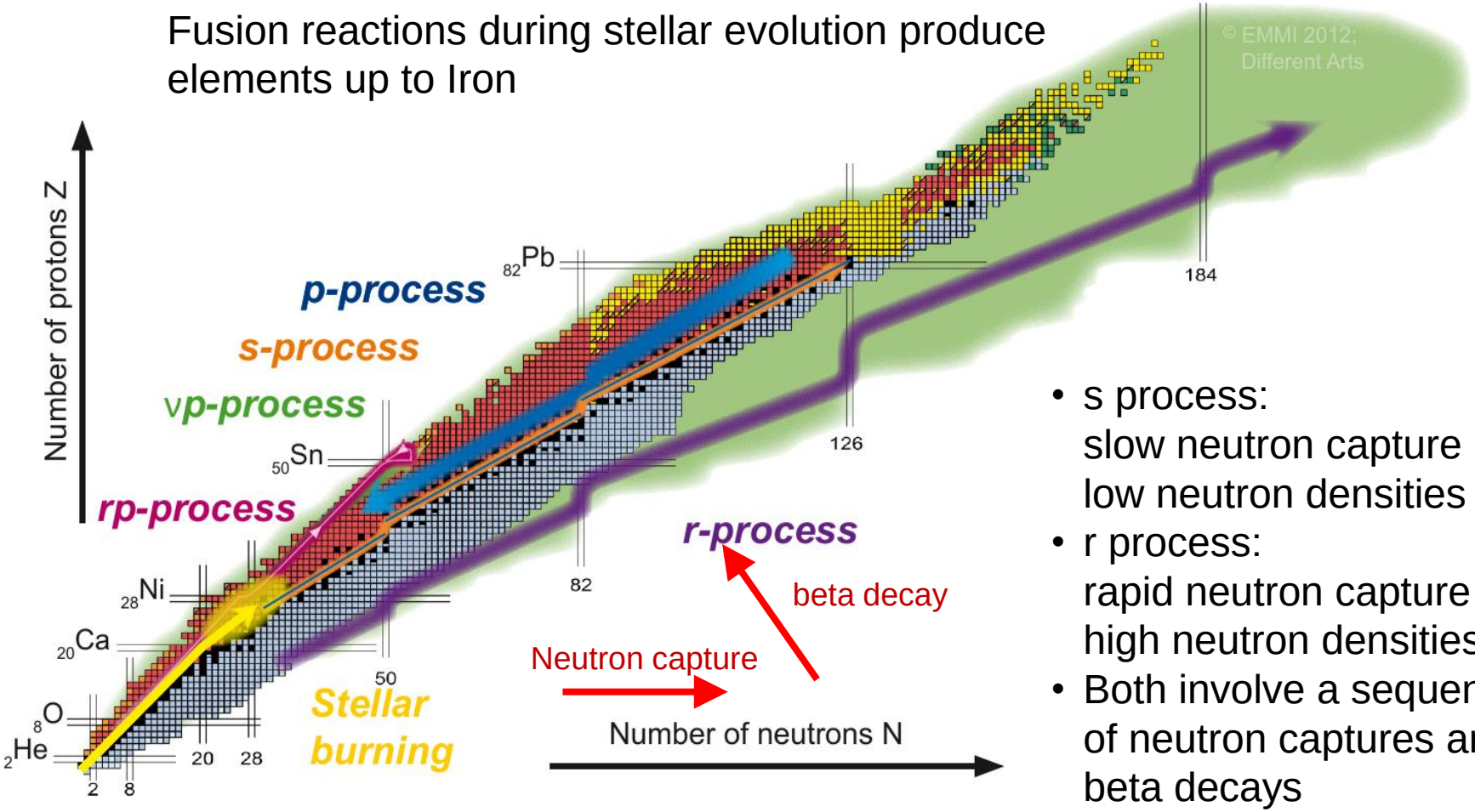

- s process:
  slow neutron capture
  low neutron densities
- r process:
  rapid neutron capture
  high neutron densities
- Both involve a sequence of neutron captures and beta decays

s and r process peaks

Maximum abundances related to neutron magic numbers

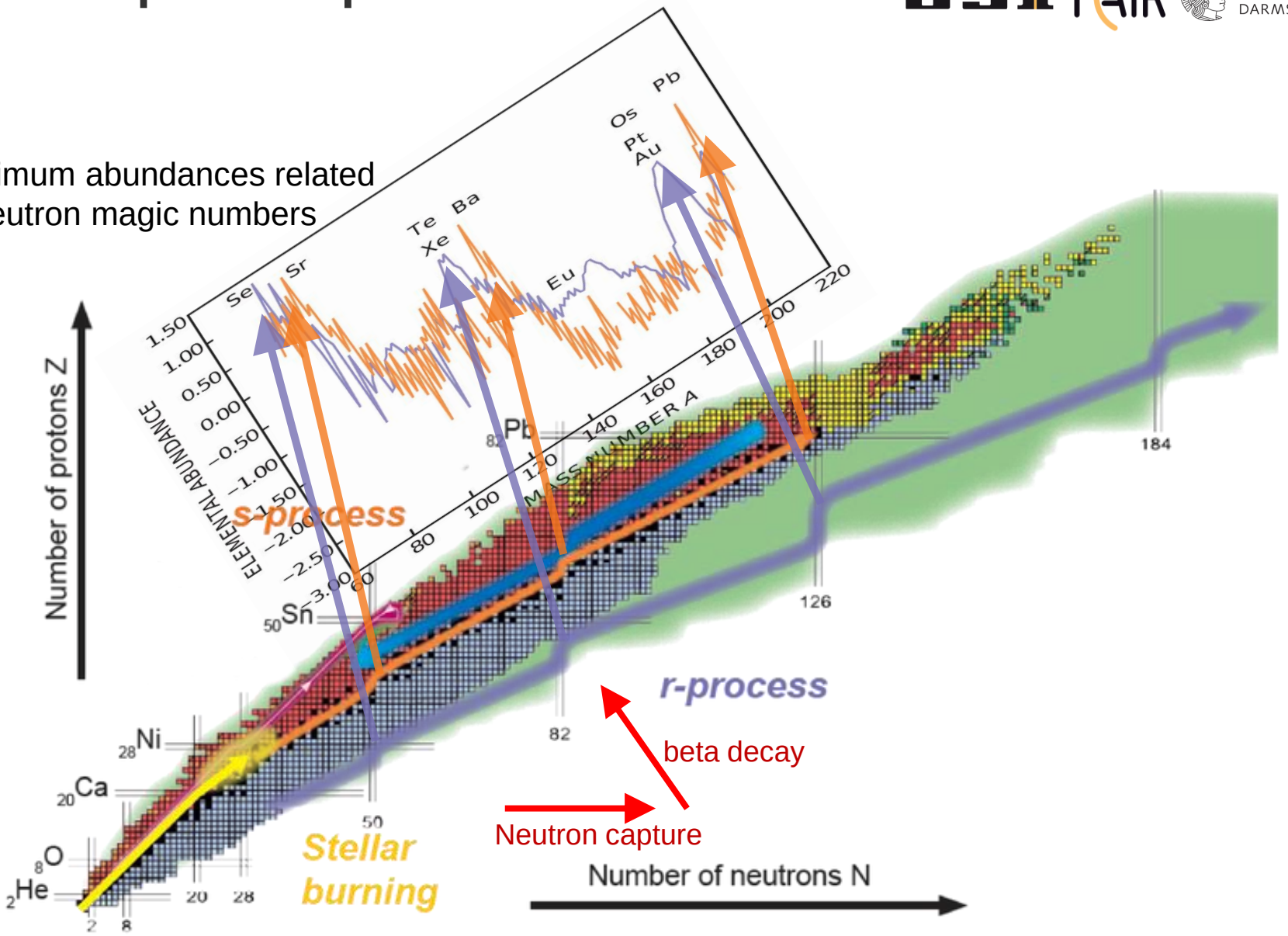

Nucleosynthesis beyond iron

Several processes contribute to the nucleosynthesis beyond Iron: s-process, r-process and p-process (γ-process)

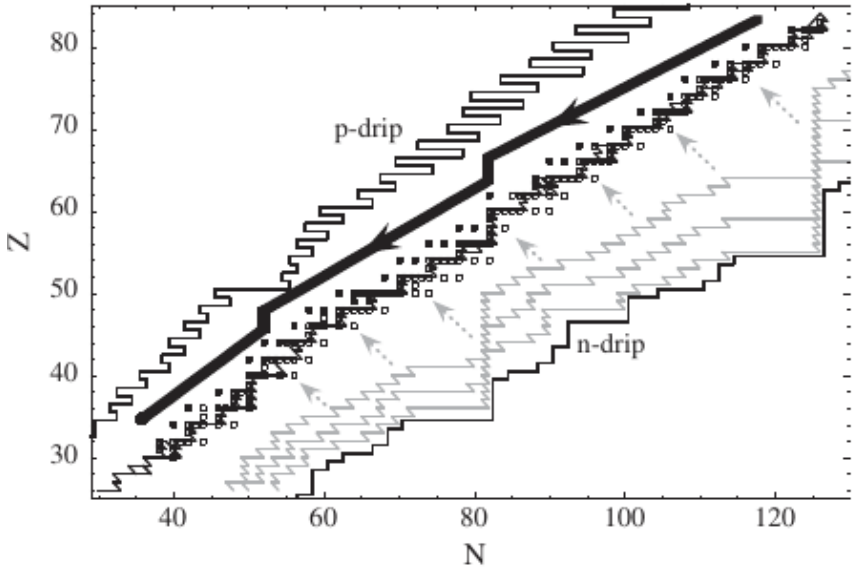

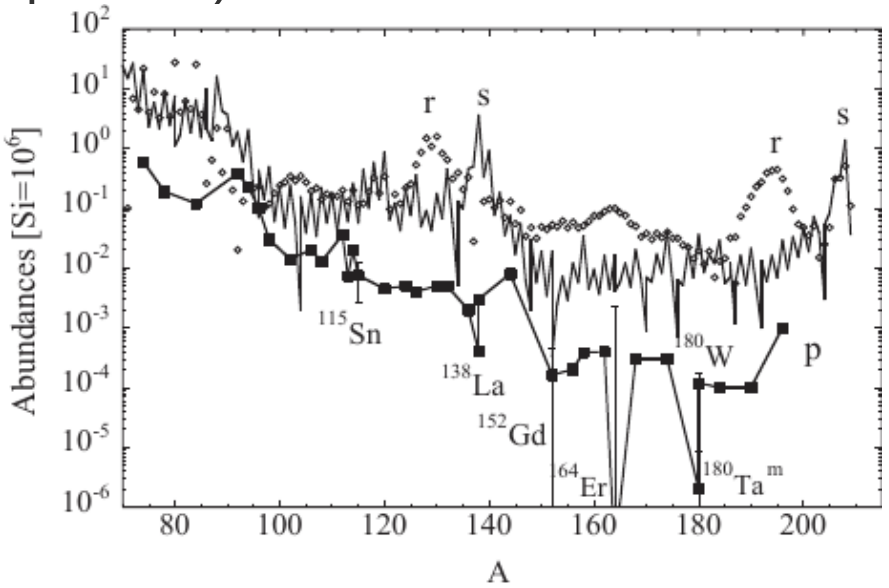

M. Arnould, S. Goriely / Physics Reports 384, 1 (2003)

- s process: low neutron densities, $n_n = 10^{10-12}$ cm^{-3}, $\tau_n > \tau_\beta$
  (site: intermediate mass stars)
- r process: large neutron densities, $n_n > 10^{20}$ cm^{-3}, $\tau_n \ll \tau_\beta$
  (site: binary neutron star mergers?)
- Additional process(es) required to produce neutron-deficient p-nuclei
  - p-process or γ-process: photodissociation material enriched by s-process
  - νp-process: (p,γ) and (n,p) reactions catalysed by $\bar{\nu}_e + p \rightarrow n + e^+$

Metal-poor stars observations

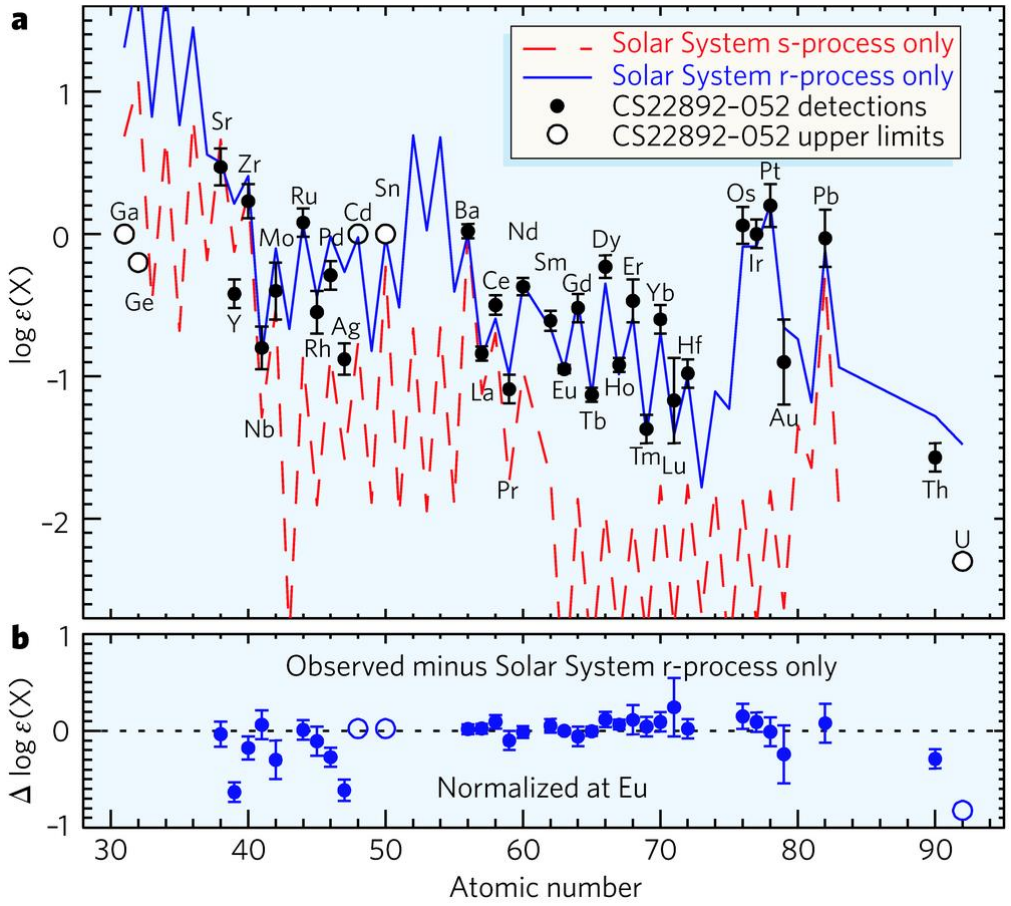

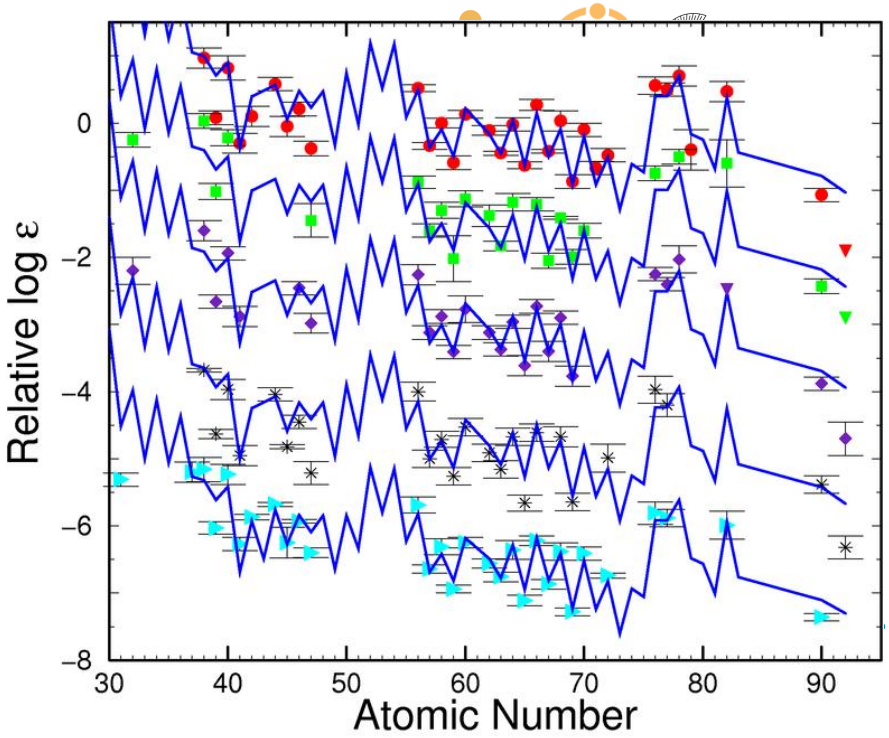

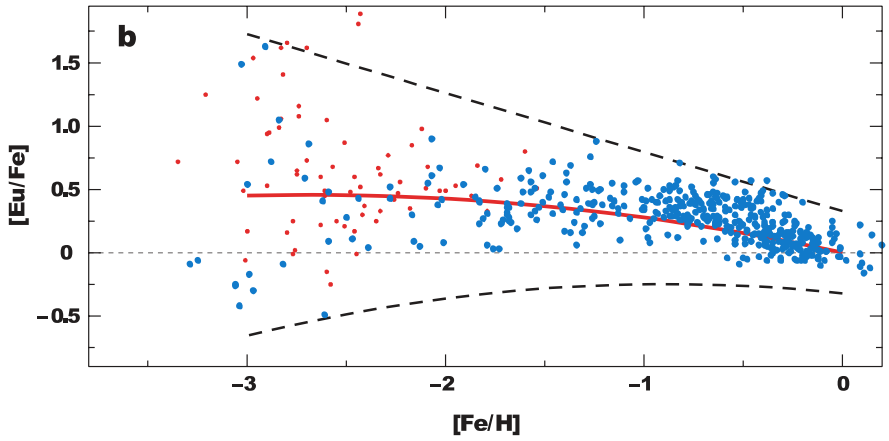

- Observations indicate that r process operates from early Galactic history in rare (high yield) events

Kilonova: signature of the r-process

Line of view GW170817

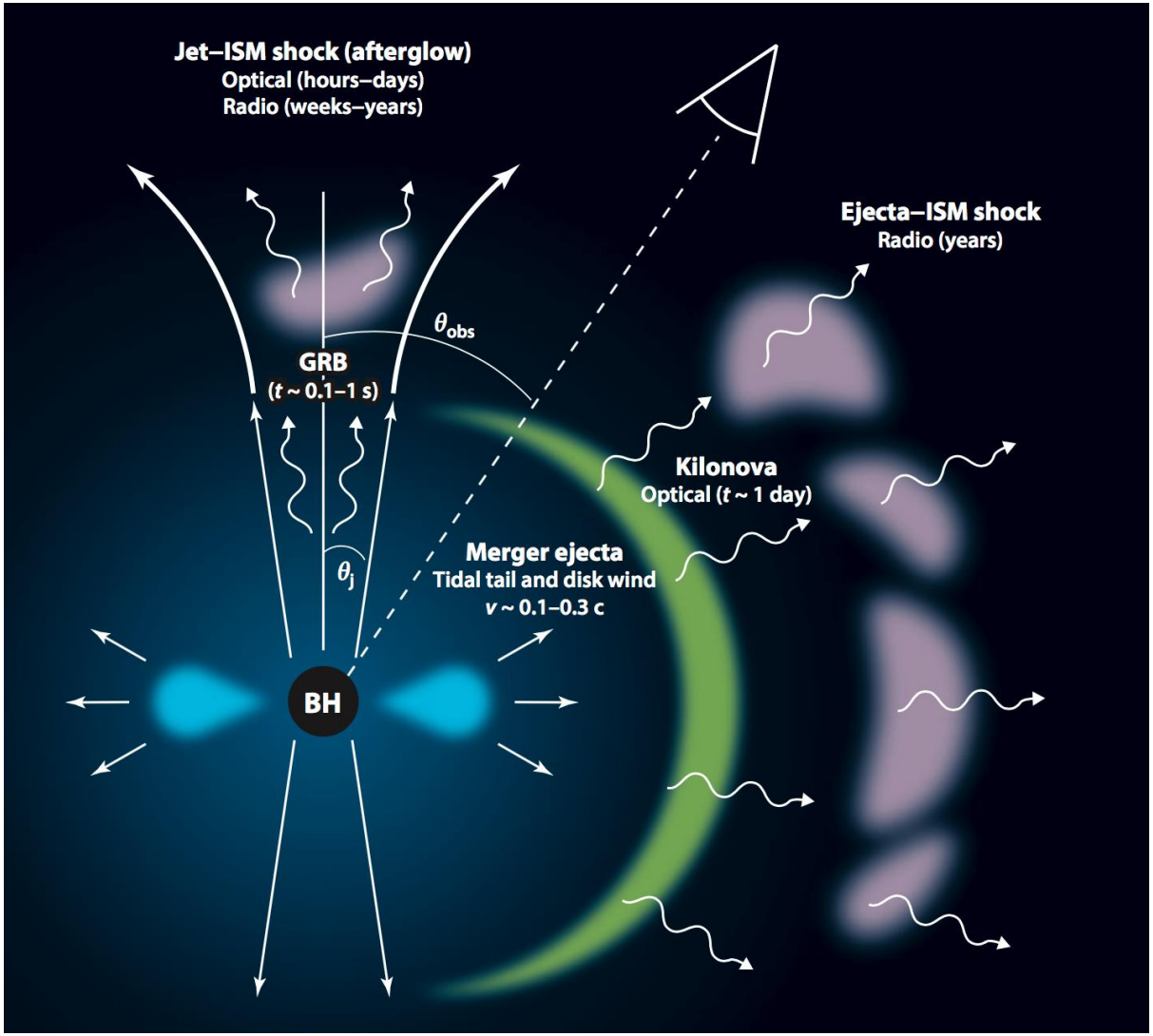

Metzger & Berger 2012

Kilonova: An electromagnetic transient due to long term radioactive decay of r-process nuclei

- Electromagnetic counterpart to Gravitational Waves
- Diagnostics physical processes at work during merger
- Direct probe of the formation r-process nuclei

R process modelling

Astrophysical environment should provide enough neutrons per seed for the r process to operate

$$A_{\text{final}} = A_{\text{initial}} + n_{\text{seed}}$$

n_{seed} depends mainly on neutron richness ejecta

Neutron stars are an important reservoir of neutrons

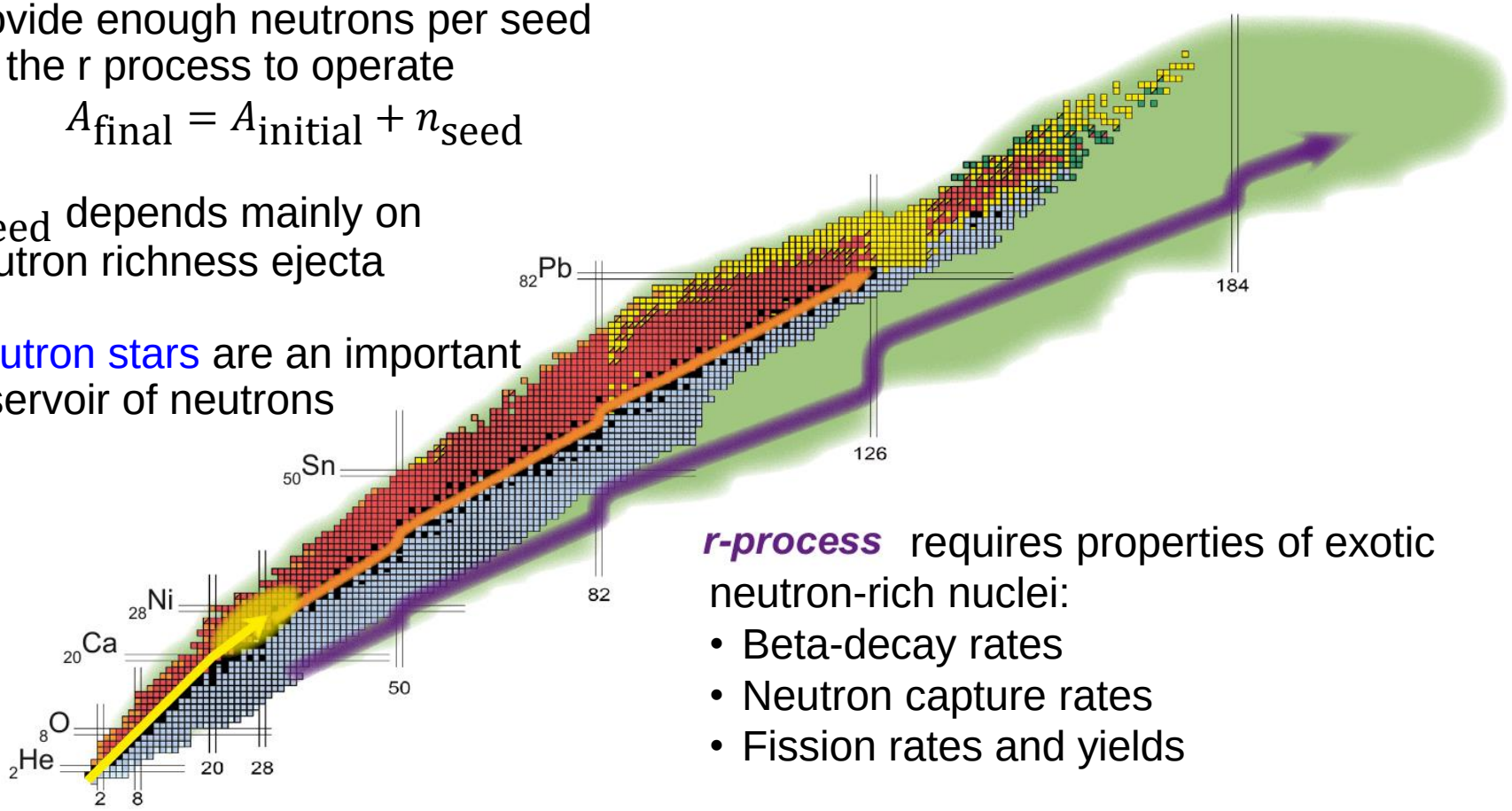

r-process requires properties of exotic neutron-rich nuclei:

- Beta-decay rates
- Neutron capture rates
- Fission rates and yields

Benchmark against observations:

- Solar and stellar abundances (indirect)
- Electromagnetic emission, kilonova (direct), sensitive Atomic and Nuclear Physics

R-process operation

Heavy elements produced by the r-process. Radioactive decay liberates energy

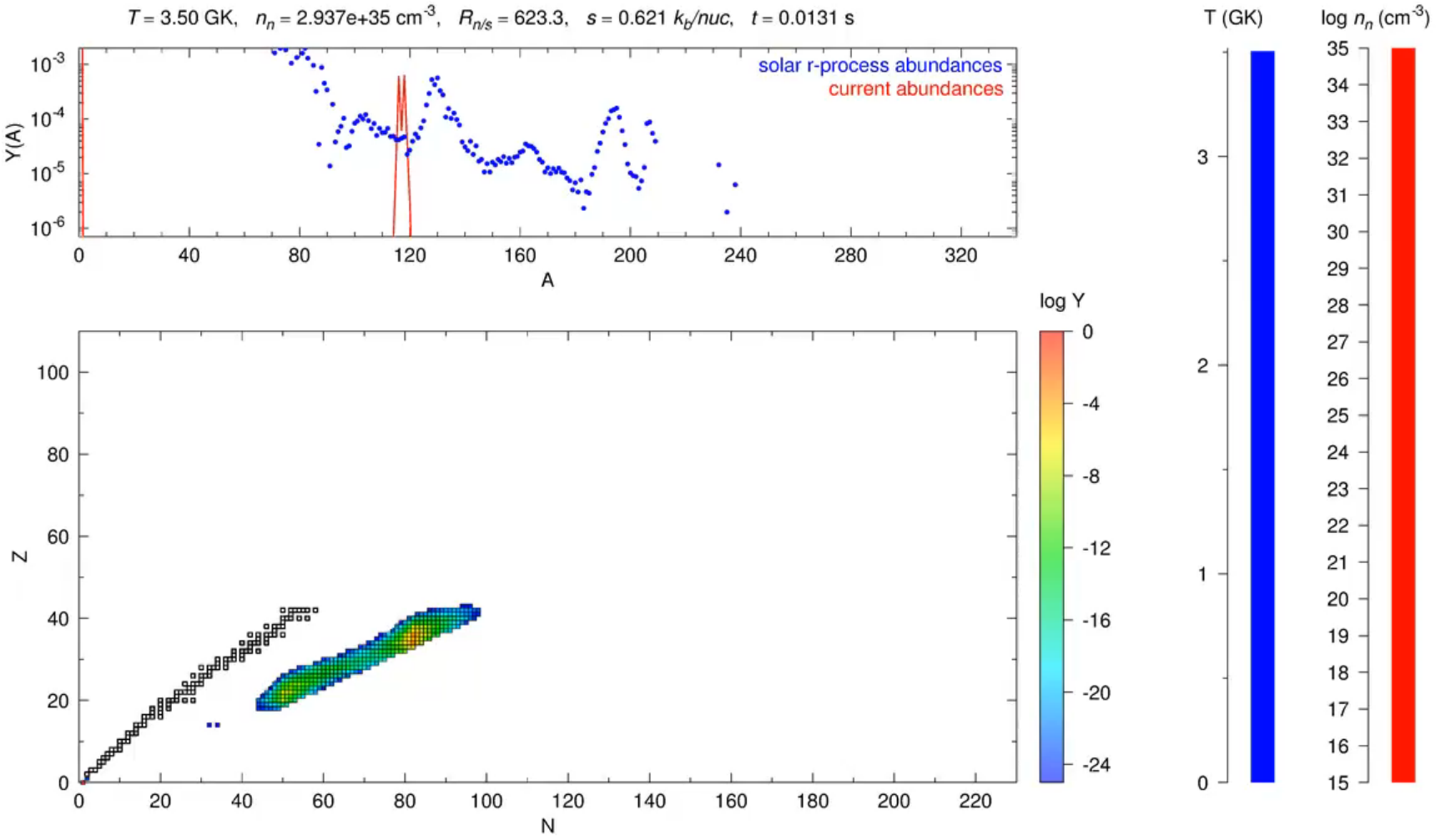

Types of reactions

Nuclei in the astrophysical environment can suffer different reactions:

- Decay (decay rate: $\lambda = \ln 2/t_{1/2}$)

$$^{56}\mathrm{Ni} \rightarrow {}^{56}\mathrm{Co} + e^{+} + \nu_e$$
$$^{15}\mathrm{O} + \gamma \rightarrow {}^{14}\mathrm{N} + p$$

$$\frac{dn_a}{dt} = -\lambda_a n_a$$

In order to dissentangle changes in the density (hydrodynamics) from changes in the composition (nuclear dynamics), the abundance is introduced:

$$Y_a = \frac{n_a}{n}, \quad n \approx \frac{\rho}{m_u} = \text{Number density of nucleons (constant)}$$

$$\frac{dY_a}{dt} = -\lambda_a Y_a$$

Rate can depend on temperature and density

Types of reactions

Nuclei in the astrophysical environment can suffer different reactions:

- Capture processes

$$a + b \rightarrow c + \gamma$$

$$\frac{dn_a}{dt} = -n_a n_b \langle \sigma v \rangle$$

$$\frac{dY_a}{dt} = -\frac{\rho}{m_u} Y_a Y_b \langle \sigma v \rangle$$

  destruction rate particle a by reaction with b: $\lambda_a(b) = \rho Y_b \langle \sigma v \rangle / m_u$

- photodissociation rates

$$\gamma + c \rightarrow a + b$$

$$\frac{dY_c}{dt} = -Y_c \lambda_c = -Y_c n_\gamma \langle \sigma c \rangle$$

  $\langle \sigma c \rangle$ photodissociation cross section averaged over thermal photon spectrum.
  The balance between capture and photodissociation is determined by the photon-to-baryon ratio or entropy.

Three body reactions

Due to the fact that there is no stable nuclei with $A = 5$ and 8, nuclei heavier than ^{4}He have to be build by 3-body reactions. The most relevant reactions are:

3-α Dominant in proton-rich environments

$$3\,{}^4\mathrm{He} \rightarrow {}^{12}\mathrm{C} + \gamma$$

$$\frac{dY_\alpha}{dt} = -\frac{3}{3!} Y_\alpha^3 \left(\frac{\rho}{m_u}\right)^2 \langle \alpha\alpha\alpha \rangle$$

$\alpha\alpha n$ Dominant in neutron-rich environments

$$2\,{}^4\mathrm{He} + n \rightarrow {}^9\mathrm{Be} + \gamma$$

$$\frac{dY_\alpha}{dt} = -\frac{2}{2} Y_\alpha^2 Y_n \left(\frac{\rho}{m_u}\right)^2 \langle \alpha\alpha n \rangle$$

These reactions are key for the build-up of heavy nuclei during the r-process.

Reaction rates

Consider n_a and n_b particles per volume of species a and b. The number of nuclear reactions per unit of time and volume

$$a + A \rightarrow B + b$$

is given by:

$$r_{aA} = \frac{n_a(v_a) n_A(v_A)}{(1+\delta_{aA})} \sigma(v) v, \quad v = |\boldsymbol{v}_a - \boldsymbol{v}_A| \text{ (relative velocity)}$$

In stellar environment the velocity (energy) of particles follows a thermal distribution that depends of the type of particles.

- Nuclei (Maxwell-Boltzmann)

$$n(v)dv = n 4\pi v^2 \left(\frac{m}{2\pi kT}\right)^{3/2} \exp\left(-\frac{mv^2}{2kT}\right) dv = n\phi(v)dv$$

- Electrons, Neutrinos (if thermal) (Fermi-Dirac)

$$n(p)dp = \frac{g}{(2\pi\hbar)^3} \frac{4\pi p^2}{e^{(E(p)-\mu)/kT} + 1} dp$$

- photons (Bose-Einstein)

$$n(p)dp = \frac{2}{(2\pi\hbar)^3} \frac{4\pi p^2}{e^{pc/kT} - 1} dp$$

Stellar reaction rate

The product σv has to be averaged over the relative velocity distribution $\phi(v)$ (Maxwell-Boltzmann)

$$\langle \sigma v \rangle = \int_0^\infty \phi(v)\sigma(v)v dv$$

that gives:

$$\langle \sigma v \rangle = 4\pi \left(\frac{m}{2\pi kT}\right)^{3/2} \int_0^\infty v^3 \sigma(v) \exp\left(-\frac{mv^2}{2kT}\right) dv, \quad m = \frac{m_a m_b}{m_a + m_b}$$

or using $E = mv^2/2$

$$\langle \sigma v \rangle = \left(\frac{8}{\pi m}\right)^{1/2} \frac{1}{(kT)^{3/2}} \int_0^\infty \sigma(E) E \exp\left(-\frac{E}{k_B T}\right) dE \qquad (1)$$

Function of temperature with strong T-dependence for charged-particle reactions

Systematics $\langle \sigma v \rangle$ and neutron separation energies

Neutron capture rates reflect the behavior of neutron separation energies

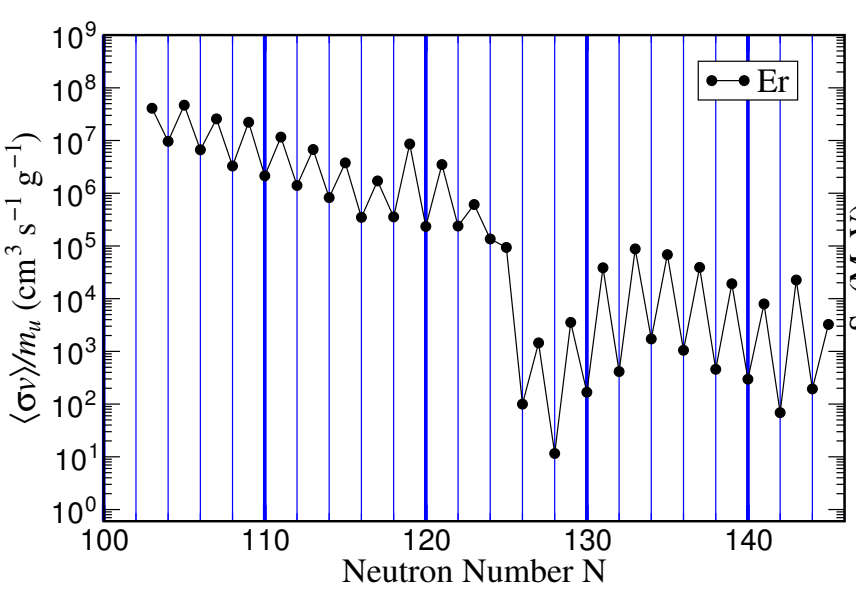

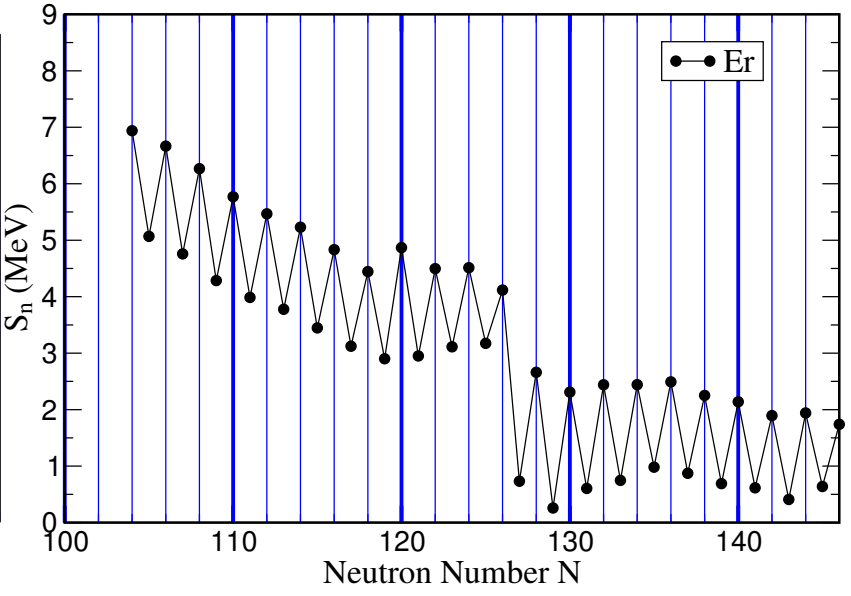

Rates computed at $T = 1$ GK.

Inverse reactions

Let's have the reaction

$$a + A \rightarrow B + \gamma \quad Q = m_a + m_A - m_B$$

We are interested in the inverse reaction. One can use detailed-balance to determine the inverse rate:

$$\lambda_\gamma = \frac{G_a G_A}{(1+\delta_{aA}) G_B} \left(\frac{m_a m_A}{m_B}\right)^{3/2} \left(\frac{k_B T}{2\pi\hbar^2}\right)^{3/2} e^{-Q/k_B T} \langle \sigma v \rangle$$

For a reaction $a + A \rightarrow B + b$ ($Q = m_a + m_A - m_B - m_b$):

$$\langle \sigma v \rangle_{bB} = \frac{(1+\delta_{bB})}{(1+\delta_{aA})} \frac{G_a G_A}{G_b G_B} \left(\frac{m_a m_A}{m_b m_B}\right)^{3/2} e^{-Q/k_B T} \langle \sigma v \rangle_{aA}$$

G partition function nuclei.

Beta-decay

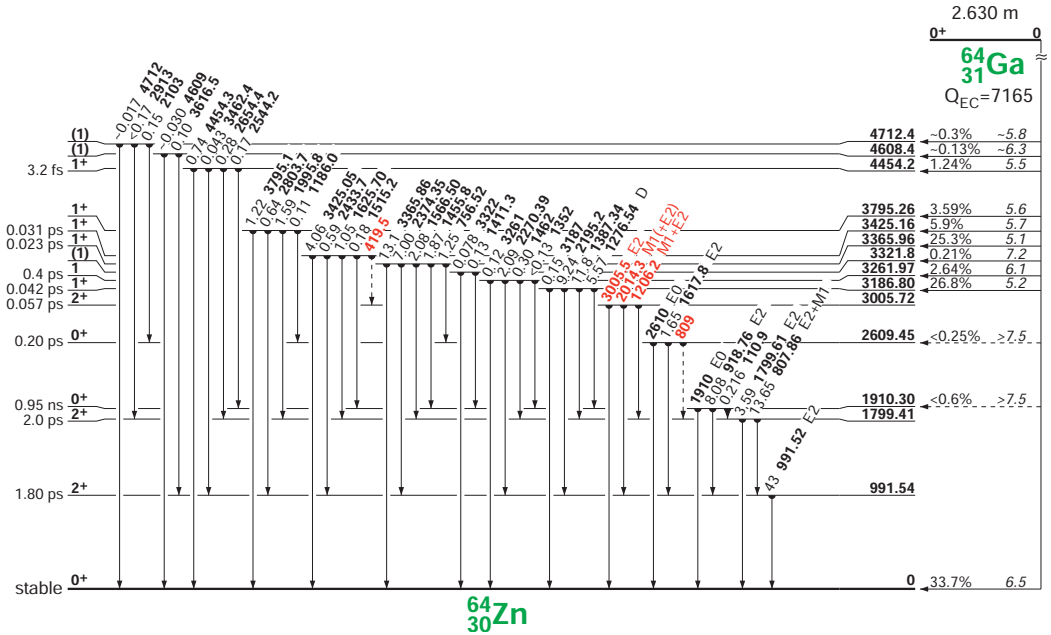

$$\lambda_\beta = \frac{\ln 2}{K} f(Q)[B(F) + B(GT)], \qquad K = \frac{2\pi^3 (\ln 2)\hbar^7}{G_F^2 V_{ud}^2 g_V^2 m_e^5 c^4} = 6147.0 \pm 2.4\ s$$

- $f(Q)$ phase space function ($\sim Q^5$).
- $B(F)$ Fermi matrix element ($\sim \langle f| \sum_k \boldsymbol{t}_+^k |i\rangle$).
- $B(GT)$ Gamow-Teller matrix element ($\sim \langle f| \sum_k \boldsymbol{\sigma t}_+^k |i\rangle$).
- Heavier nuclei contributions from forbidden decays (leptons carry angular momentum)

Systematics beta-decay Q-values

The decay Q-value increases with neutron excess.

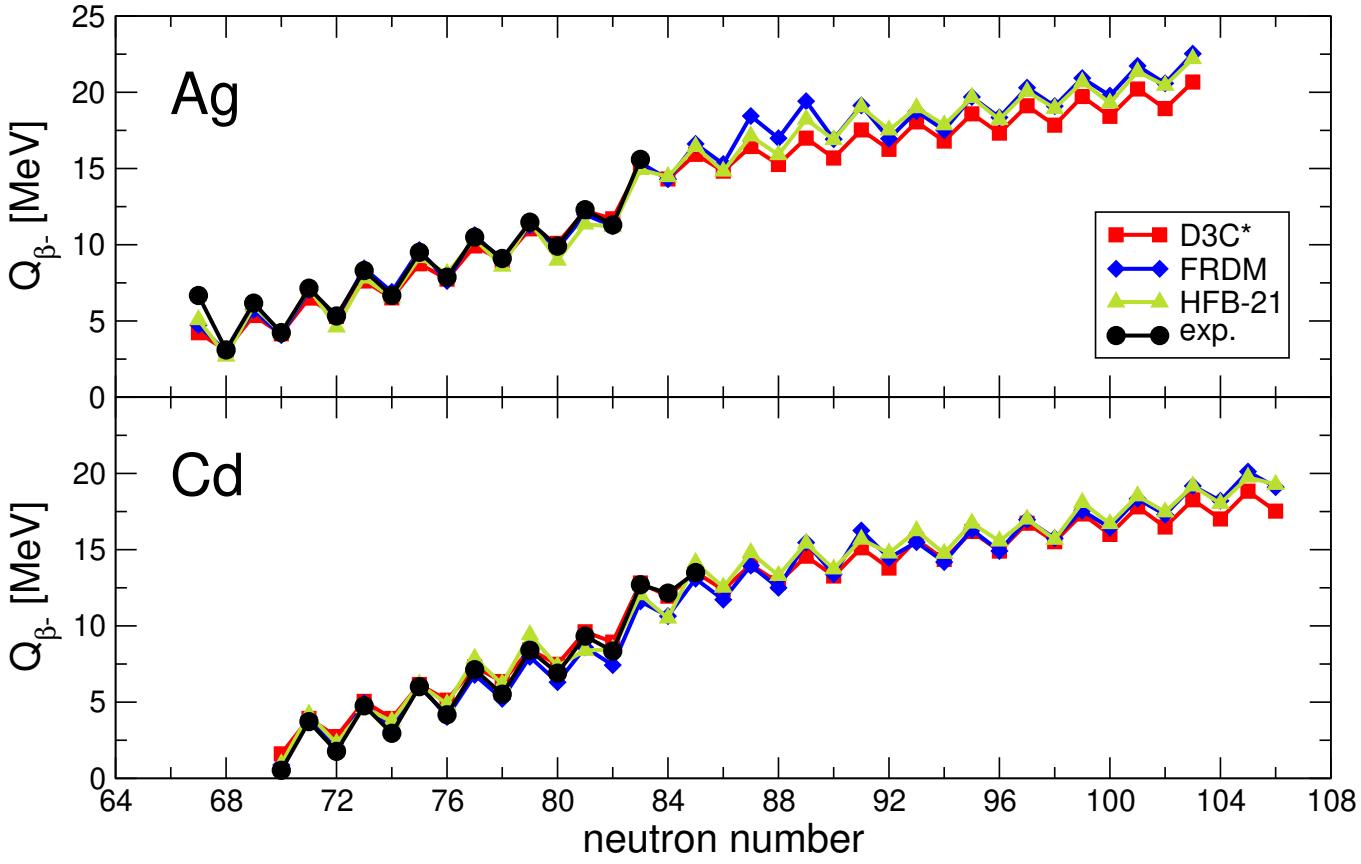

Structure Gamow-Teller strength

- Gamow-Teller strength is characterized by the presence of a resonance at excitation energies around 10-15 MeV.
- With increasing neutron-excess Q increases and a larger fraction of strength is in the decay window. Half-lives become shorter.
- Low-lying strength is rather sensitive to correlations.

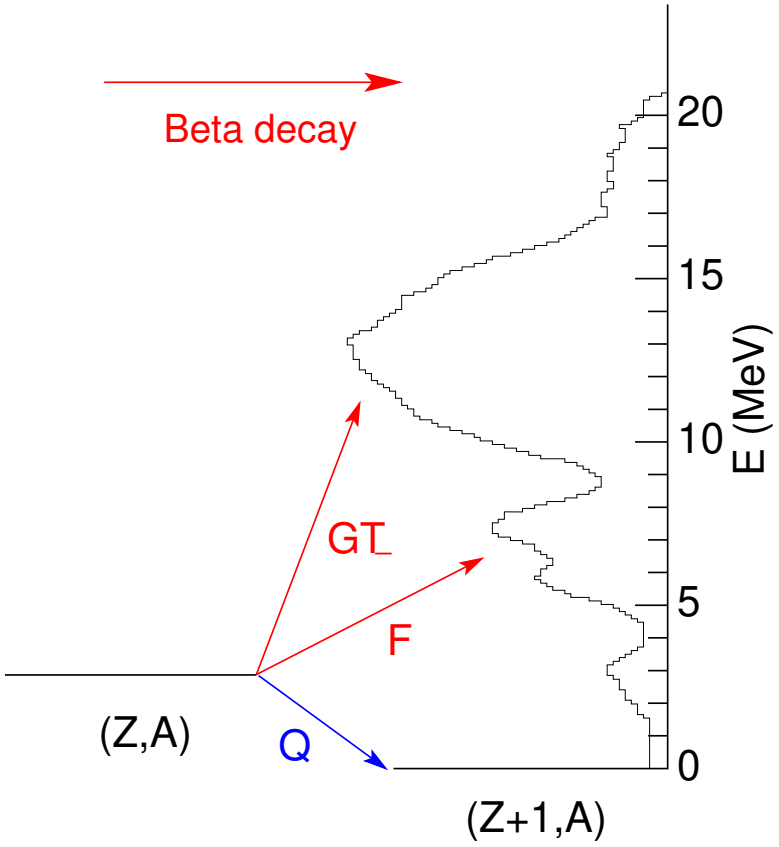

Systematics half-lives

Half-lives decrease with neutron excess. Strong sensitivity to decay energy.

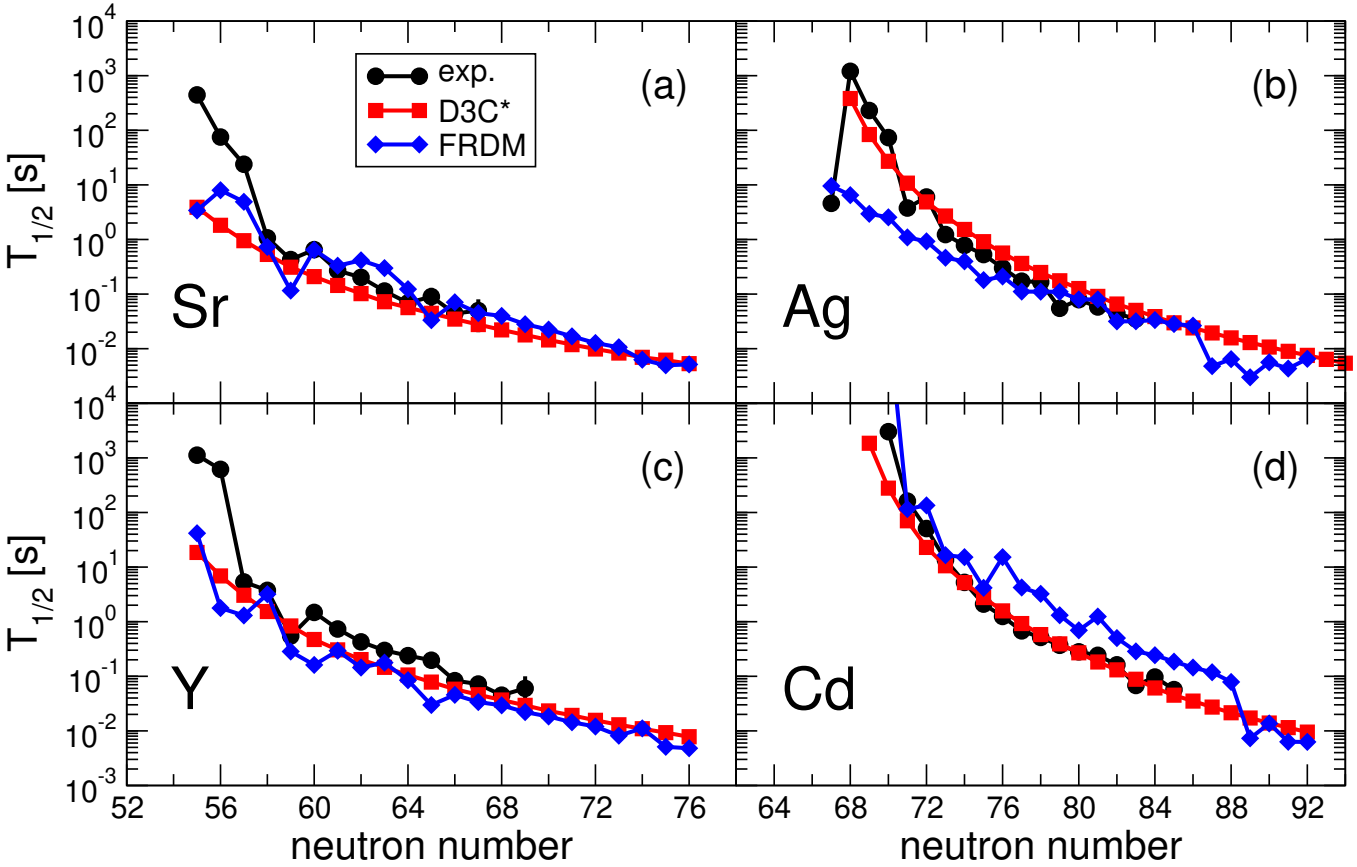

T. Marketin, L. Huther, and G. Martínez-Pinedo, Phys. Rev. C **93**, 025805 (2016).

Neutrino-nucleus reactions

If nuclei are subject to large neutrino fluxes absorption of ν_e charge-current interactions can accelerate the "decay" of neutron rich nuclei ($\lambda = \lambda_\beta + \lambda_{\nu_e}$)

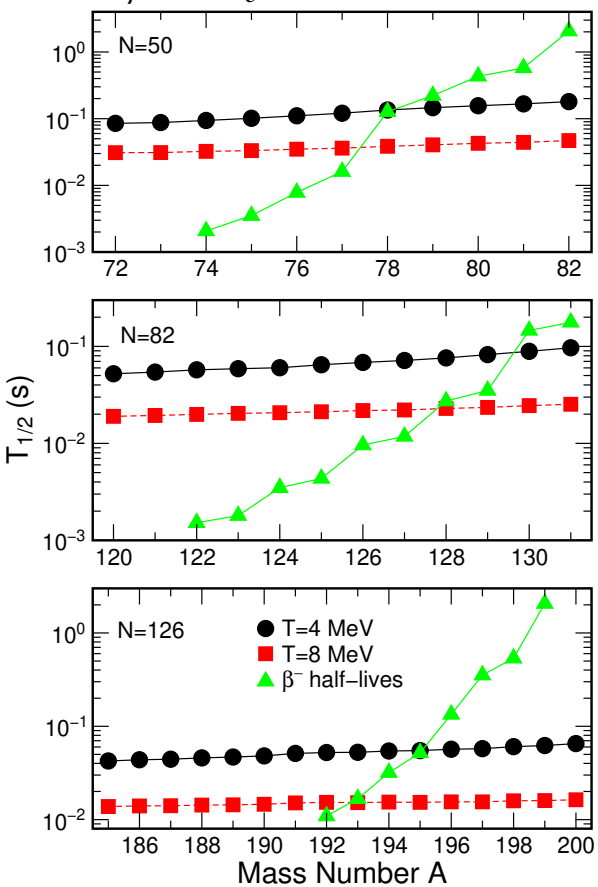

Neutrino rates are not sensitive to shell-effects $\sigma \propto (N - Z)$.

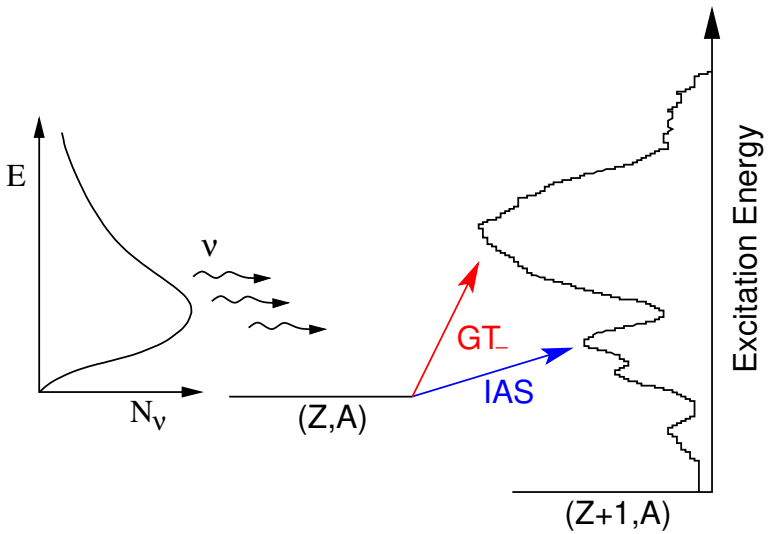

Due to large neutrino energies cross section is dominated to transitions to Gamow-Teller resonance.

Rate Examples: $^4\mathrm{He}(\alpha\alpha,\gamma)$

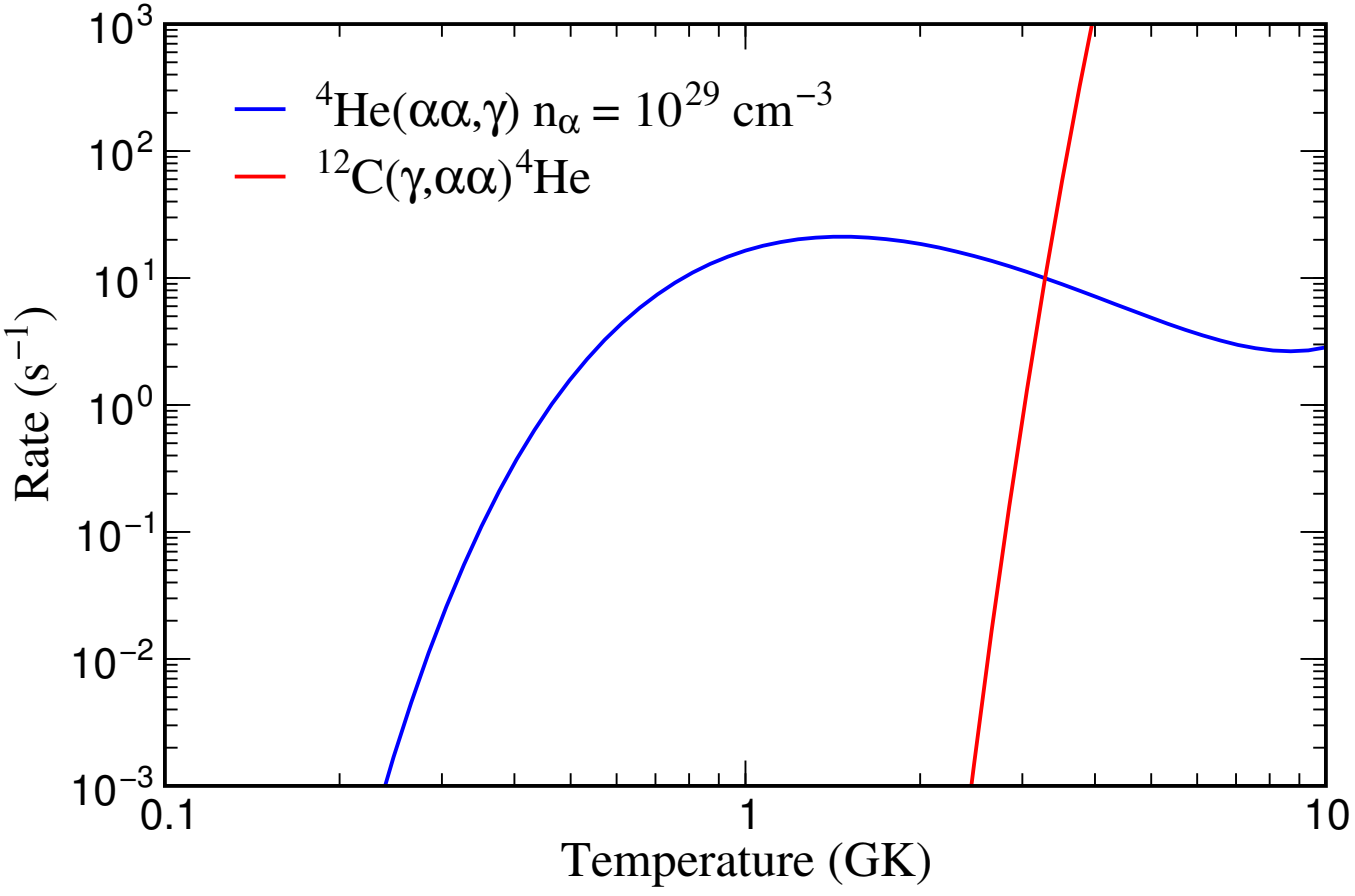

Rate Examples: (p, γ)

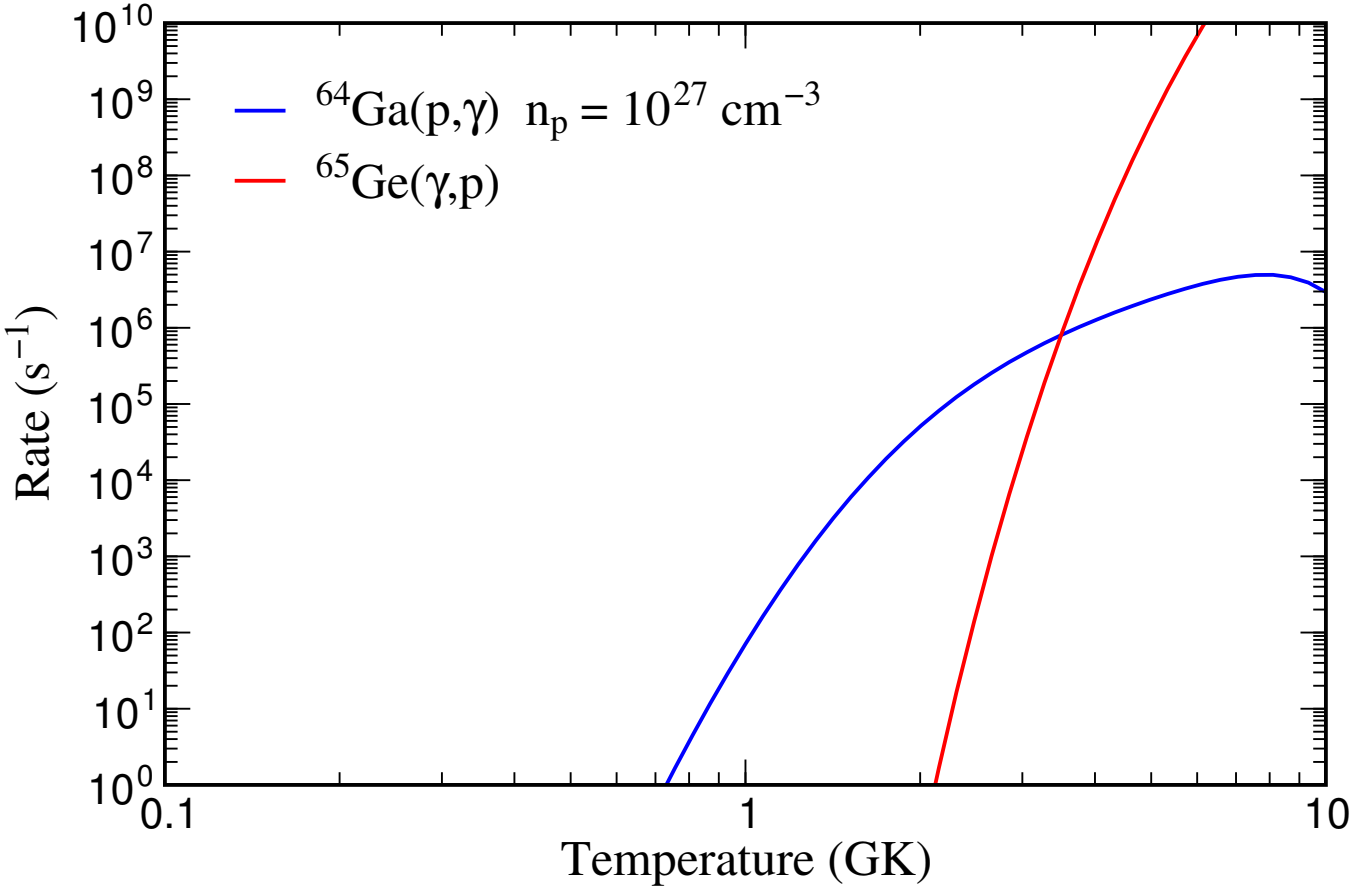

Rate Examples: (α, γ)

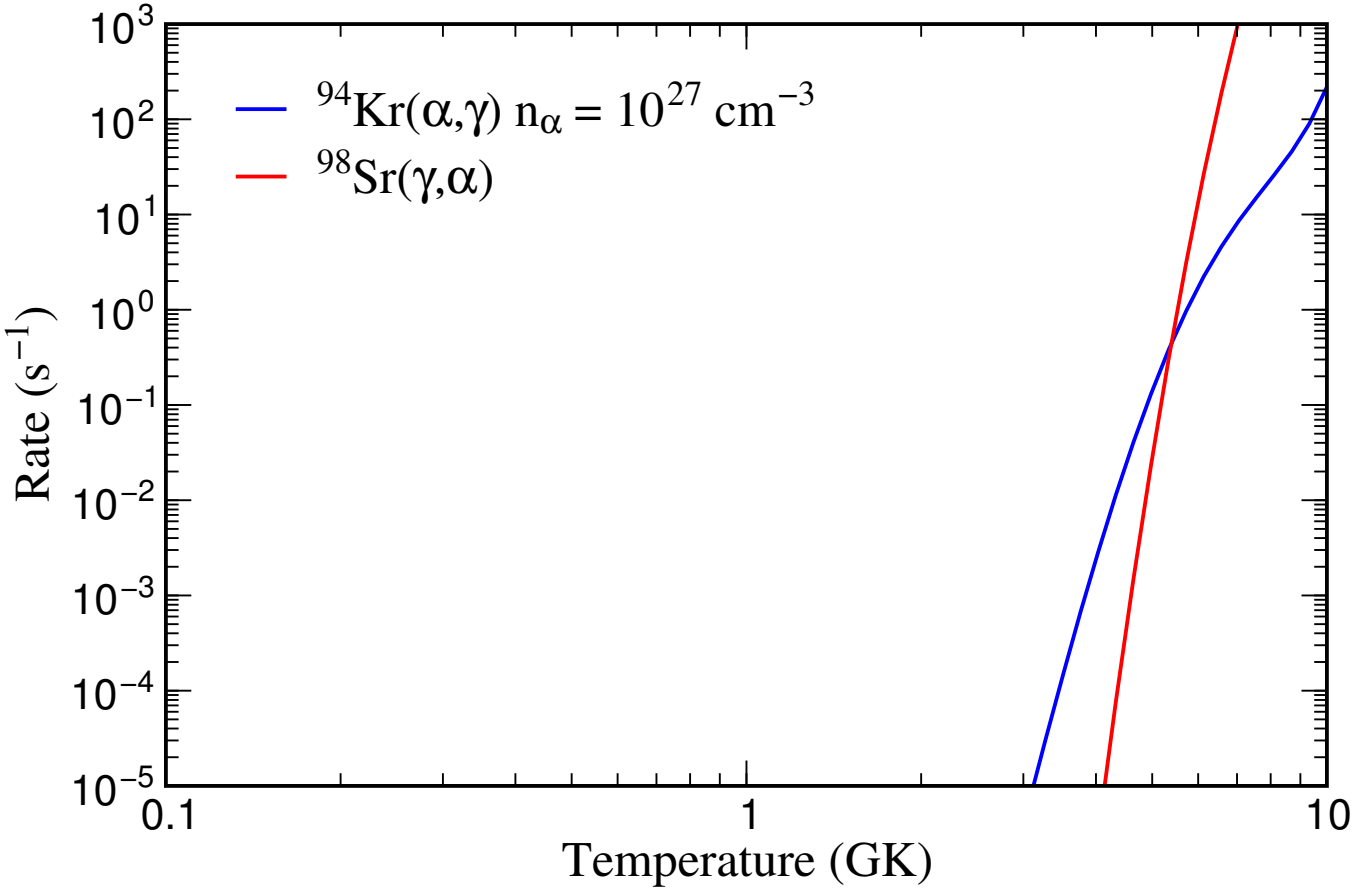

Rate examples: (n, γ)

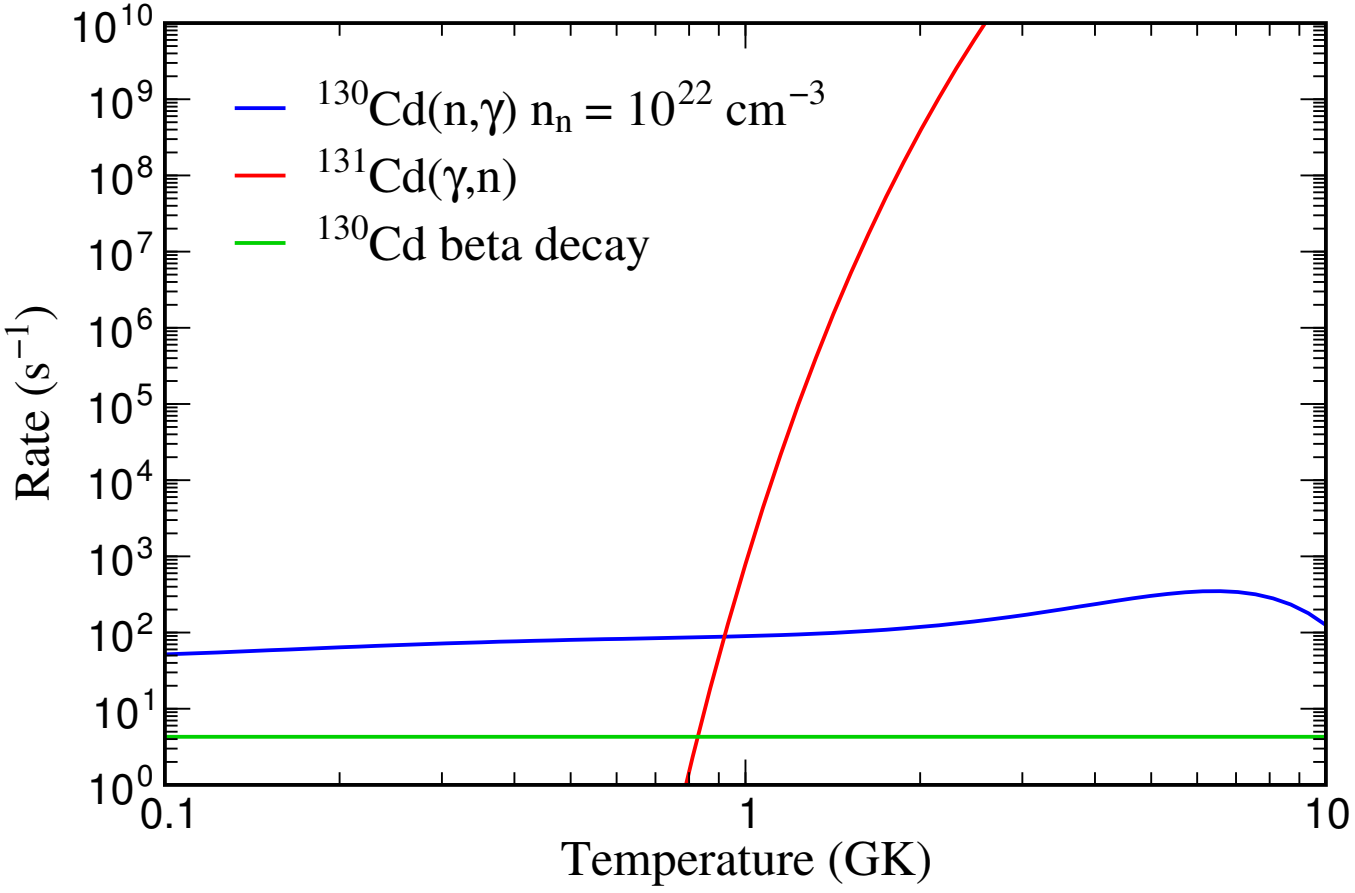

R-process sites

- Any r-process site should be able to produce both the "seed" nuclei where neutrons are captured and the neutrons that drive the r-process. The main parameter describing the feasibility of a site to produce r-process nuclei is the neutron-to-seed ratio: n_n/n_{seed}.
- If the seed nuclei have mass number A_{seed} and we have n_n/n_{seed} neutrons per seed, the final mass number of the nuclei produced will be $A = A_{\text{seed}} + n_n/n_{\text{seed}}$.
- For example, taking $A_{\text{seed}} = 90$ we need $n_n/n_{\text{seed}} = 100$ if we want to produce the 3rd r-process peak ($A \sim 195$) and $n_n/n_{\text{seed}} = 150$ to produce U and Th.

r-process nucleosynthesis relevant parameters

Independently of the astrophysical site the nucleosynthesis is sensitive to a few parameters that determine the neutron-to-seed ratio and the heavy elements that can be produced:

$$A_f = A_i + n_s, \quad n_s = n_n/n_{\text{seed}} \sim s^3/(Y_e^3 \tau_{\text{dyn}})$$

Y_e The lower the value of Y_e more neutrons are available and the larger n_s

entropy Large entropy $s \sim T^3/\rho$, means low density and high temperature (large amount of photons). Both are detrimental to the build up of seeds.

expansiton time scale The faster the matter expands, smaller τ_{dyn}, the less time one has to build up seeds

Dependence abundances on entropy

All calculations use a constant $Y_e = 0.45$

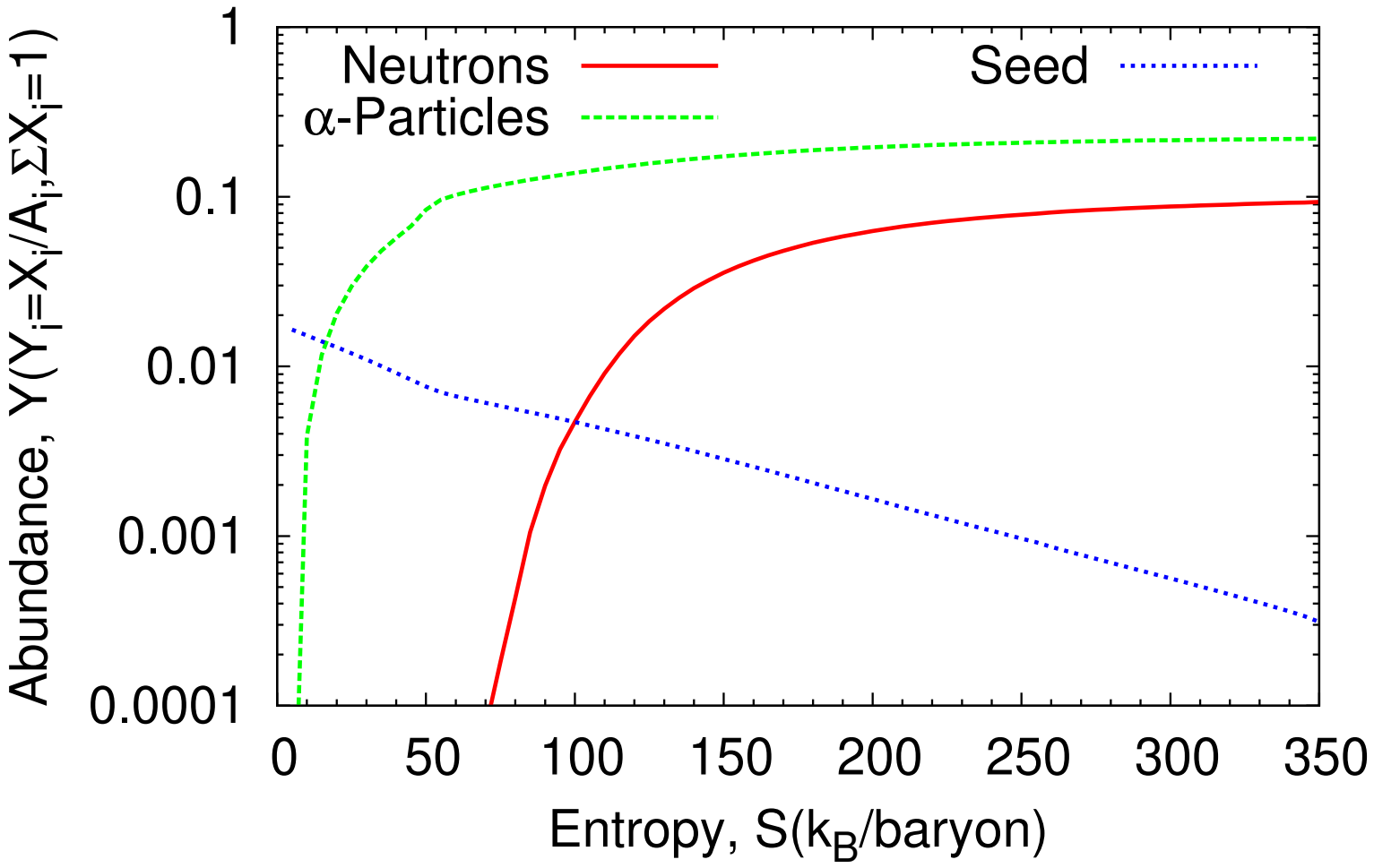

Farouqi, et al, Astrophys. J. 694, L49 (2009).

Seed dependence on Y_e

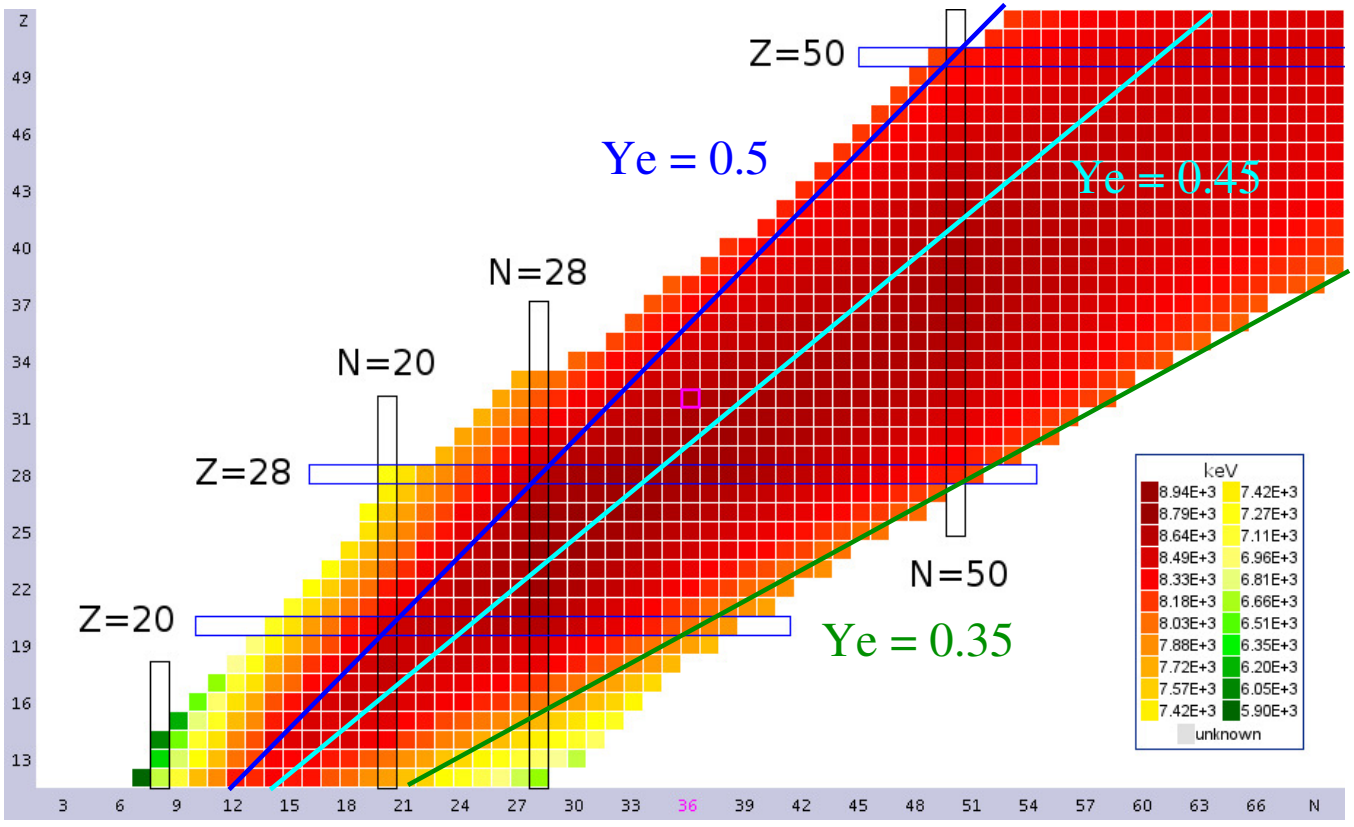

With reduced Y_e the peak of the nuclear abundance distribution moves from ^{56}Ni ($Y_e \sim 0.5$) to heavier neutron rich nuclei (^{90}Zr for $Y_e \sim 0.45$). For low Y_e becomes energetically favourable to have free neutrons.

Dependence on Y_e

For moderate entropies r process depends mainly on Y_e.

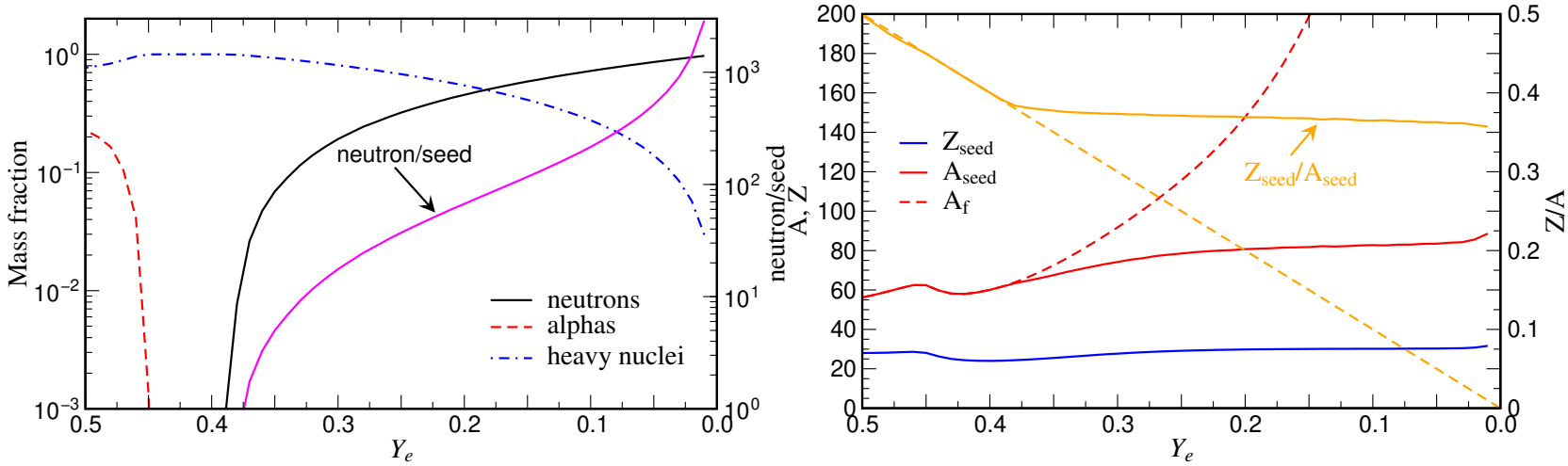

For neutron-rich moderate entropy ejecta ($s \sim 20$) we have:

$$n_s = A_s\left(\frac{Z_s}{A_s}\frac{1}{Y_e} - 1\right), \quad A_f = A_s + n_s$$

Calculation by Bowen Jiang

Dependence nucleosynthesis on Y_e

For moderate entropies $s \lesssim 30$ nucleosynthesis depends on neutron richness of ejecta. Determined by

$$\nu_e + n \rightleftarrows p + e^- \qquad \bar{\nu}_e + p \rightleftarrows n + e^+$$

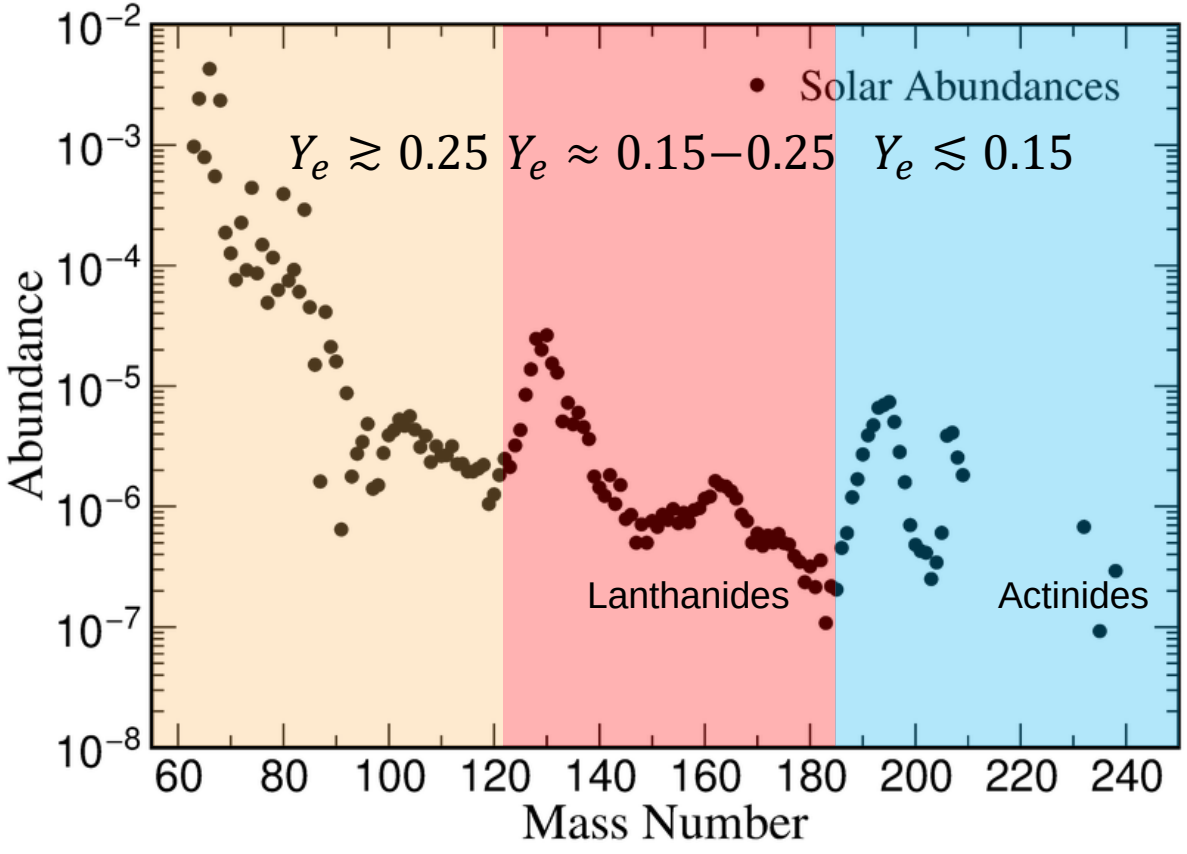

The relevant nuclear physics depends on the particular Y_e conditions.

r process calculations

r process calculations require to solve the system of differential equations:

$$\begin{aligned}\frac{dY(Z,A)}{dt} = & \left(\frac{\rho}{m_u}\right)\langle\sigma v\rangle_{Z,A-1}Y_n Y(Z,A-1) + \lambda_\gamma(Z,A+1)Y(Z,A+1) \\ & + \sum_{j=0}^{J}\lambda_{\beta jn}(Z-1,A+j)Y(Z-1,A+j) \\ & - \left(\left(\frac{\rho}{m_u}\right)\langle\sigma v\rangle_{Z,A}Y_n + \lambda_\gamma(Z,A) + \sum_{j=0}^{J}\lambda_{\beta jn}(Z,A)\right)Y(Z,A)\end{aligned}$$

$$\begin{aligned}\frac{dY_n}{dt} = & - \sum_{Z,A}\left(\frac{\rho}{m_u}\right)\langle\sigma v\rangle_{Z,A}Y_n Y(Z,A) \\ & + \sum_{Z,A}\lambda_\gamma(Z,A)Y(Z,A) \\ & + \sum_{Z,A}\left(\sum_{j=1}^{J} j\lambda_{\beta jn}(Z,A)\right)Y(Z,A)\end{aligned}$$

We are neglecting fission

Phases during the operation of the r-process

- **Weak freeze-out:** proton-to-nucleon ratio determined by (anti)neutrino absorption and their inverses
- **Seed production**: Charged particle reactions operating for $T \gtrsim 2\ GK$ produce the seed nuclei and neutrons
- **Neutron-capture phase:** neutrons are captured on the available seed nuclei on a typical times of $\sim 1\ s$. Different equilibria are achieved:
  - $(n,\gamma) \rightleftarrows (\gamma,n)$ equilibrium defines the r-process path that is mainly sensitive to the nuclear masses
  - Beta-flow equilibrium: abundance given element is proportional to the beta-decay half-lives. R-process peaks associated to nuclei with longest half-lives.
- **Freeze-out and decay to stability:** fully dynamical phase in which competition between neutron-captures, beta-decay (and fission) determines the final abundance pattern. Most sensitive phase to the nuclear input

Evolution during r process

Example of r process calculation for very neutron rich ejecta (Based on trajectory from merger simulation from A. Bauswein)

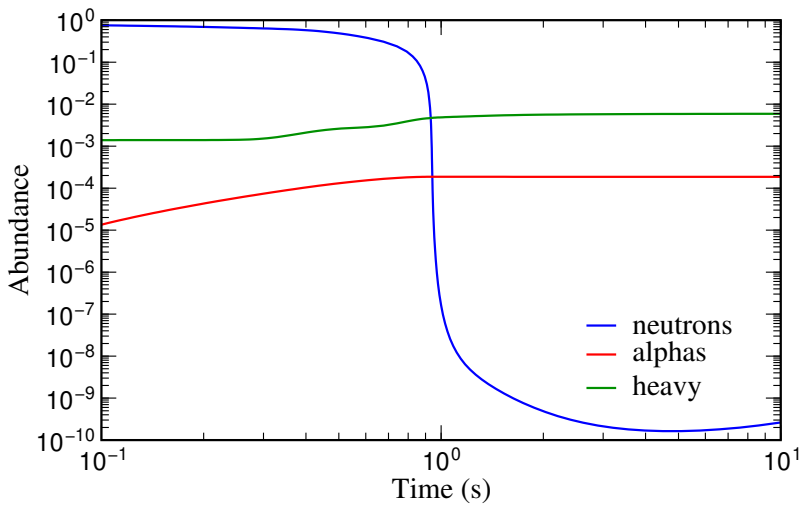

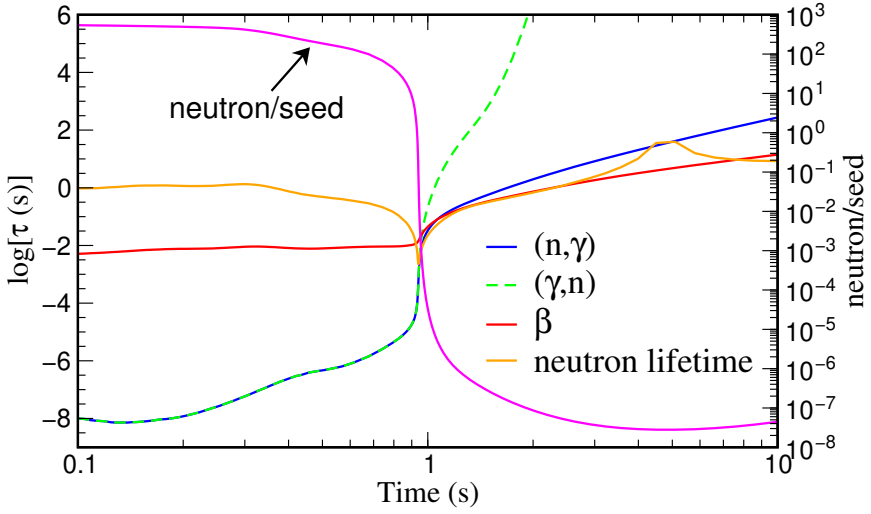

$$\frac{1}{\tau_n} = \frac{1}{n_s}\left(\frac{1}{\tau_{(n,\gamma)}} - \frac{1}{\tau_{(\gamma,n)}}\right)$$

The last phase of the r process when the neutron-to-seed decreases very fast is known as freeze-out. During this phase neutron captures and beta-decays compete with each other. It is during this phase that the final abundances are shaped.

From Meng-Ru Wu

Classical r-process, $(n,\gamma) \rightleftarrows (\gamma,n)$ equilibrium

Need:
- mix of suitable heavy seed nuclei (A=56-90) and neutrons
- sufficient large number density of neutrons (max at least ~1e24 cm^{-3})
- sufficient large neutron/seed ratio (at least ~100)

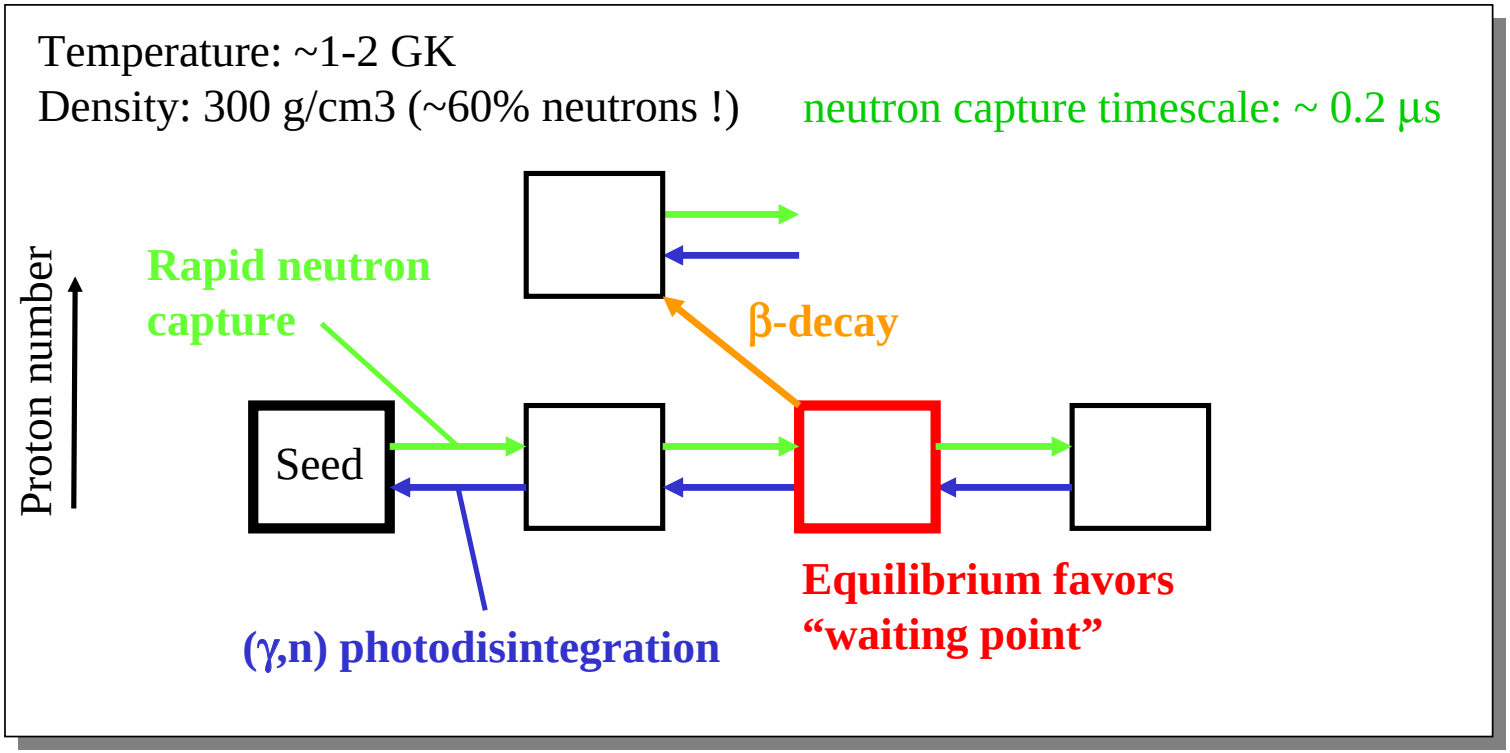

$(n,\gamma) \rightleftarrows (\gamma,n)$ equilibrium

Neutron capture reactions proceed much faster than beta-decays and an $(n,\gamma) \rightleftarrows (\gamma,n)$ equilibrium is achieved

$$\mu(Z,A+1) = \mu(Z,A) + \mu_n$$

$$\frac{Y(Z,A+1)}{Y(Z,A)} = n_n \left(\frac{2\pi\hbar^2}{m_u k_B T}\right)^{3/2} \left(\frac{A+1}{A}\right)^{3/2} \frac{G(Z,A+1)}{2G(Z,A)} \exp\left[\frac{S_n(Z,A+1)}{k_B T}\right]$$

Only even-even nuclei participate in the path so we can write:

$$\frac{Y(Z,A+2)}{Y(Z,A)} = n_n^2 \left(\frac{2\pi\hbar^2}{m_u k_B T}\right)^{3} \left(\frac{A+2}{A}\right)^{3/2} \frac{G(Z,A+2)}{4G(Z,A)} \exp\left[\frac{S_{2n}(Z,A+2)}{k_B T}\right]$$

The maximum of the abundance defines the r-process path:

$$S^0_{2n}(\mathrm{MeV}) = \frac{2T_9}{5.04}\left(34.075 - \log n_n + \frac{3}{2}\log T_9\right)$$

For $n_n = 5\times10^{21}\ \mathrm{cm}^{-3}$ and $T = 1.3$ GK corresponds at $S^0_{2n} = 6.46$ MeV, $S^0_n = S^0_{2n}/2 = 3.23$ MeV,

r process path

Path depends on nuclear masses

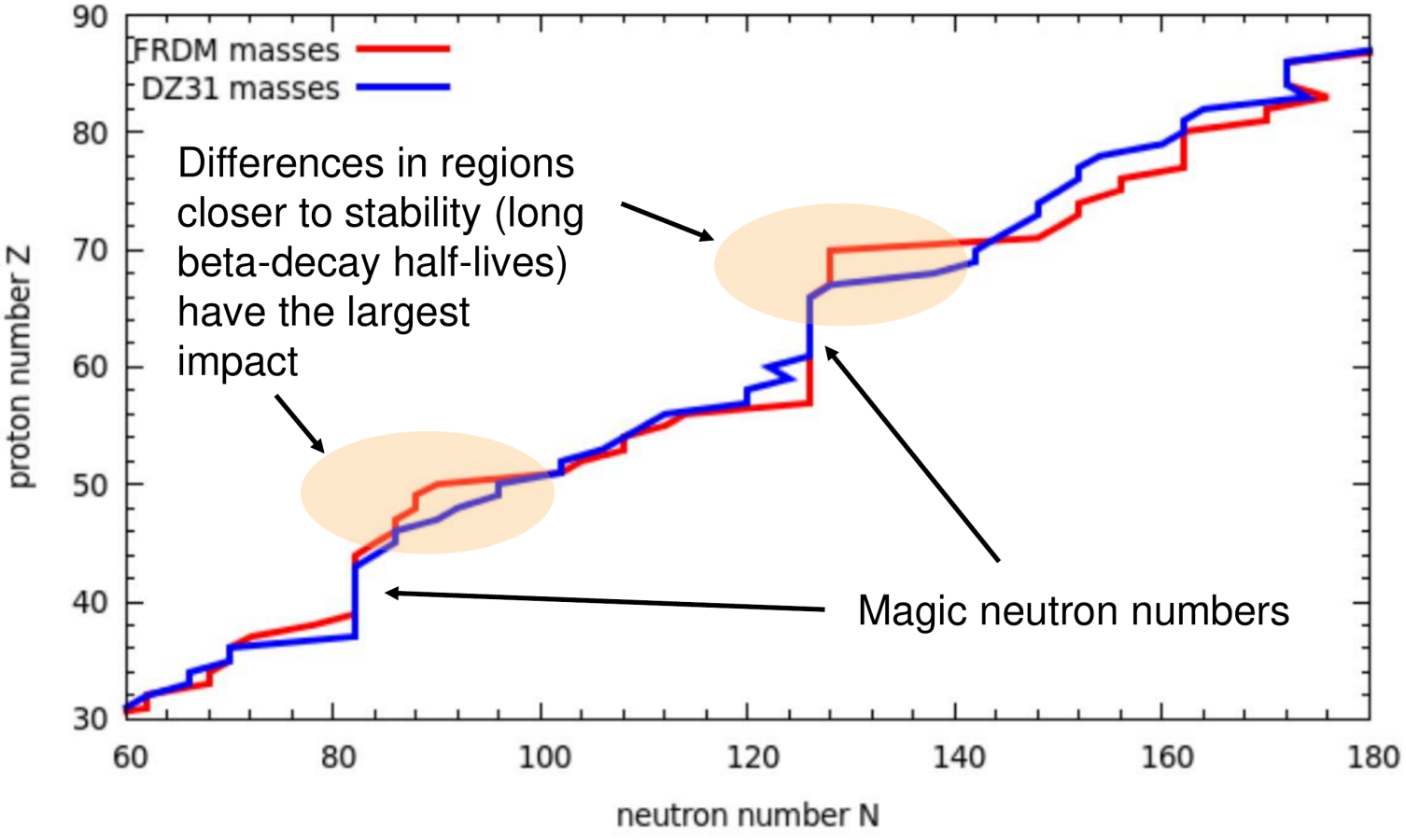

Two-neutron separation energies

r-process path defined by those nuclei with: $S_{2n}(Z,A) \gtrsim S^0_{2n}$

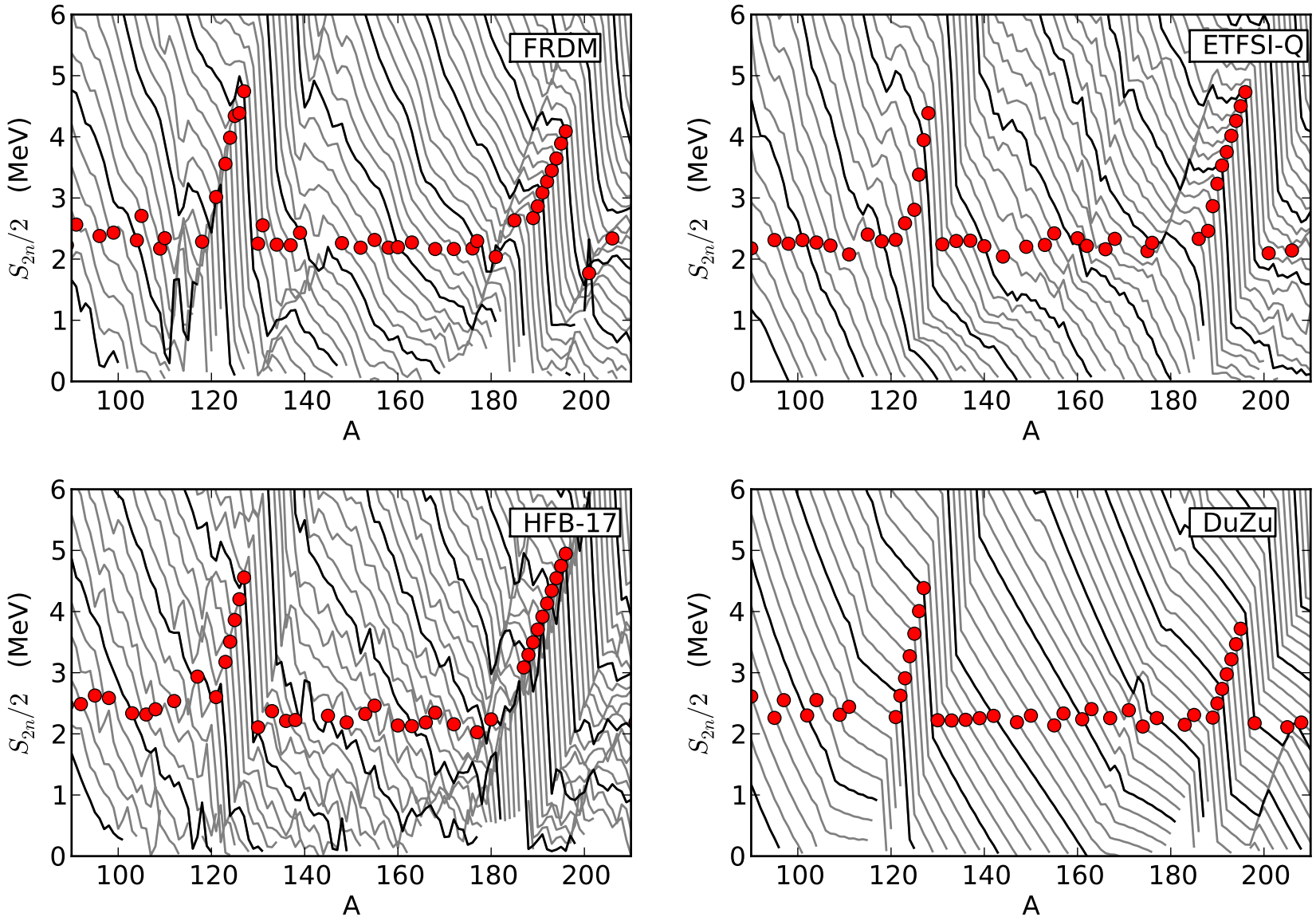

A. Arcones, GMP, Phys. Rev. C **83**, 045809 (2011)

path dependence on time

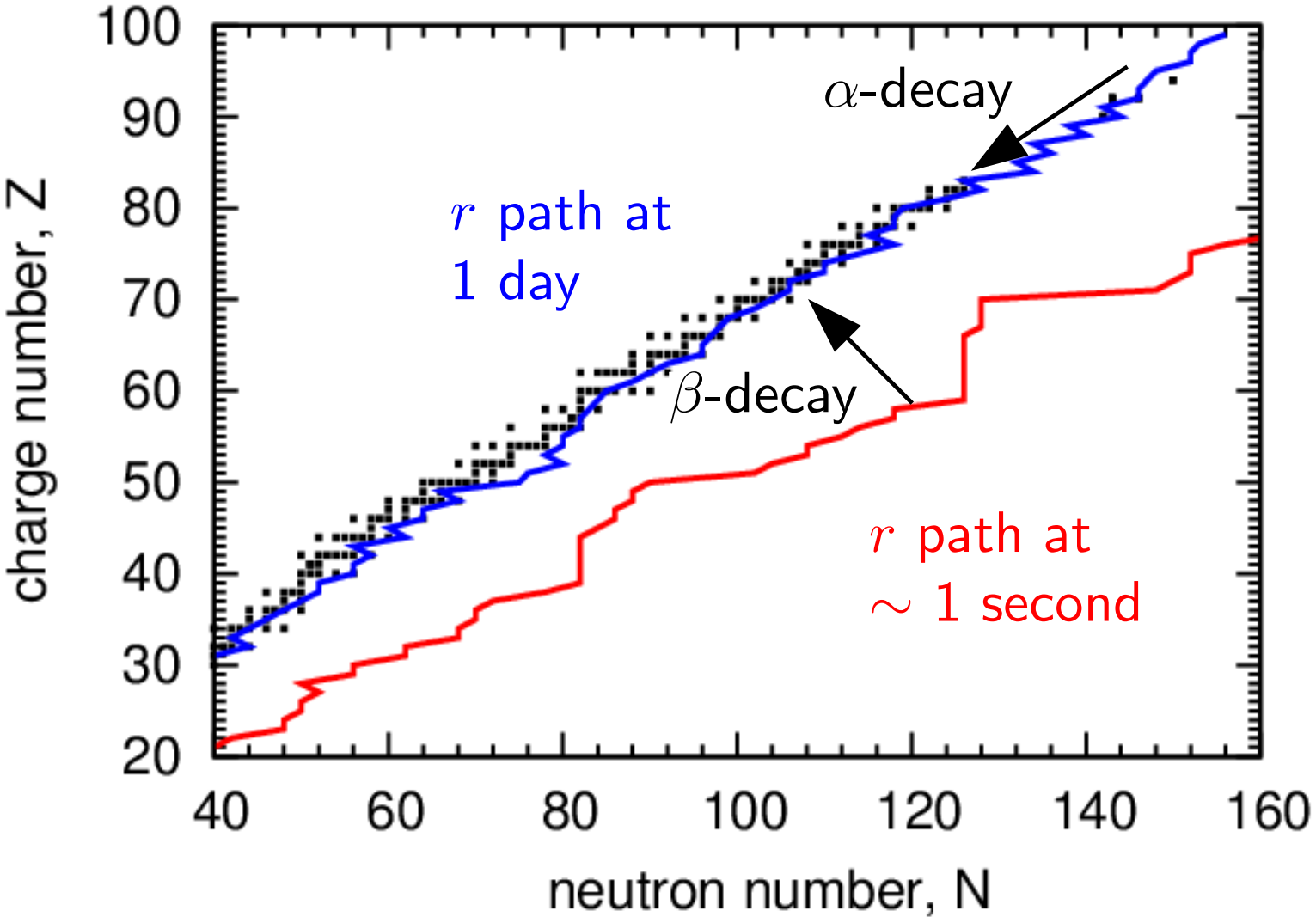

Beta-flow equilibrium

Assuming $(n,\gamma) \rightleftarrows (\gamma,n)$ equilibrium, it is sufficient to compute the time evolution of the total abundance for an isotopic chain

$$Y(Z) = \sum_A Y(Z,A)$$

The differential equation reduces to

$$\frac{dY(Z)}{dt} = \lambda_\beta(Z-1)Y(Z-1) - \lambda_\beta(Z)Y(Z)$$

with

$$\lambda_\beta(Z) = \frac{1}{Y(Z)} \sum_A \lambda_\beta(Z,A)Y(Z,A)$$

Only beta-decays are necessary to determine the evolution. If the duration of the r process is larger than the beta-decay lifetimes an equilibrium is reaches denotes as steady β flow equilibrium that satisfies for each Z value

$$\lambda_\beta(Z-1)Y(Z-1) = \lambda_\beta(Z)Y(Z), \quad \text{i.e. } Y(Z) \propto \tau_\beta(Z)$$

Abundances vs beta lifetimes

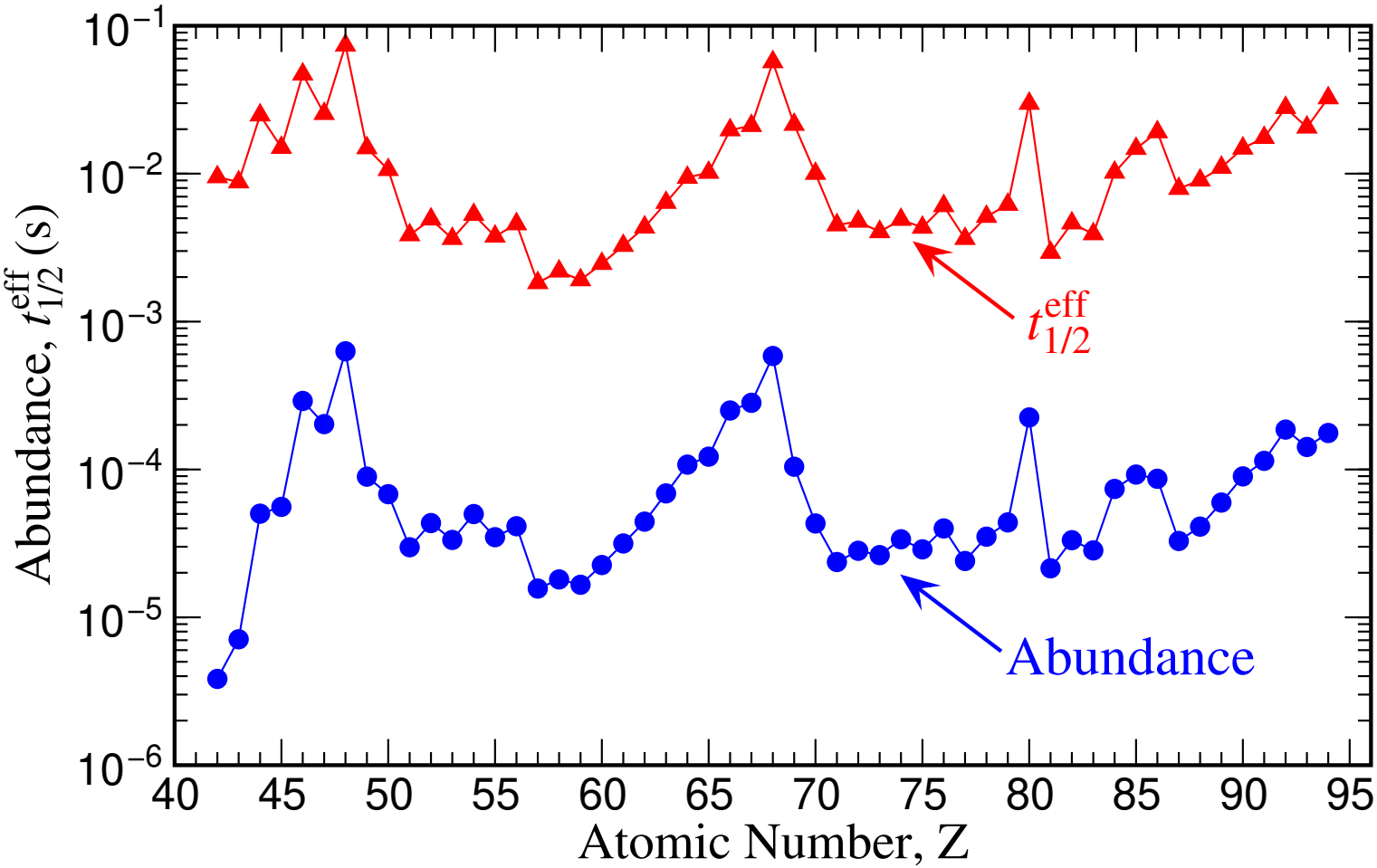

$$\frac{1}{t_{1/2}^{\mathrm{eff}}(Z)} = \frac{1}{\sum_N Y(Z,N)} \sum_N \frac{Y(Z,N)}{t_{1/2}(Z,N)}$$

Nuclear masses

Exact impact of nuclear masses depends on the particular astrophysical conditions. For neutron-rich conditions, 3rd peak abundances are sensitive to the particular mass model used.

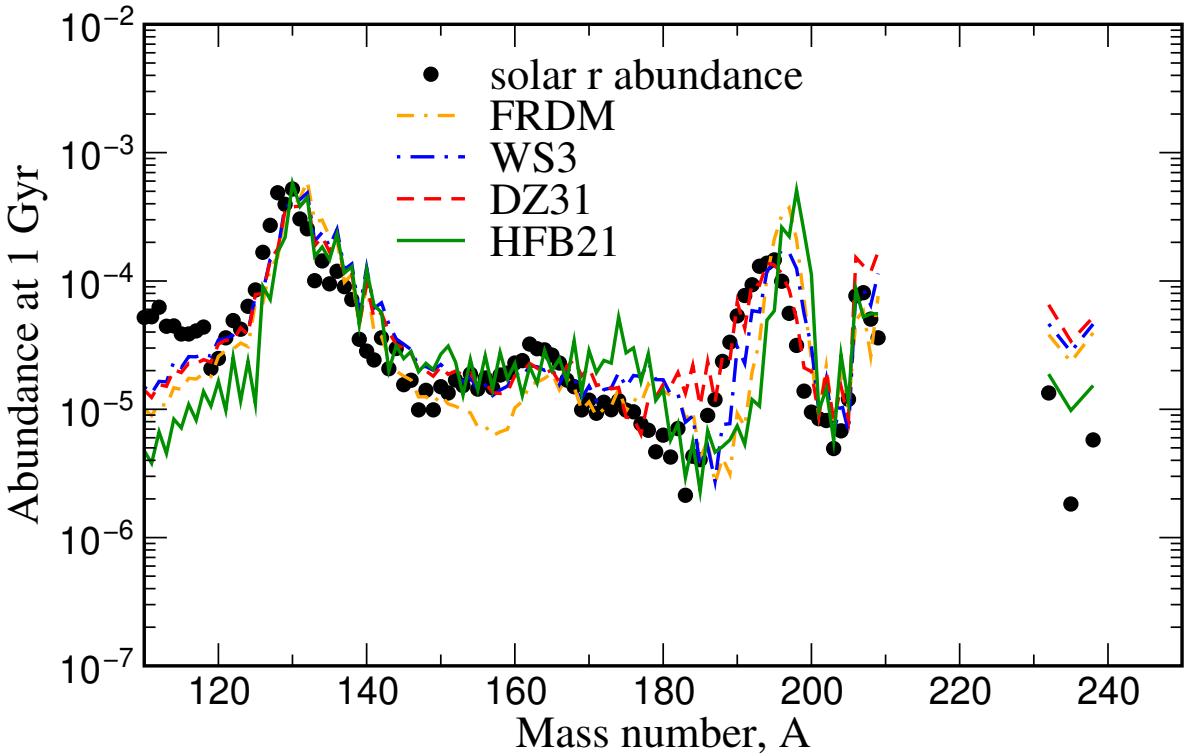

Correlation between the magnitude of the 3rd peak abundances and the production of actinides.

Beta-decays

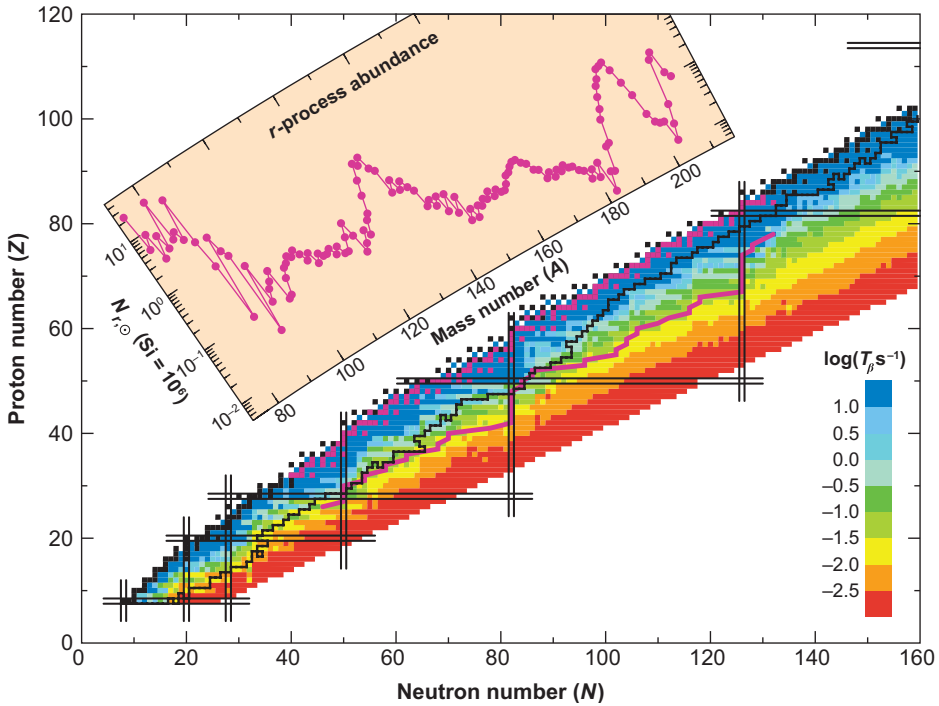

- Beta decays determine the speed at which light elements are converted into heavy elements.
- Material tends to accumulate on nuclei with longest beta-decay half-lives. Around magic neutron numbers r-process path moves closer to stability producing the observed r-process peaks.
- Relatively few half-lives are known experimentally. Global theoretical calculations are necessary.

Nuclear physics input: beta-decay half-lives

- Beta-decay half-lives determine the speed at which heavy elements are build starting from light ones
- N~126 Half-lives have a strong impact on the position of the A ~ 195 peak

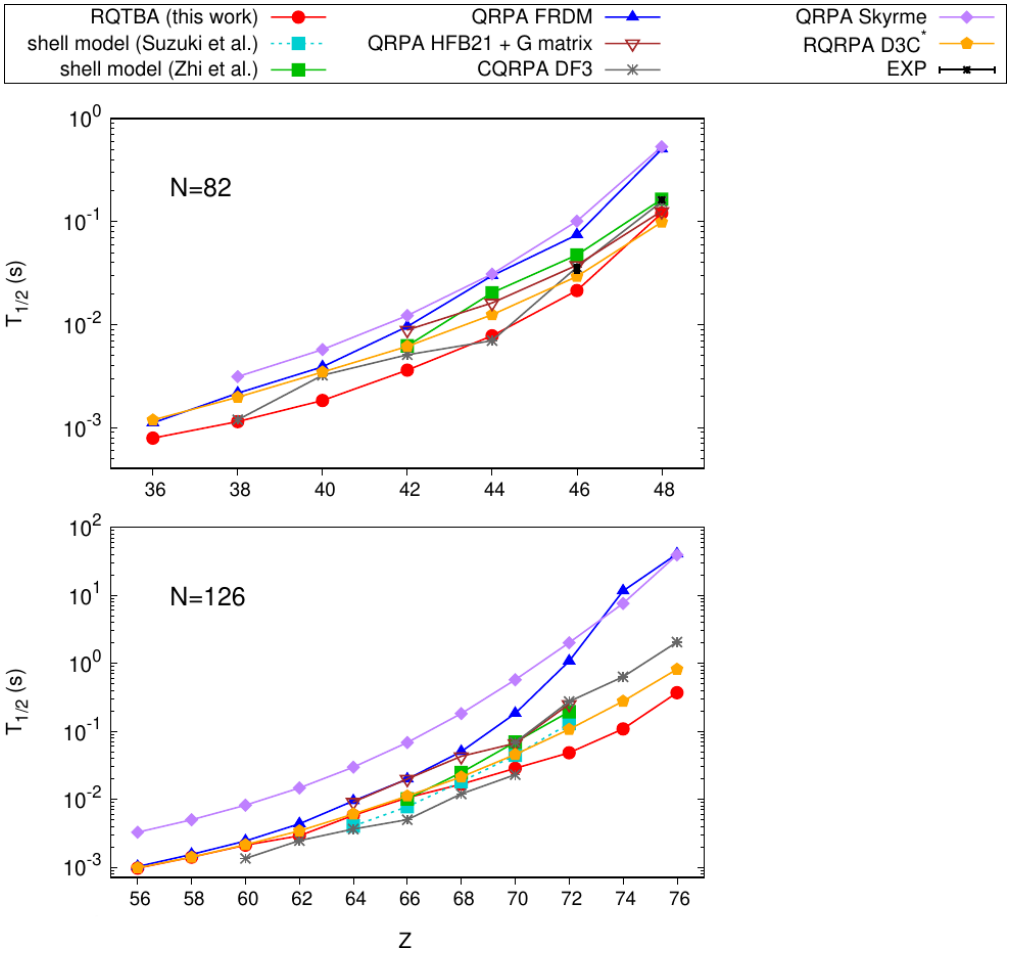

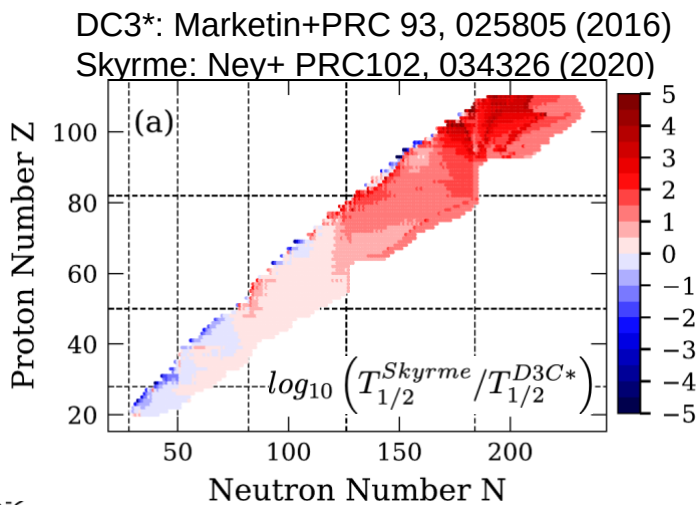

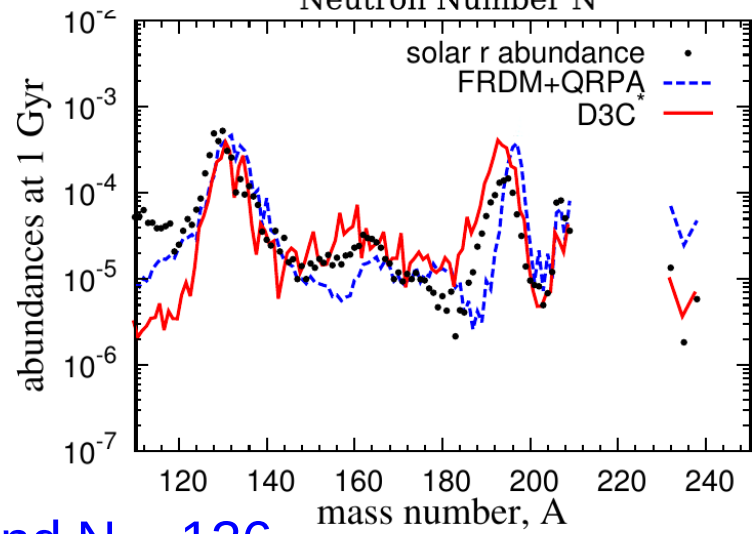

C. Robin, GMP, in preparation

Need data for beta decay half-lives around N ~ 126

Fission

- Fission determines heavier nuclei produced by the r-process
- Important for energy production electromagnetic transients
- Challenge: extrapolate known data to neutron-rich nuclei

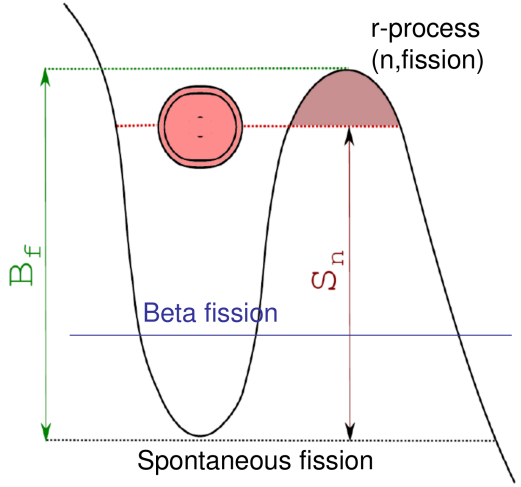

Fission is described as a tunneling process through a barrier. neutron-induced fission is the dominating process for nuclei at which $S_n \approx B_f$.

Giuliani, GMP, Robledo, Phys. Rev. C 97, 034323 (2018)

What is the role of fission in the r-process nucleosynthesis?

Giuliani et al PRC 97, 034323 (2018)

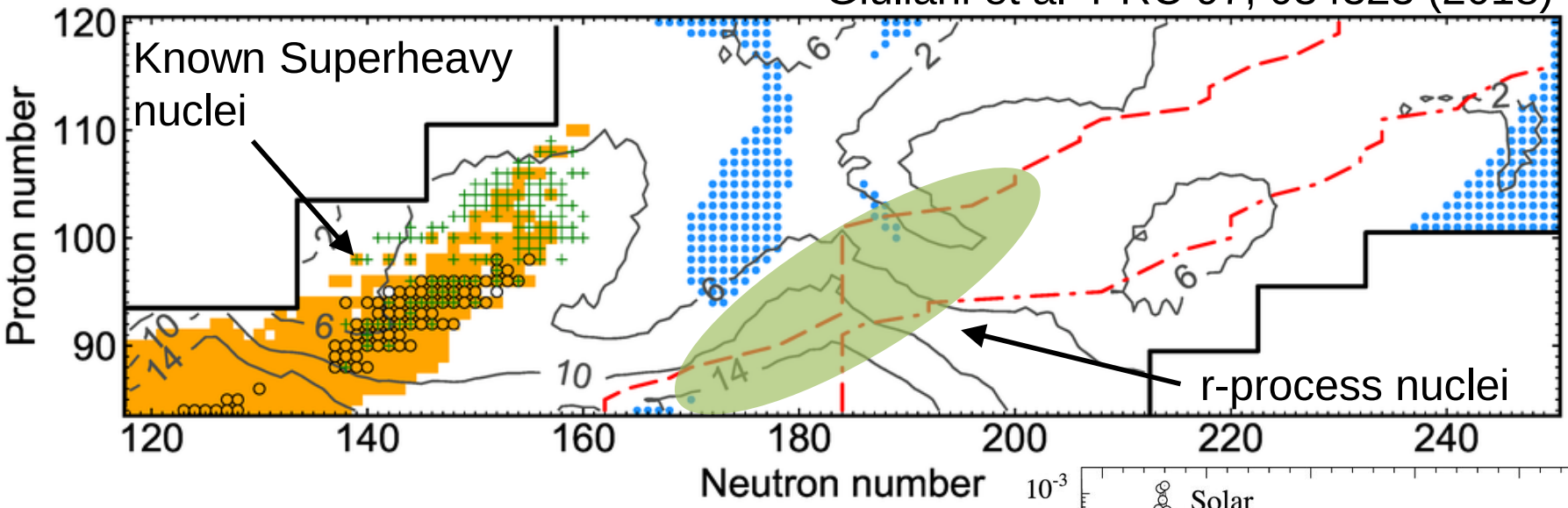

Current r-process modes predict substantial production of nuclei around A~ 280 (Z ~ 96 N ~ 184)

However during their decay to beta stability they fission on timescales of seconds to hours.

Can we find signatures of (super)heavy nuclei in kilonova light curves?

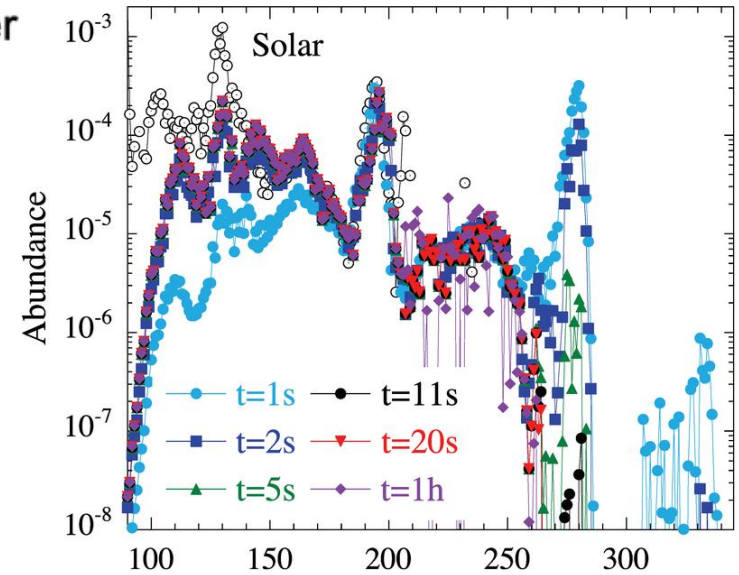

Goriely and GMP NPA **944**, 158 (2015).

Superheavy region: mine-field due to low fission barriers

- During the r-process operation mainly (n,fiss) limits the production of superheavy nuclei
- After freeze-out a competition between beta-delayed, spontaneous and neutron induced fission.
- Similar results for different barriers sets

Giuliani, GMP, Robledo, PRC 97, 034323 (2018).

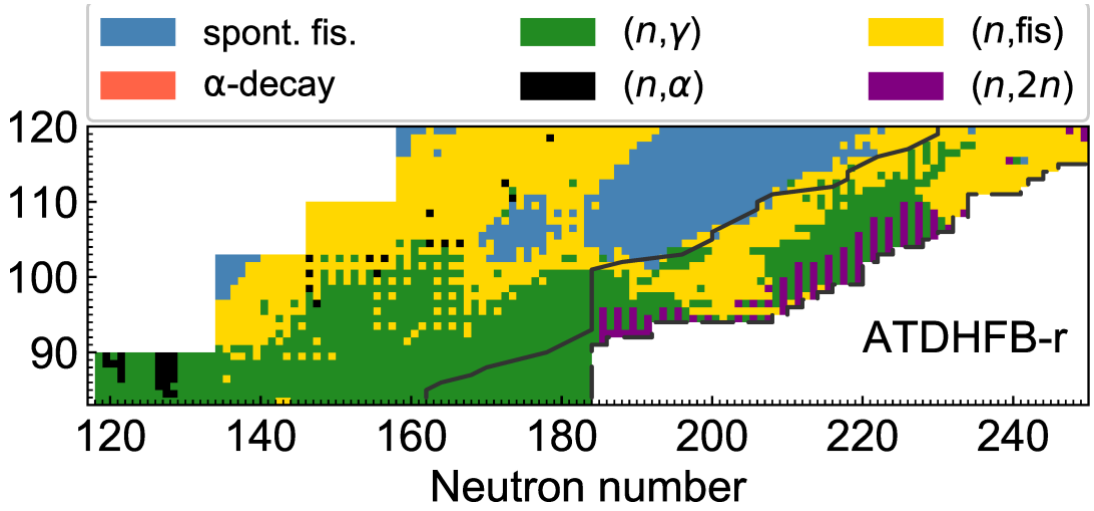

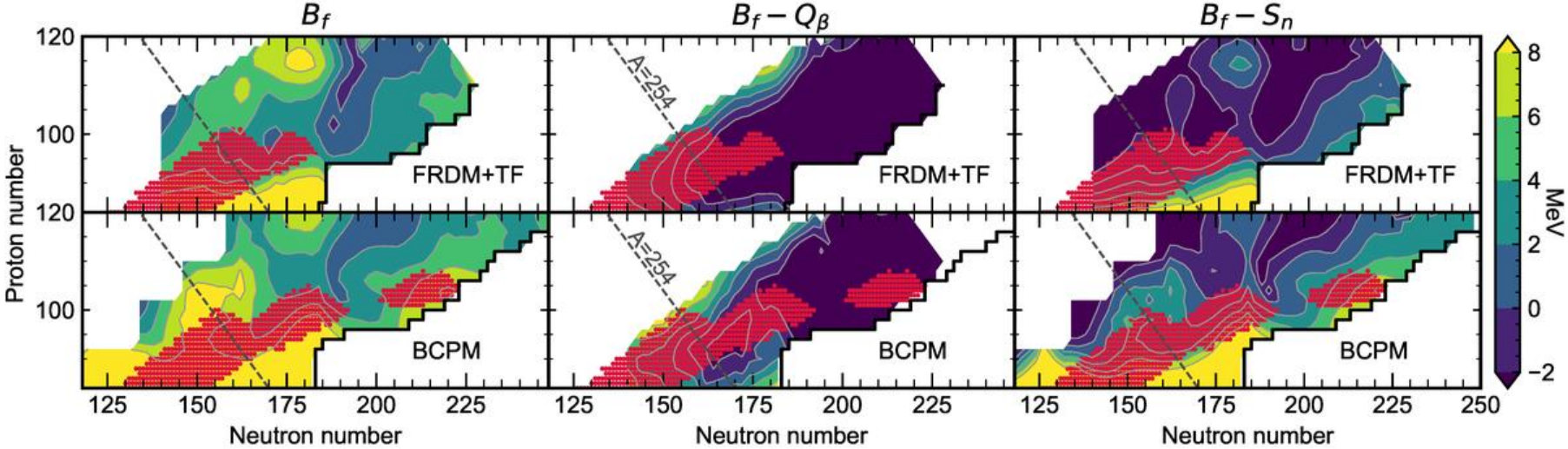

Giuliani, GMP, Wu, Robledo, PRC 102, 045804 (2020)

Fission yields

The fission fragment distribution impacts the final abundance pattern.

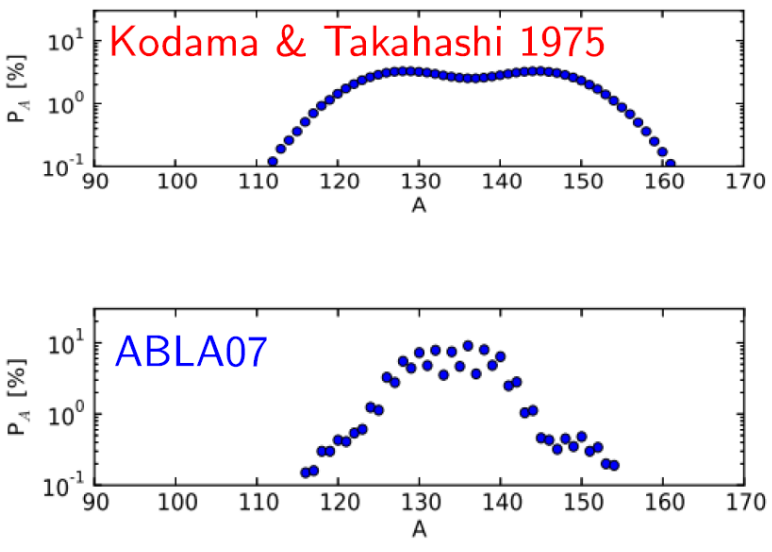

[From Eichler et al, ApJ 808, 30 (2015)]

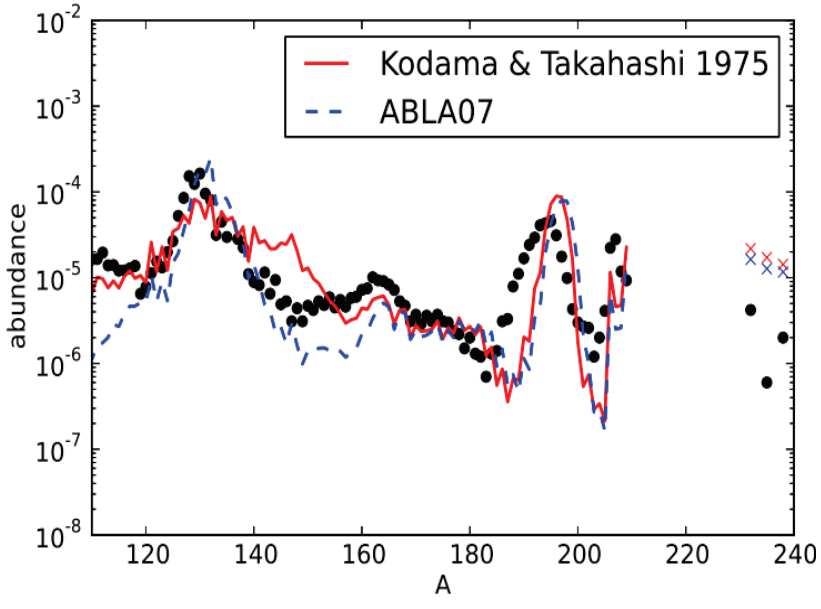

Multiphysics picture of r-process

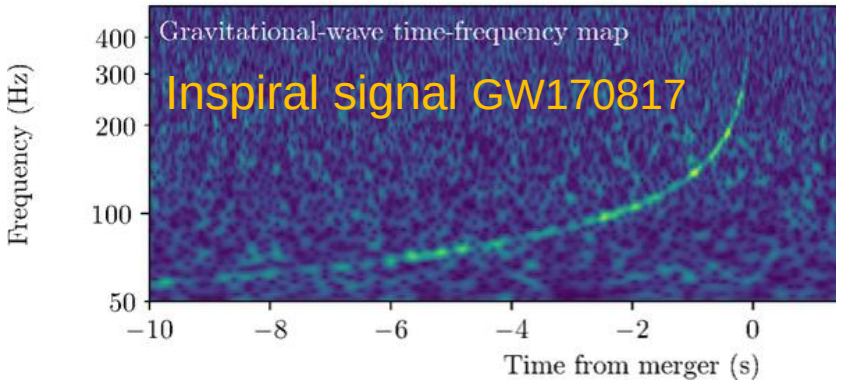

r-process: nucleosynthesis and electromagnetic transient

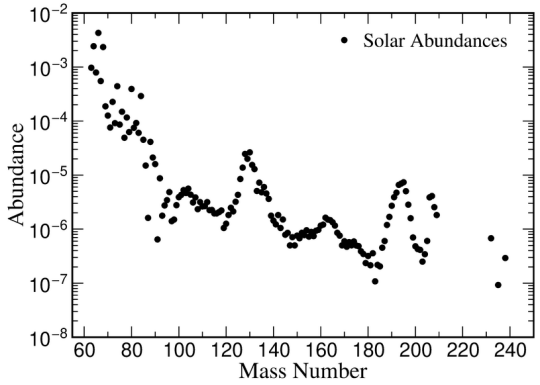

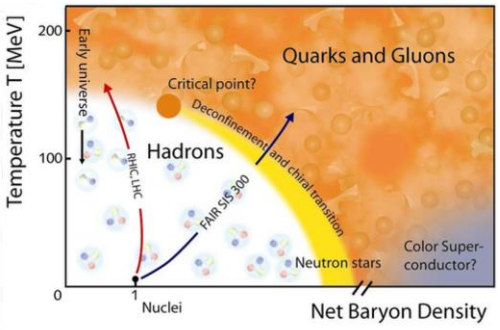

Phase diagram QCD matter

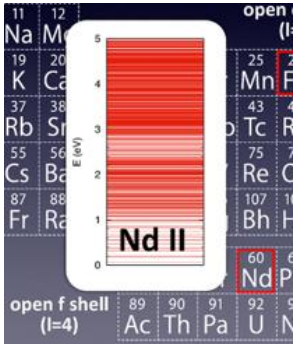

Atomic opacities

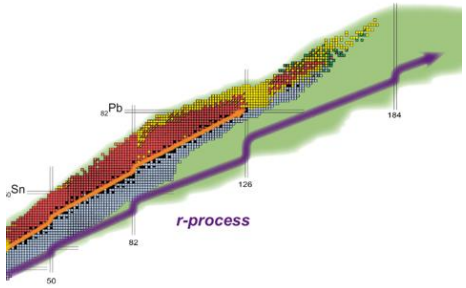

Neutron-rich exotic nuclei

Nucleosynthesis dependence on Y_e

Nucleosynthesis mainly sensitive to proton-to-nucleon ratio, $Y_e = n_p/(n_n + n_p)$

$\nu_e + n \rightleftarrows p + e^-$ vs $\bar{\nu}_e + p \rightleftarrows n + e^+$

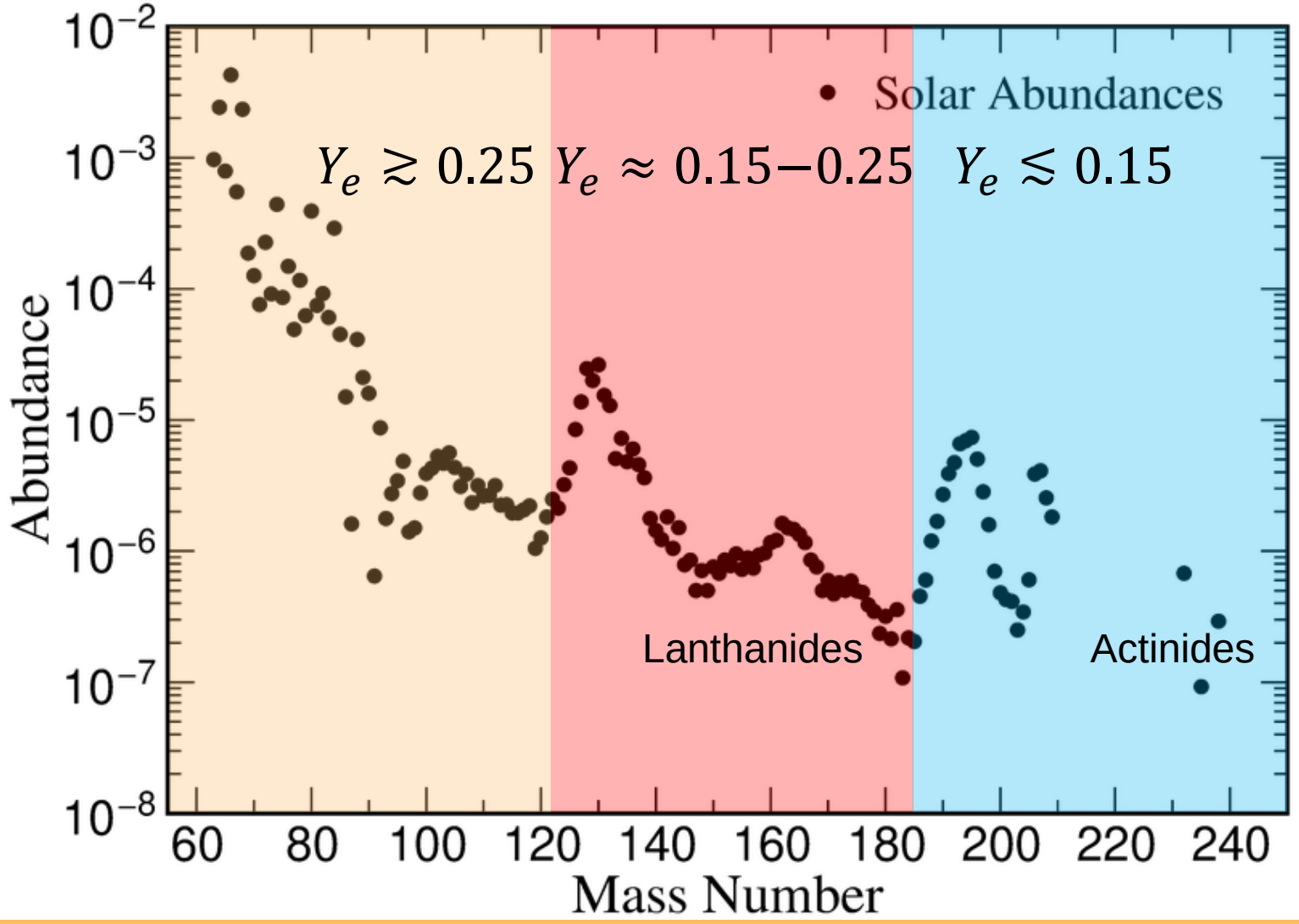

Ejecta in neutron star mergers

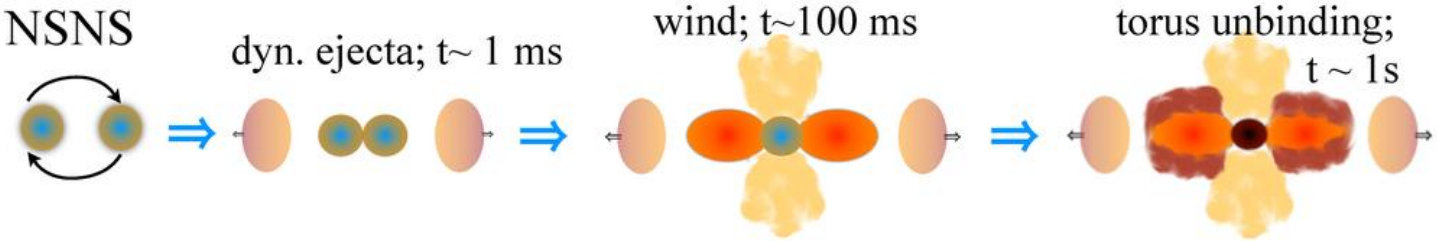

Two main sources of ejecta:

- Dynamical ejecta ($M \lesssim 0.01\ \mathrm{M}_{\odot}$)
- Disk (secular) ejecta ($M \lesssim 0.1\ \mathrm{M}_{\odot}$)

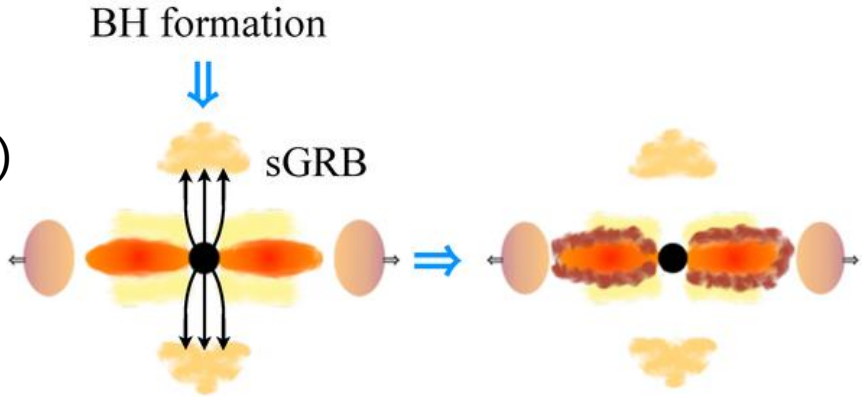

Ejecta properties depend on central remnant (neutron star or black hole). It determines the strength of neutrino emission

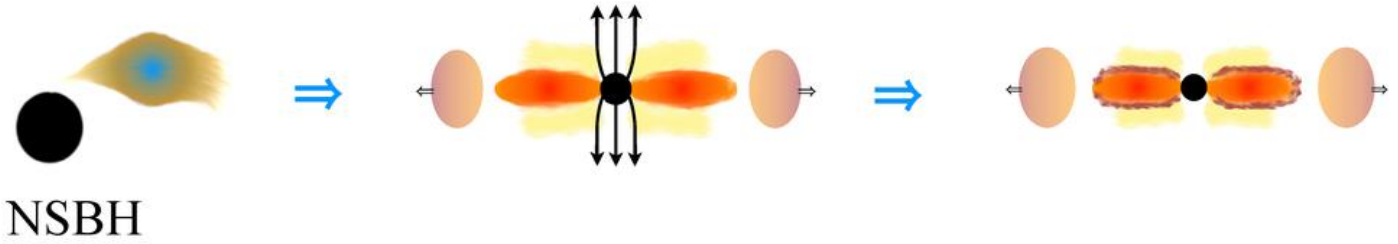

S. Rosswog, et al, Class. Quantum Gravity 34, 104001 (2017).

Mass ejection neutron star merger

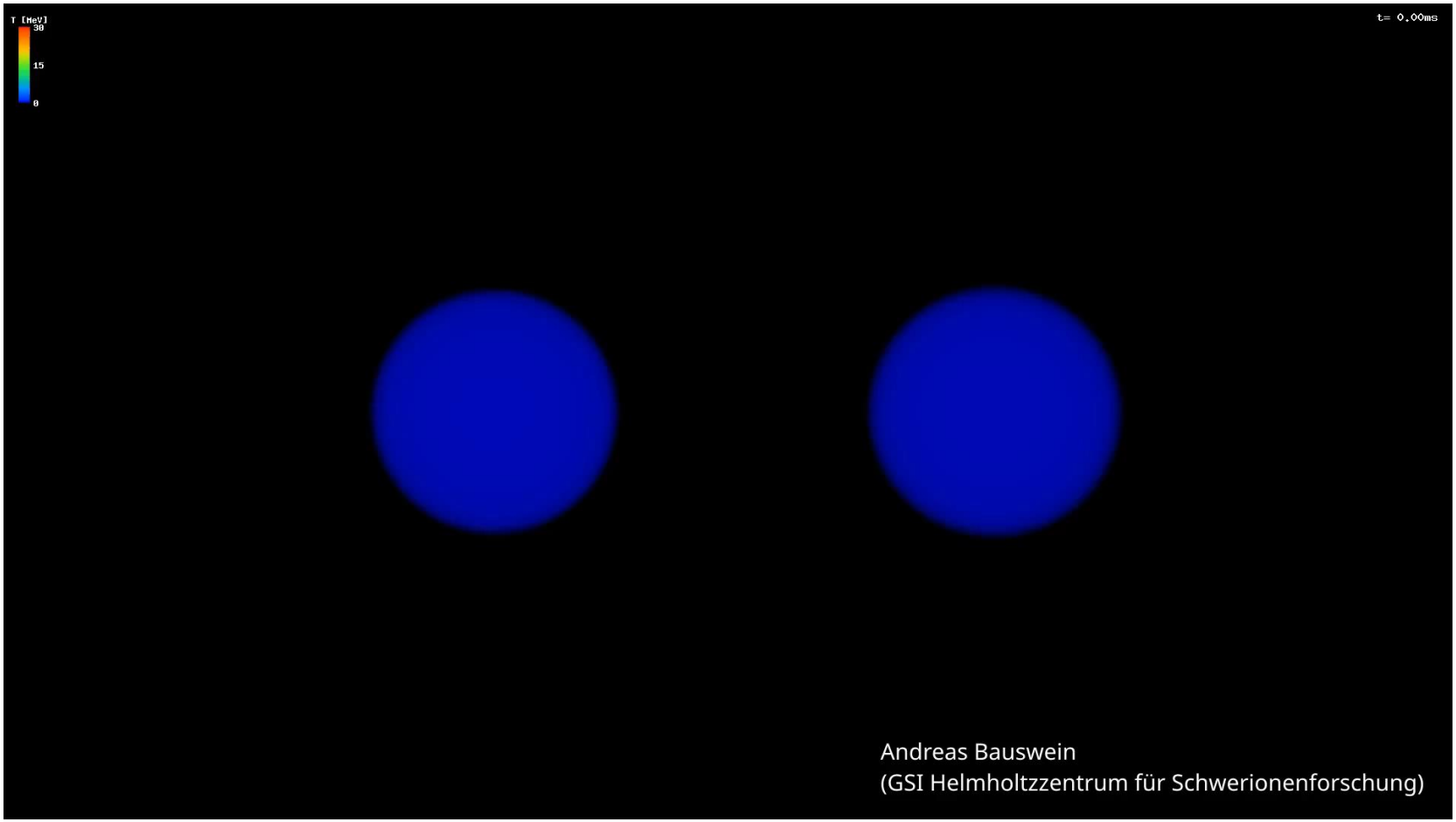

Two sources of ejecta:

- Dynamical during the early phases of the merger ($M \lesssim 0.01\ M_{\odot}$)
- Accretion disc on longer timescales (($M \lesssim 0.05\ M_{\odot}$)

Ejecta properties depend on central remnant (neutron star or black hole).
Determines the strength of neutrino emission

Post merger structure

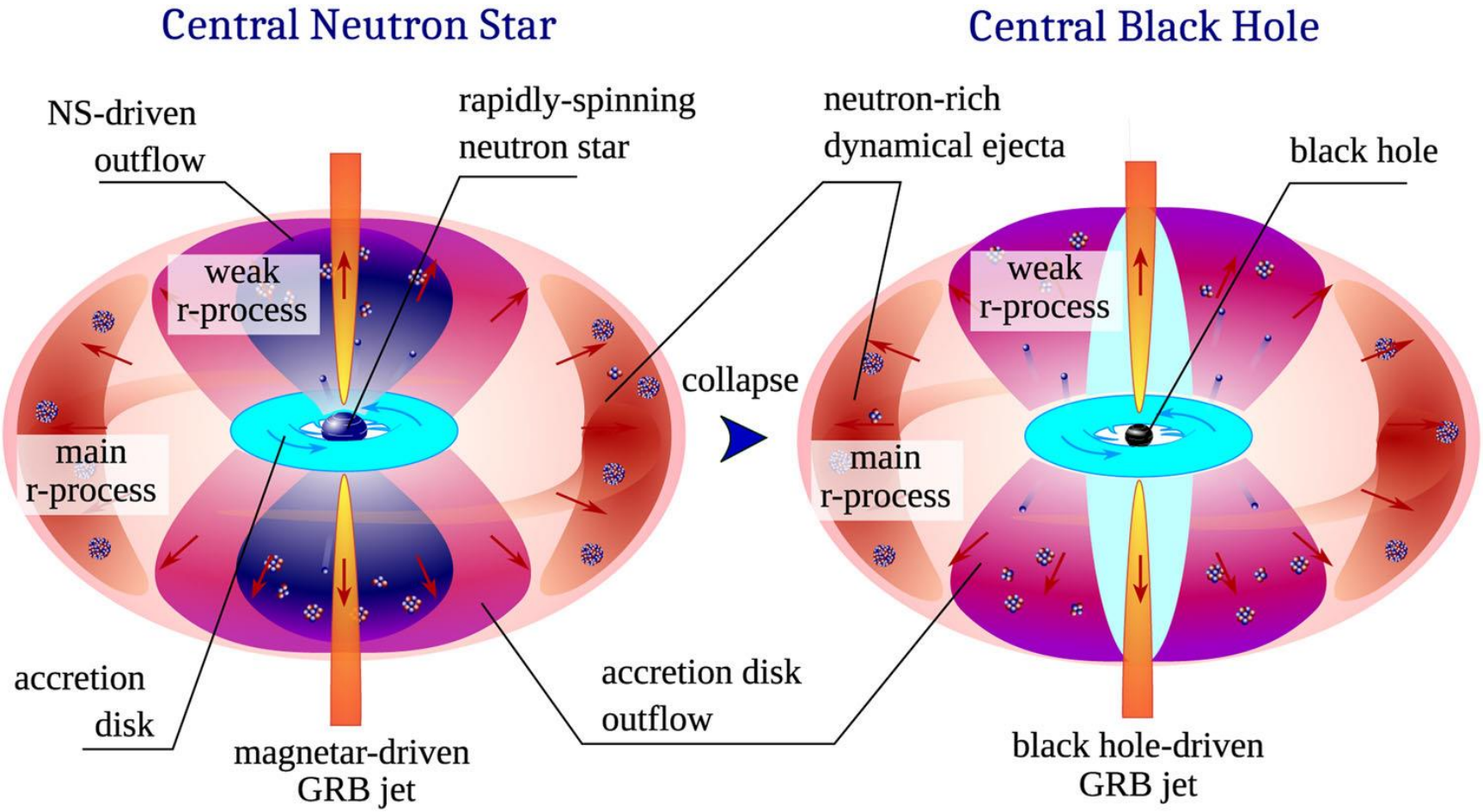

S. Rosswog and O. Korobkin, Annalen Der Physik **2022**, 2200306 (2022).

Dynamical ejecta (simulations)

- Initially dynamical ejecta was assumed to be very neutron rich ($Y_e \lesssim 0.1$).
- Starting with the work of Wanajo et al 2014, several studies have shown that weak processes modify the neutron-to-proton ratio
- Largest impact in the polar regions

SPH Simulation **Vimal Vijayan**
Neutrino transport: ILEAS
1.35 – 1.35 $M_\odot$, SFHo EoS

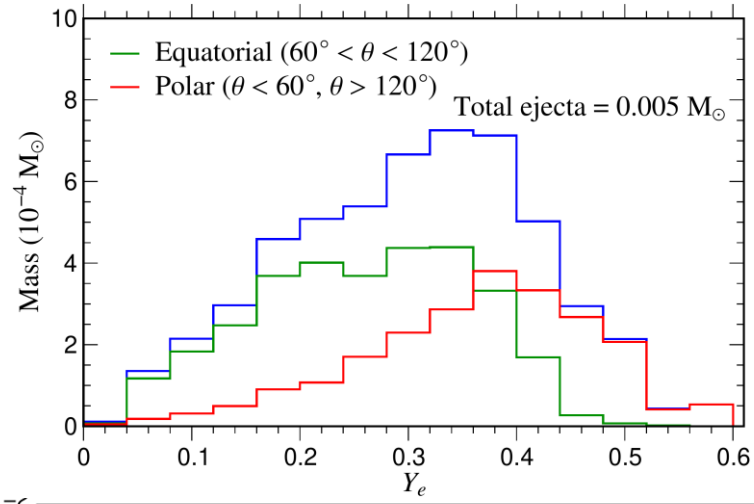

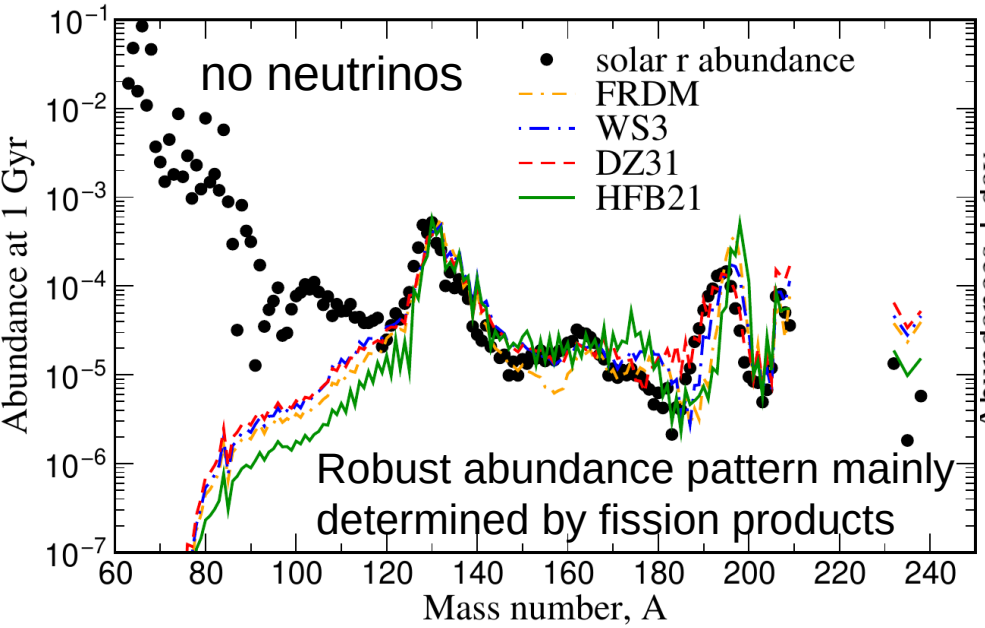

Mendoza-Temis, et al, PRC 92, 055805 (2015)

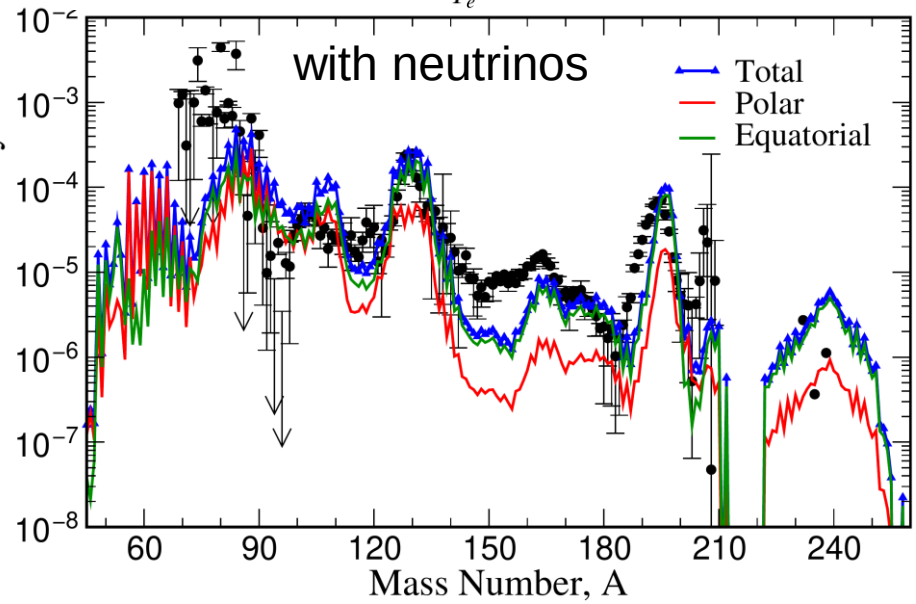

Collins et al, arXiv::2209.05246
See also: Kullman+ 2022, Just+ 2022

Elemental abundances

- At kilonova timescales (days) elemental abundances have not yet converged to final abundances

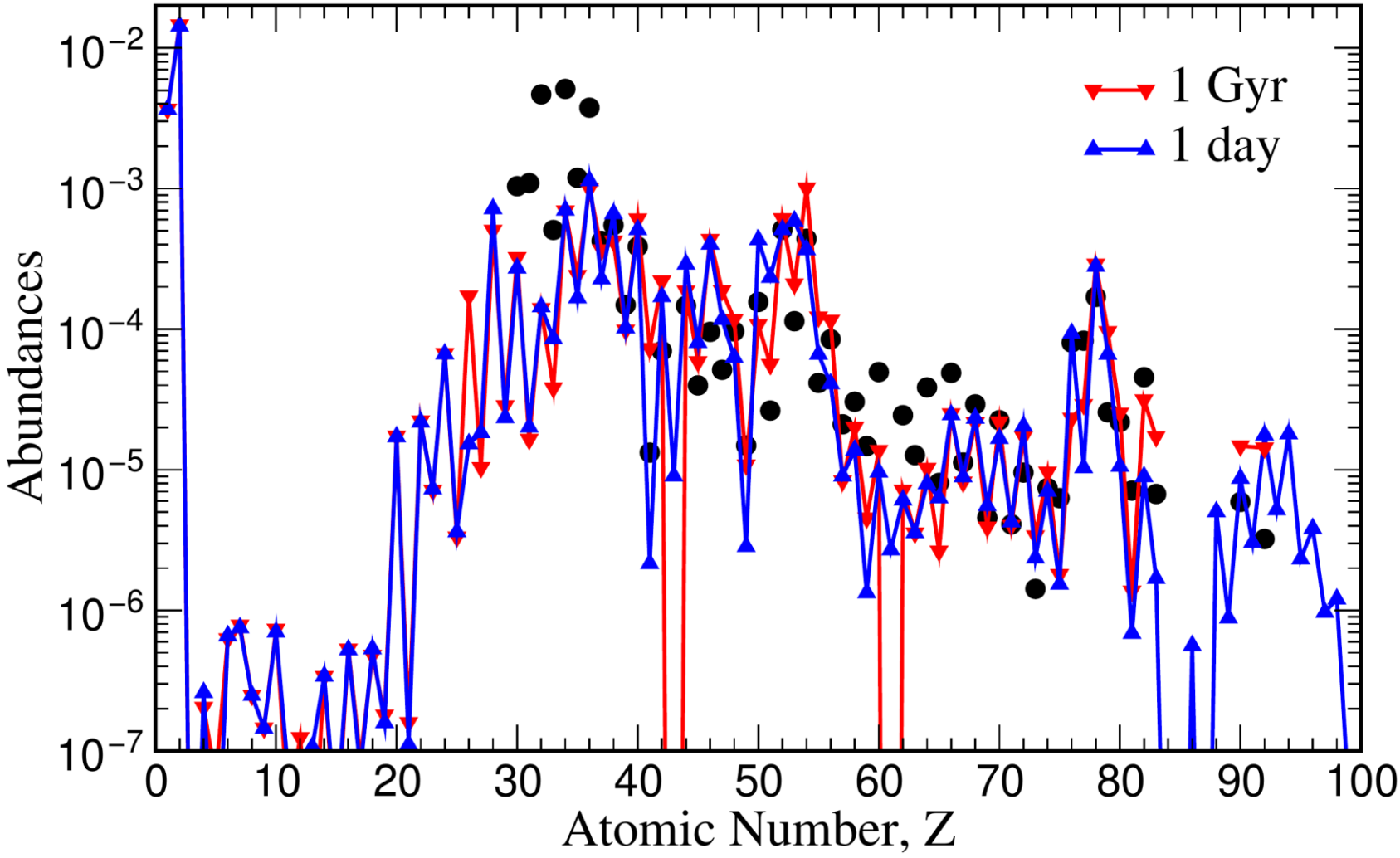

Disk (secular) ejecta

After the merger, a hyper massive neutron star is formed that can be temporarily stable before collapsing to a black hole

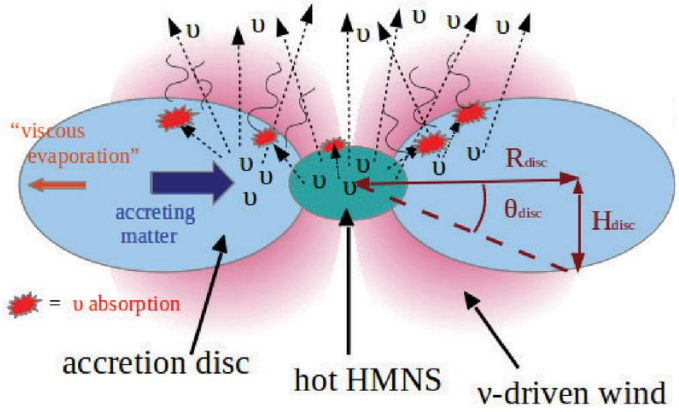

Large neutrino fluxes mainly in polar region decrease neutron-to-proton ratio by reactions

$$\nu_e + n \rightarrow p + e^-$$
$$\bar{\nu}_e + p \rightarrow n + e^+$$

Martin, et al, ApJ 813, 2 (2015)

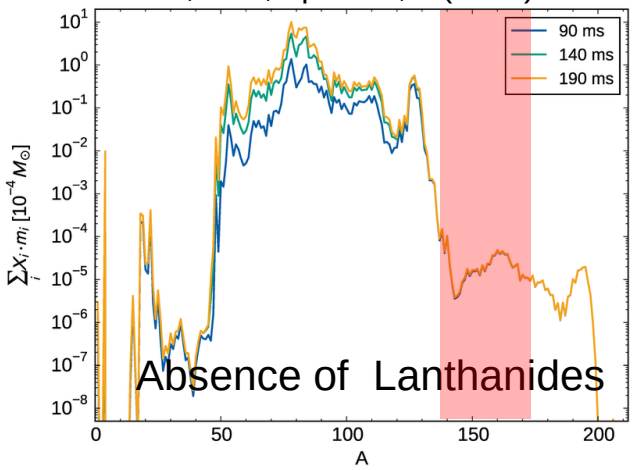

Once neutron star collapses to a black hole neutrinos emission ceases. Larger neutron-to-proton ratio

Wu et al, MNRAS 463, 2323 (2016)

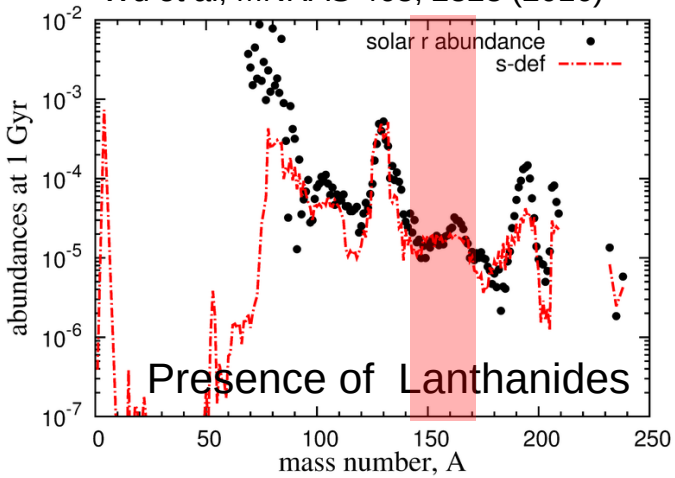

see also Lippuner et al, MNRAS 472 904 (2017)

See also Just et al, MNRAS **448**, 541 (2015), Siegel and Metzger PRL **119**, 231102 (2017).

Long term merger simulations

First long-term simulations with neutron star lifetimes 0.1-1 s and describe all components of the ejecta*: d*ynamical, NS-remnant ejecta, and final viscous ejecta from BH torus.

Just et al, arXiv:2302.10928

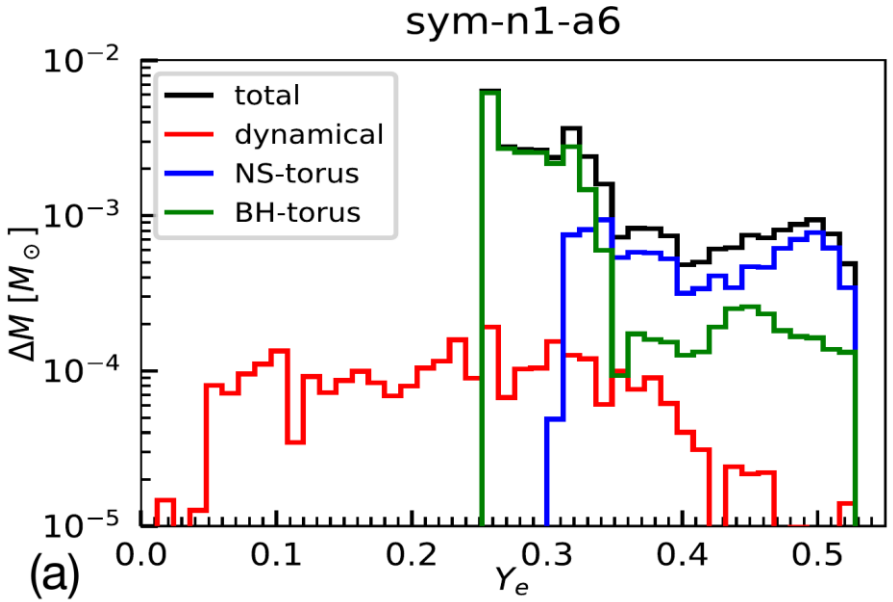

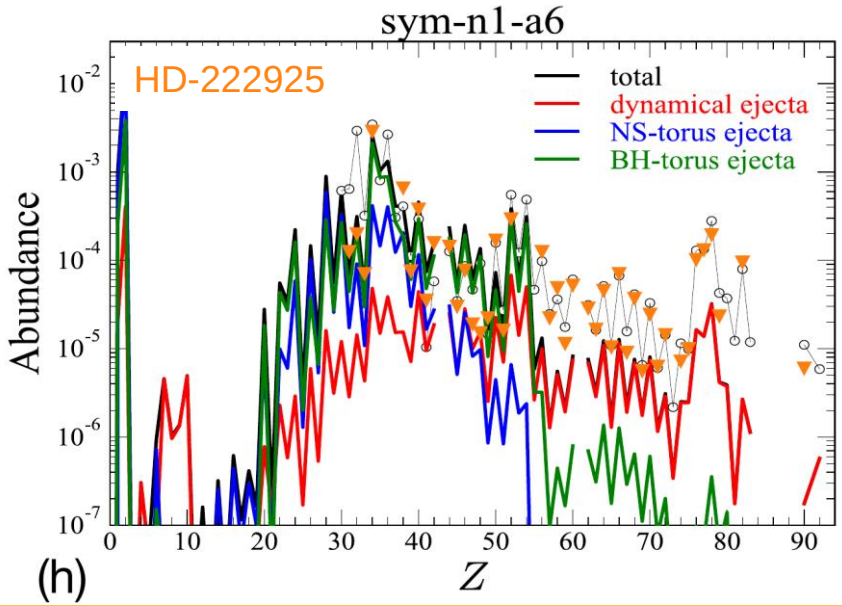

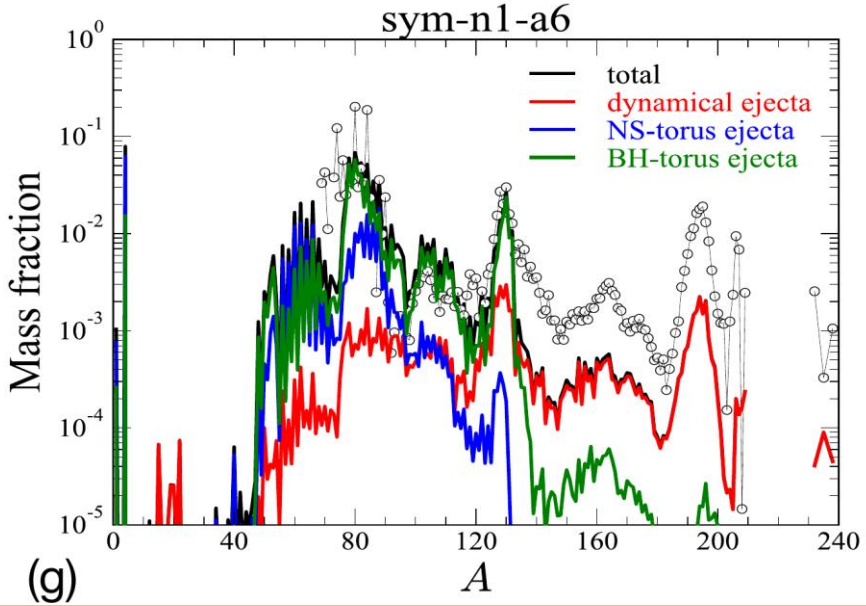

Electromagnetic signatures of nucleosynthesis

Supernova light curves follow the decay of ^{56}Ni ($t_{1/2} = 6$ d) and later ^{56}Co ($t_{1/2} = 77$ d)

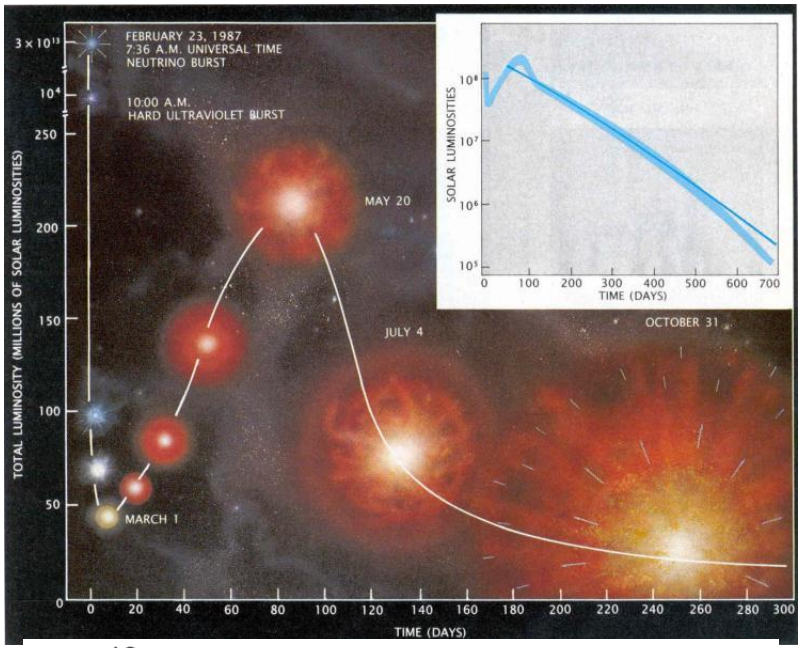

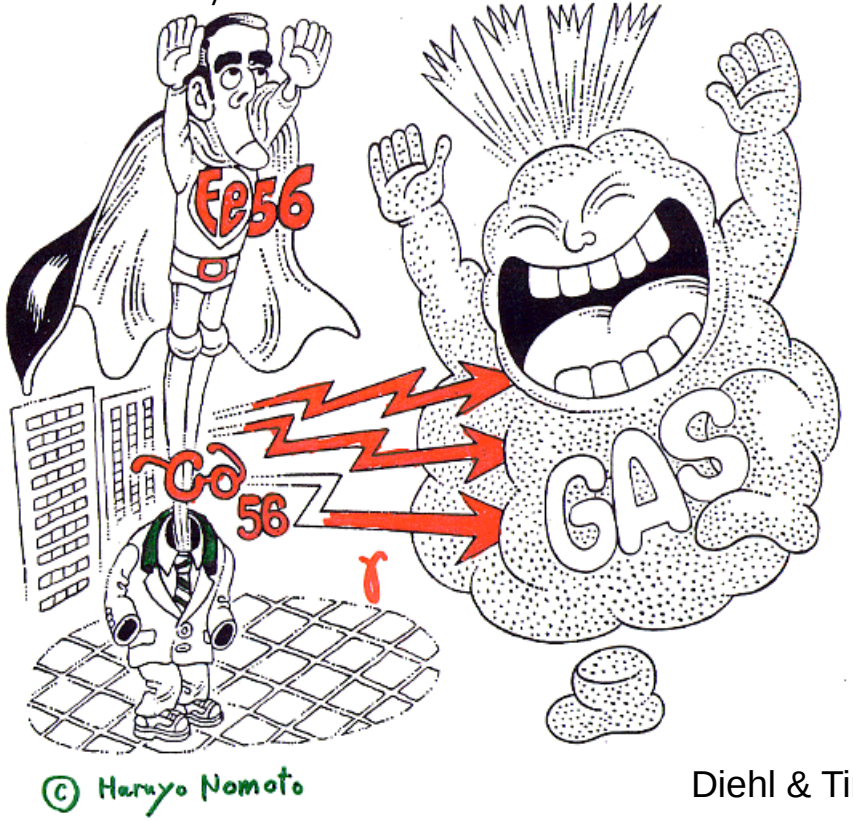

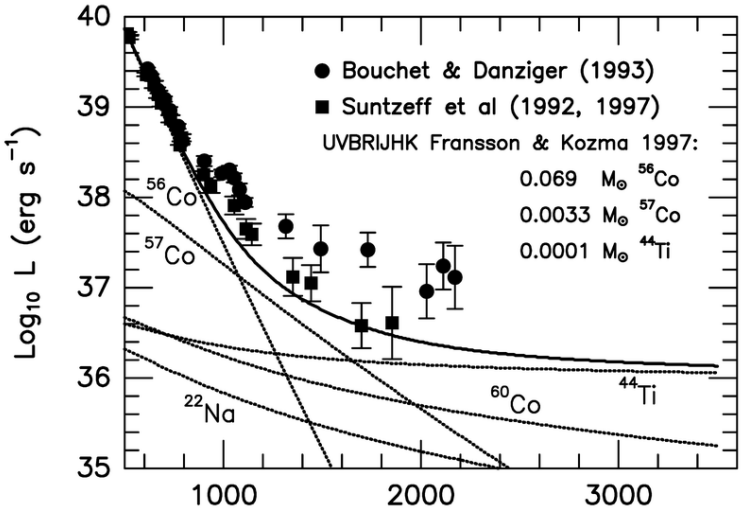

Diehl & Timmes, PASP 110, 637 (1998)

Electromagnetic transient from r process

At early times (days), the decay of r process products produces energy following a power law $\dot{\varepsilon} \sim t^{-1.3}$ (Way & Wigner 1948, Metzger et al 2010). Many nuclei decaying at the same time heating up the ejecta

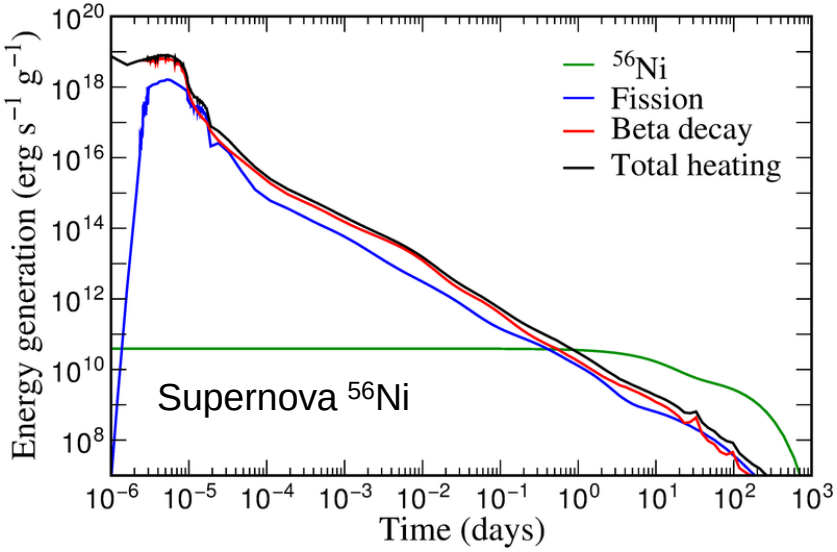

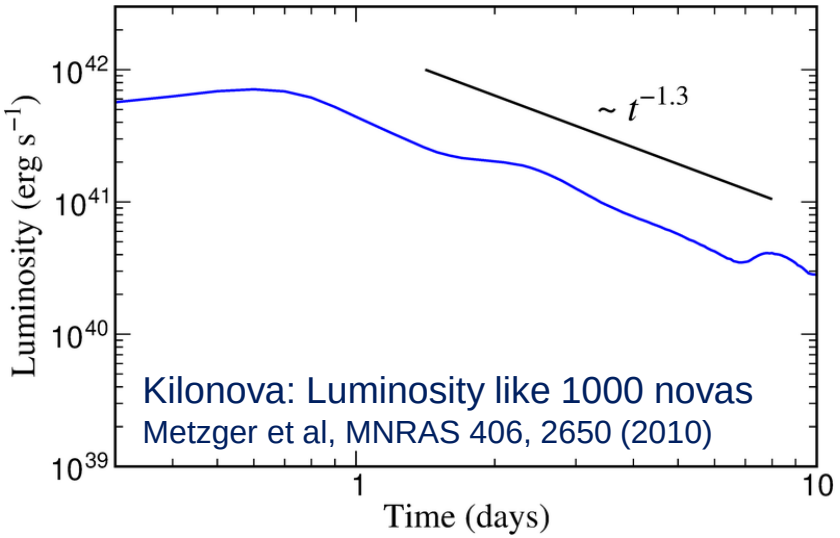

We expect an electromagnetic transient with properties depending:

- Energy production rate
- Efficiency energy is absorbed by the gas (thermalization efficiency)
- Opacity of the gas (depends on composition, presence of Lanthanides/Actinides)

Ejected mass and velocity can be inferred from observations

Impact of opacity

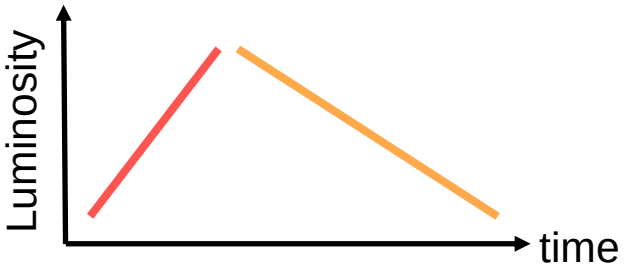

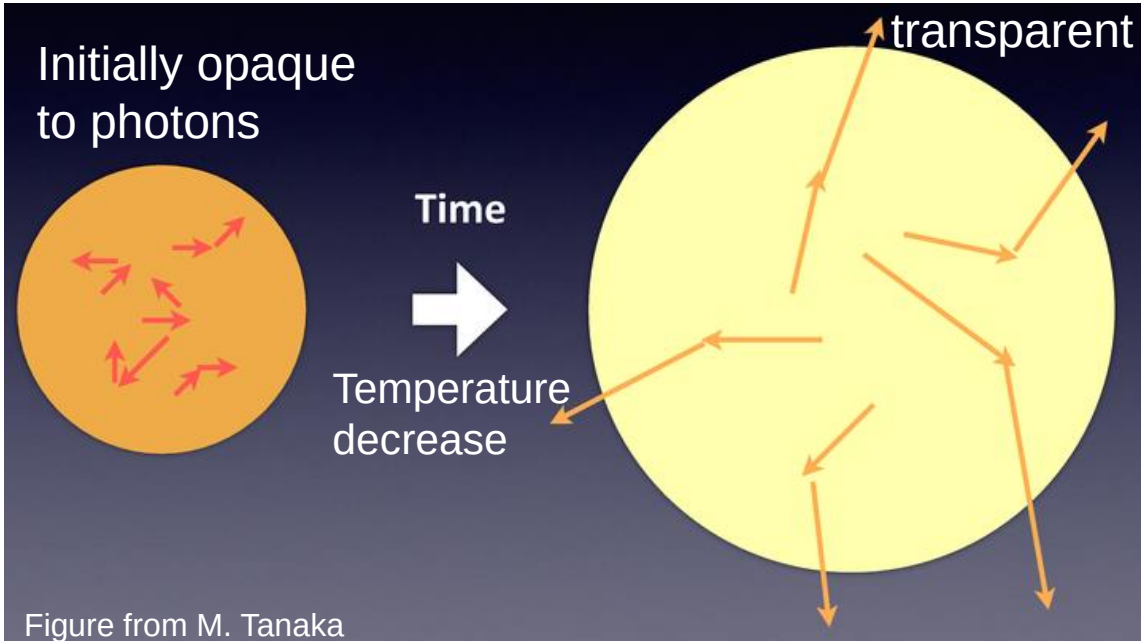

The transition from an opaque to transparent regime depends on the interaction probability of the photons (opacity). Depends on the structure of the atoms (presence of Lanthanides/Actinides)

Low opacity: early emission from hot material at short wavelengths (blue)

High opacity: late emission from colder material at longer wavelengths (red)

Simple Kilonova model

Light curve is expected to peak when photon diffusion time is comparable to elapsed time (Metzger et al 2010, Kasen et al 2017)

$$t_{\rm diff} = \frac{\rho \kappa R^2}{3\,c}, \qquad \rho = \frac{M}{4\pi R^3/3}, \qquad R = vt$$

$$t_{\rm peak} \approx \left(\frac{\kappa M}{4\pi c v}\right)^{\frac{1}{2}} \approx 1.5\ {\rm days} \left(\frac{M}{0.01\,M_\odot}\right)^{\frac{1}{2}} \left(\frac{v}{0.01c}\right)^{-\frac{1}{2}} \left(\frac{\kappa}{1\ {\rm cm^2\ g^{-1}}}\right)^{\frac{1}{2}}$$

The Luminosity is $L(t) \approx M\,\dot{\varepsilon}(t)$, $\dot{\varepsilon}(t) \approx 10^{10} \left(\frac{t}{1\ {\rm day}}\right)^{-\alpha}\ {\rm erg\ s^{-1}\ g^{-1}}$

$$L_{\rm peak} \approx 1.1 \times 10^{41} {\rm erg\ s^{-1}} \left(\frac{M}{0.01\,M_\odot}\right)^{1-\frac{\alpha}{2}} \left(\frac{v}{0.01c}\right)^{\frac{\alpha}{2}} \left(\frac{\kappa}{1\ {\rm cm^2\ g^{-1}}}\right)^{-\frac{\alpha}{2}}$$

Very sensitive to atomic opacity

$\kappa \approx 1\ {\rm cm^2\ g^{-1}}$, light r process material (blue emission)

$\kappa \approx 10\ {\rm cm^2\ g^{-1}}$, heavy (lanthanide/actinide rich) r process (red emis.)

Impact Lanthanides/Actinides

Opacity dominated by bound-bound transitions

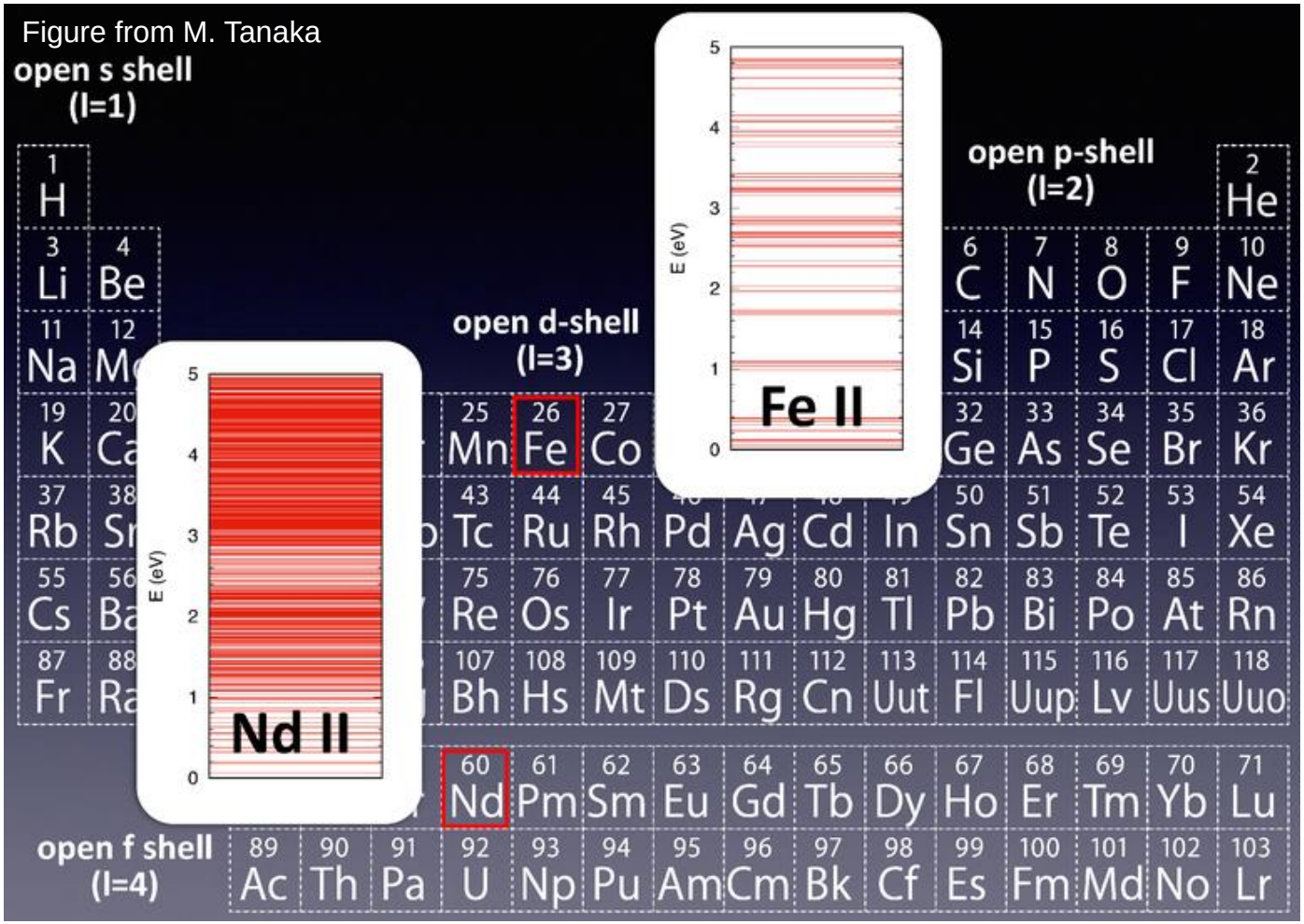

Large number of states of Lanthanides/Actinides leads to a high opacity

Barnes & D. Kasen, Astrophys. J. 775, 18 (2013);Tanaka & Hotokezaka, Astrophys. J. 775, 113 (2013).

AT2017gfo: electromagnetic transient GW170817

M. R. Drout et al. Science 2017;358:1570-1574

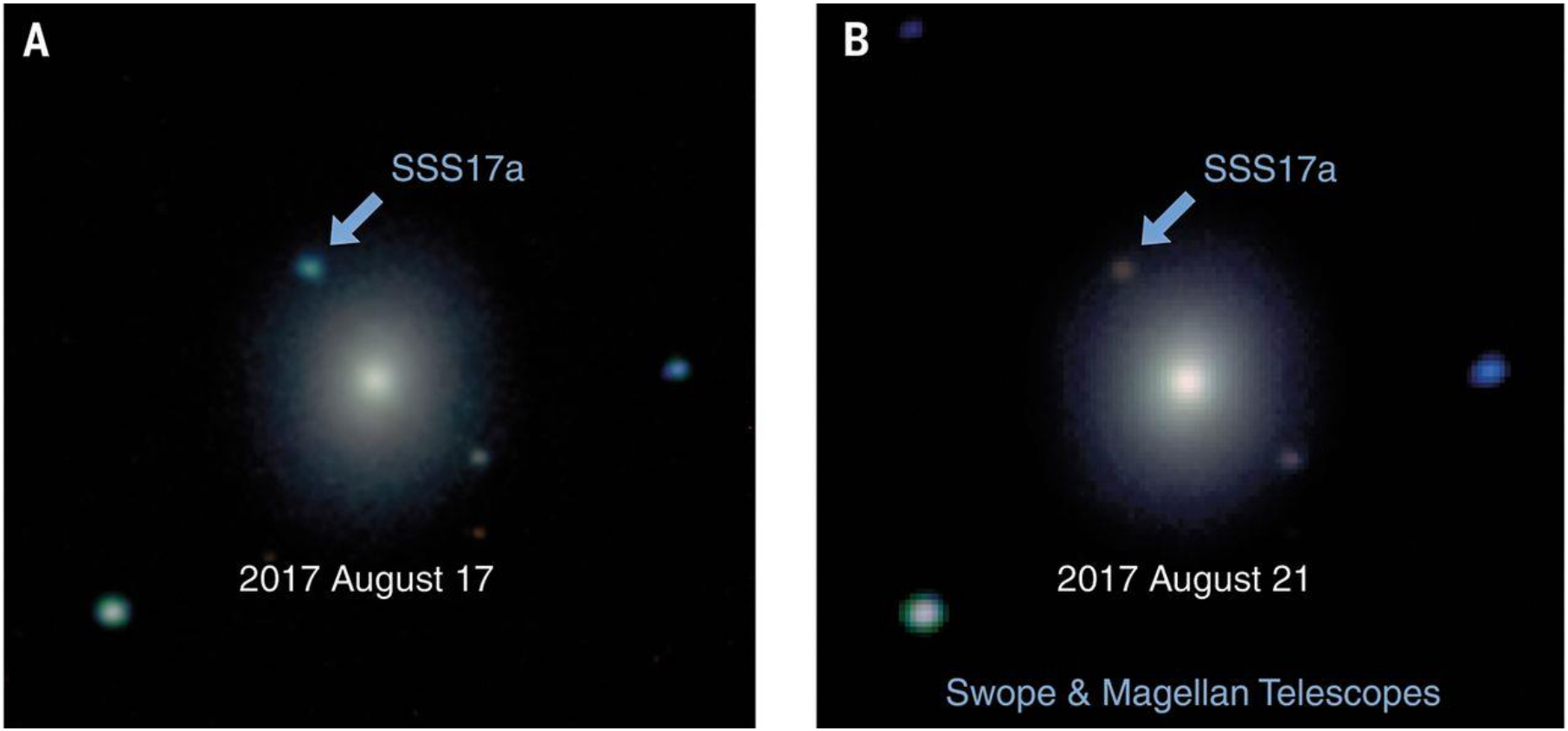

Novel fast evolving transient powered radioactive decay r-process material

Emission evolves from blue to red in a few days

Kilonova: Electromagnetic transient powered by decay of r-process nuclei

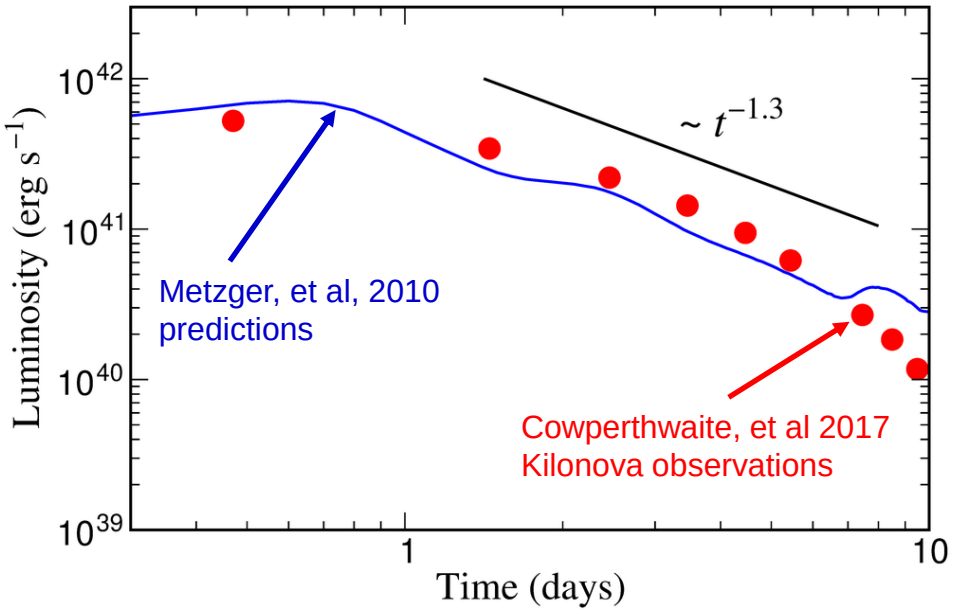

Pian et al., Nature 551, 67 (2017)

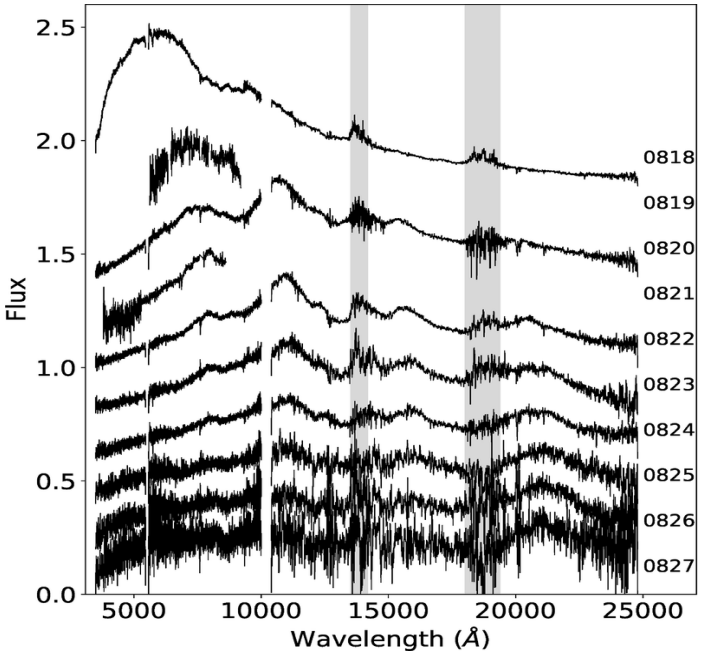

- Time evolution determined by the radioactive decay of r-process nuclei
- Two components [Kasen et al, Nature 551, 80 (2017)]
  - Blue dominated by light elements (Z < 50) ($M = 0.025\ M_{\odot}, v = 0.3c, X_{\rm lan} = 10^{-4}$, dynamical ejecta?, signature weak processes)
  - Red due to presence of Lanthanides ($M = 0.04\ M_{\odot}, v = 0.15c, X_{\rm lan} = 10^{-1.5}$, ejecta accretion disk?, points to delayed formation of a black hole), implies $M_{\rm max}(\rm NS) = 2.21^{+0.10}_{-0.13}\ M_{\odot}$ (Huth+ 2022)

Identification Sr in kilonova spectra

Watson et al, Nature **574**, 497 (2019)

Identification of strontium in the merger of two neutron stars

Darach Watson[1,2], Camilla J. Hansen[3,*], Jonatan Selsing[1,2,*], Andreas Koch[4], Daniele B. Malesani[1,2,5], Anja C. Andersen[1], Johan P. U. Fynbo[1,2], Almudena Arcones[6,7], Andreas Bauswein[7,8], Stefano Covino[9], Aniello Grado[10], Kasper E. Heintz[1,2,11], Leslie Hunt[12], Chryssa Kouveliotou[13,14] Giorgos Leloudas[1,5], Andrew Levan[15,16], Paolo Mazzali[17,18], Elena Pian[19] [See end for affiliations]

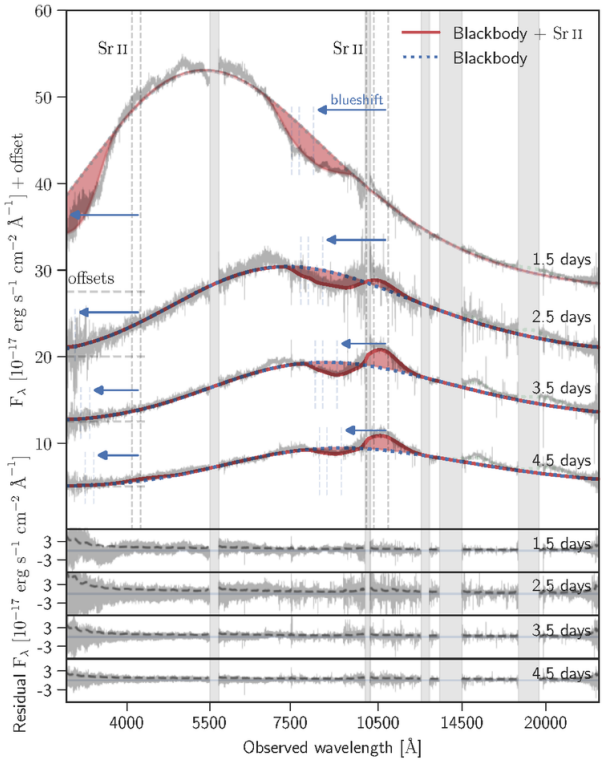

- First direct spectroscopic identification of an r-process element
- Strontium is produced in High $Y_e \sim 0.35$ ejecta: direct evidence of the role of neutrinos in merger ejecta

Lanthanum and Cerium suggested to account for features at 12000-14000 Å (Domoto et al, 2022)

Nuclear fingerprints light curve

Bolometric light curve is easy to determine theoretically ($L \sim M_{\rm ej} \dot{\varepsilon}_{\rm eff}$)

but difficult to determine observationallv

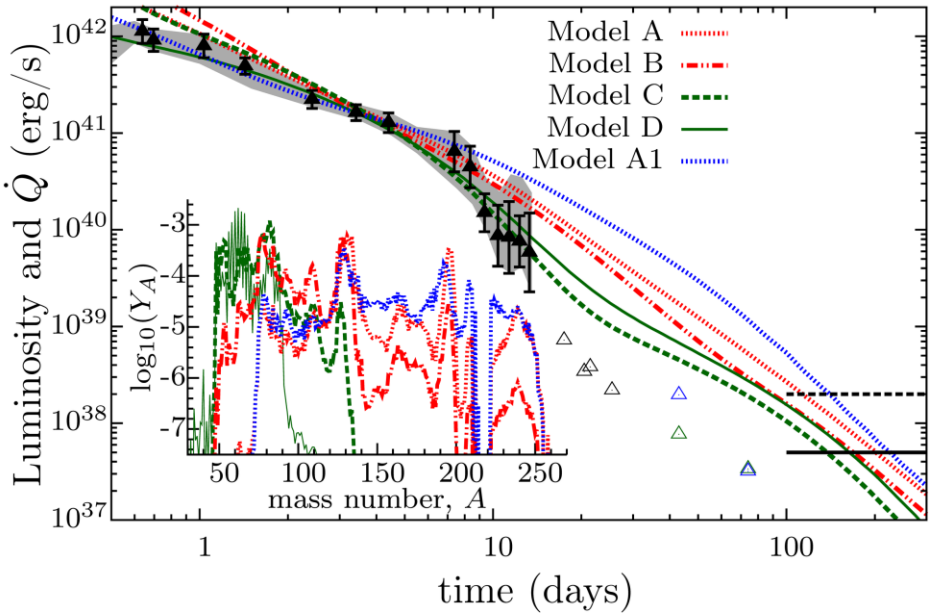

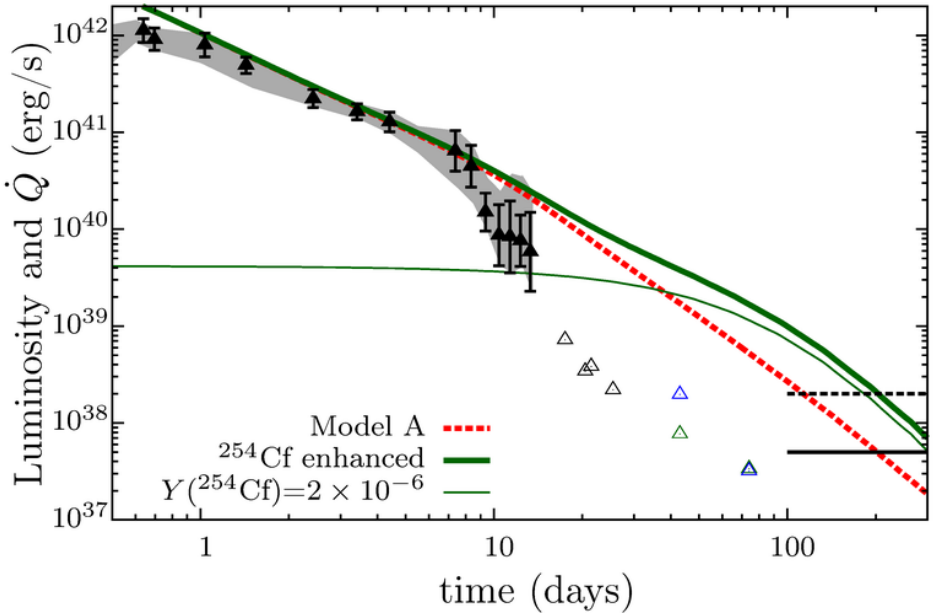

PHYSICAL REVIEW VOLUME 103, NUMBER 5 SEPTEMBER 1, 1956

Californium-254 and Supernovae*

G. R. Burbidge and F. Hoyle,† *Mount Wilson and Palomar Observatories, Carnegie Institution of Washington, California Institute of Technology, Pasadena, California*

and

E. M. Burbidge, R. F. Christy, and W. A. Fowler, *Kellogg Radiation Laboratory, California Institute of Technology, Pasadena, California*

(Received May 17, 1956)

At late times light curve is determined by nuclear heating. Opacity uncertainties play a smaller role (ejecta is transparent)

Observations between 10 and 100 days are sensitive to composition.
Light curve becomes dominated by individual decays: ^{254}Cf

Wu, Barnes, GMP, Metzger, PRL 122, 062701 (2019), Zhu+ 2018

R-process in mergers

Simulations

Bauswein et al, ApJ 773, 78 (2013)

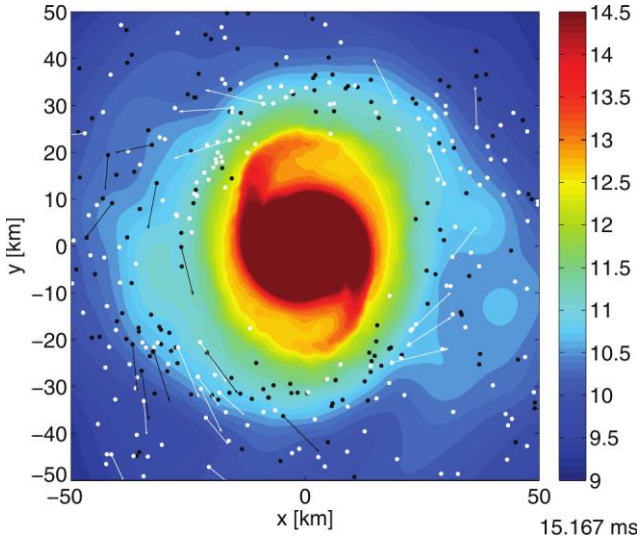

- Different sources of ejecta, dynamical and secular, with different properties (Y_e)
- Role of equation of state
- Role of neutrinos

Nucleosynthesis

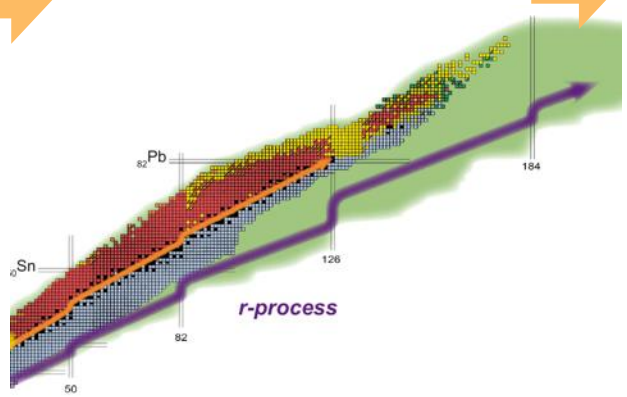

- Physics of neutron-rich and heavy nuclei

Light curve and spectra modelling

Watson et al, Nature **574**, 497 (2019)

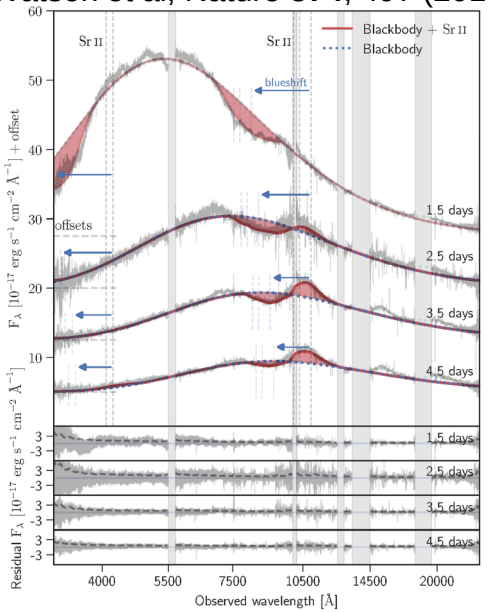

- Radioactive energy deposition
- Thermalization decay products (Barnes+ 2016, Kasen+ 2019)
- Spectra formation: atomic data depends on ejecta evolution (LTE vs NLTE)

- Which r-process elements are produced in mergers?
- Are mergers the (main) r-process site?

3D Kilonova light curves

3D modelling using radiation transport monte-carlo ARTIS code

Gray Ye dependent opacities
Lead by: **Christine Collins**
arXiv:2209.05246

Angular dependence disappears once ejecta becomes transparent

Similar blue to red color evolution to AT2017gfo

Y_e Tanaka+ 2020	κ $cm^2\ g^-$
$Y_e \leq 0.1$	19.5*
$0.1 < Y_e \leq 0.15$	32.2
$0.15 < Y_e \leq 0.2$	22.3
$0.2 < Y_e \leq 0.25$	5.60
$0.25 < Y_e \leq 0.3$	5.36
$0.3 < Y_e \leq 0.35$	3.30
$Y_e > 0.35$	0.96

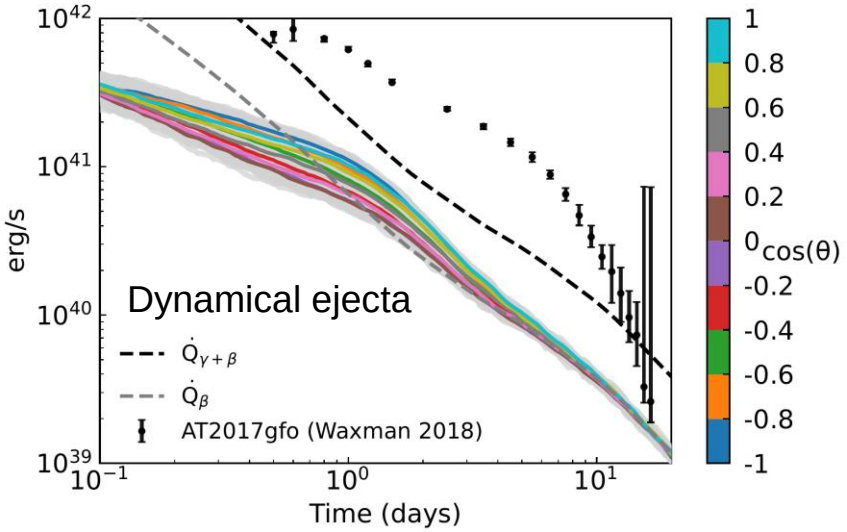

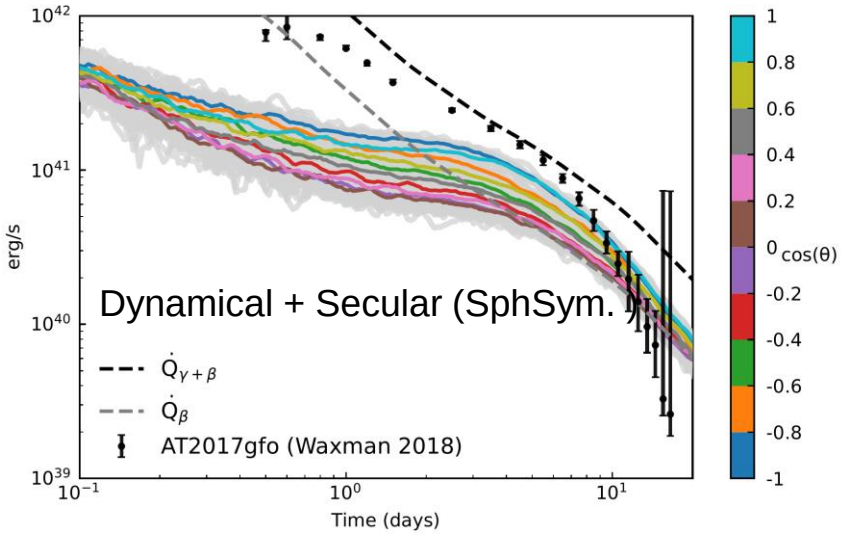

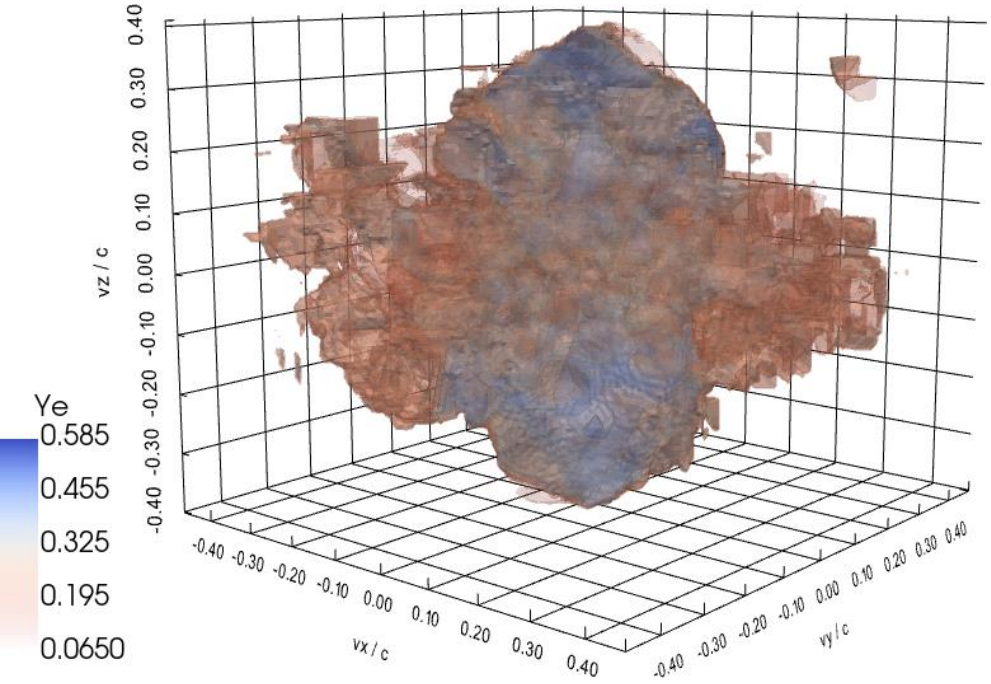

End to end kilonova models

- Based on grey opacities using approximate radiative transfer model
- promising agreement with AT2017gfo after times of several days
- inconsistencies at early times needs a more dominant neutrino-driven wind

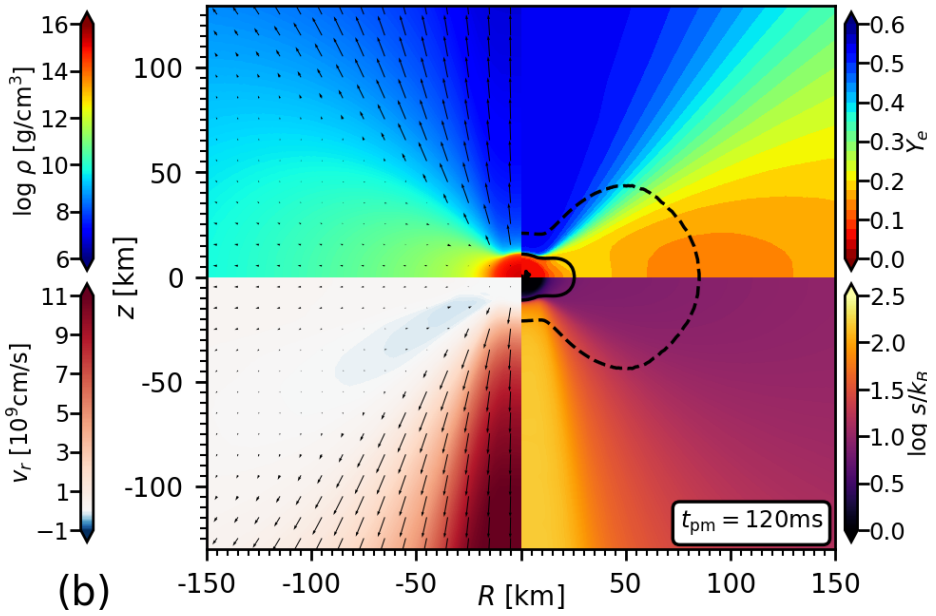

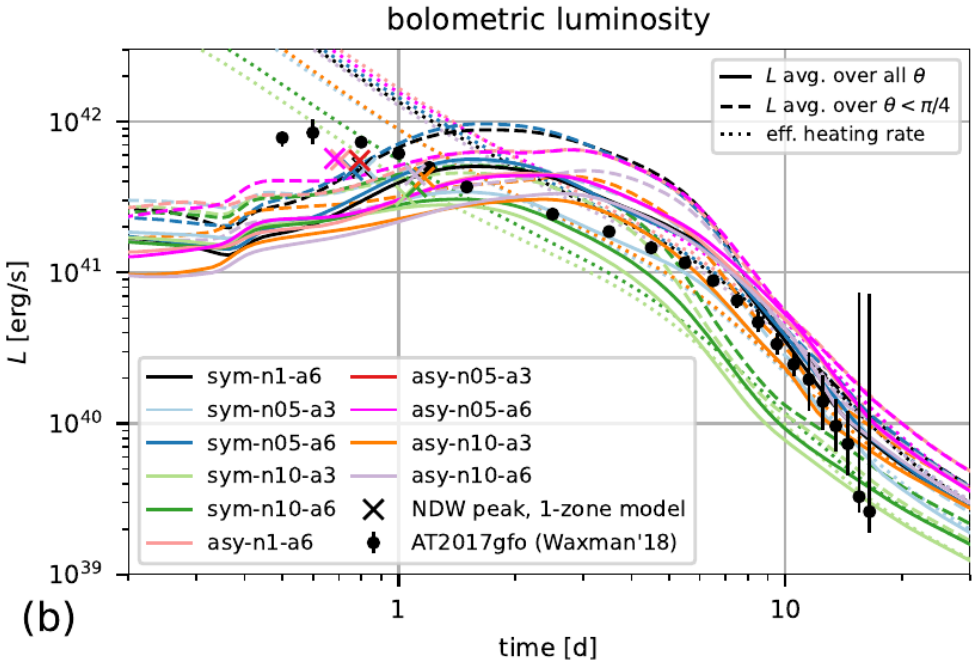

Just et al, arXiv:2302.10928

Energy levels - Opacity

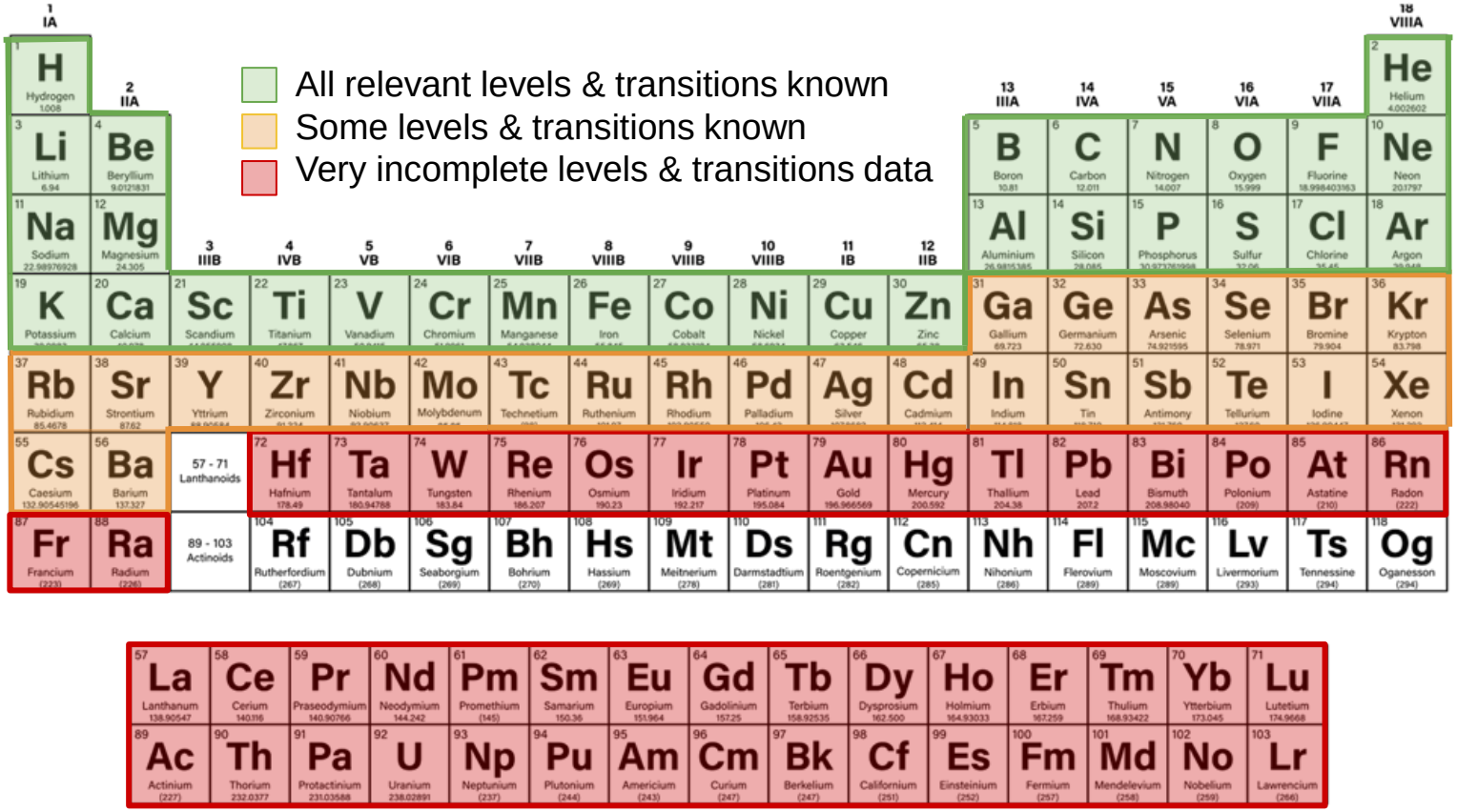

- Early evolution ($t \lesssim 1$ week, local thermodynamic equilibrium)
  - Bound-bound opacities
  - Not enough data for levels and transitions (theory: Gaigalas+ 2019, Tanaka+ 2020, Fontes+ 2020)
- Nebular evolution ($t \gtrsim 1$ week, non LTE)
  - Electron-ion cross sections, photoionization cross sections, recombination coefficients (Hotokezaka+ 2021, Pognan+ 2022)

Atomic opacities and spectral modelling

- Systematic bound-bound opacity calculations
  - Calculations for all elements between Iron and Actinides using Flexible Atomic Code [Gu CJP 86, 675 (2008), https://github.com/flexible-atomic-code/fac], U Lisbon
  - Extended set of configurations to ensure convergence low lying states and density of levels
  - Benchmark against data or calculations with alternative codes (HFR, U Mons)

R. Silva

G. Leck

A. Flörs

- **ARTIS** Kromer & Sim, MNRAS 398, 1809 (2009) https://github.com/artis-mcrt/artis
  - 3D Monte Carlo Radiative Transfer
  - Consistent description of energy deposition, transport and spectral formation
  - 3D geometry ejecta
  - Both photospheric (thermal) and nebular (non-thermal) epochs (Shingles+ 2020 and 2022)
  - Extensions: Follow individual decays including γ-ray deposition and transport. Particle energy deposition assumed local but not instantaneous.

L. Shingles

Atomic Opacities (LTE)

- Sobolev optical depth (for a line l)

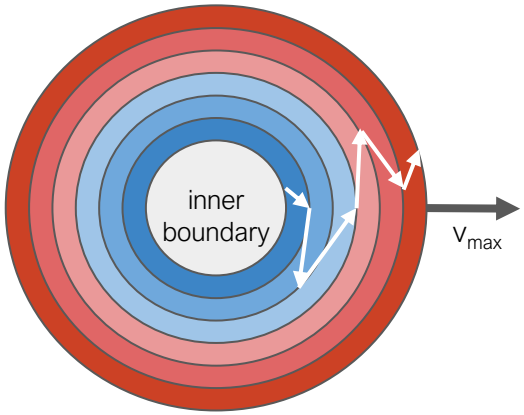

$$\tau_l = \frac{\pi e^2}{m_e c} t f_l n_l \lambda_l$$

Transition wavelength

Oscillator strength

Population lower level (Saha eq. and partition functions)

- Expansion opacity (homologous expanding material, not used in the radiation transport modelling)

$$\kappa_{\mathrm{exp}}^{\mathrm{bb}} = \frac{1}{\rho c t} \sum_l \frac{\lambda_l}{\Delta \lambda_{\mathrm{bin}}} (1 - e^{-\tau_l})$$

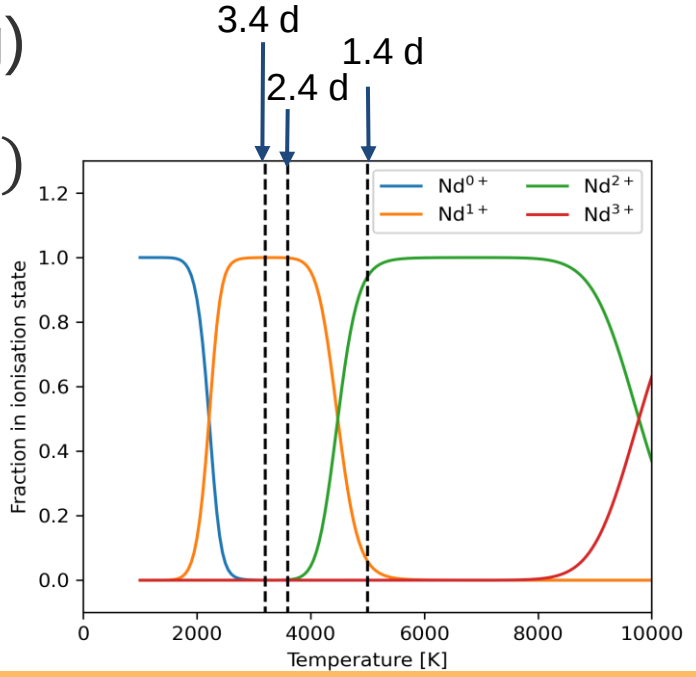

Level energies: Nd II

- Include enough configurations to achieve convergence low lying states and level densities.
- Opacities after calibration to known levels using the Flexible Atomic Code.

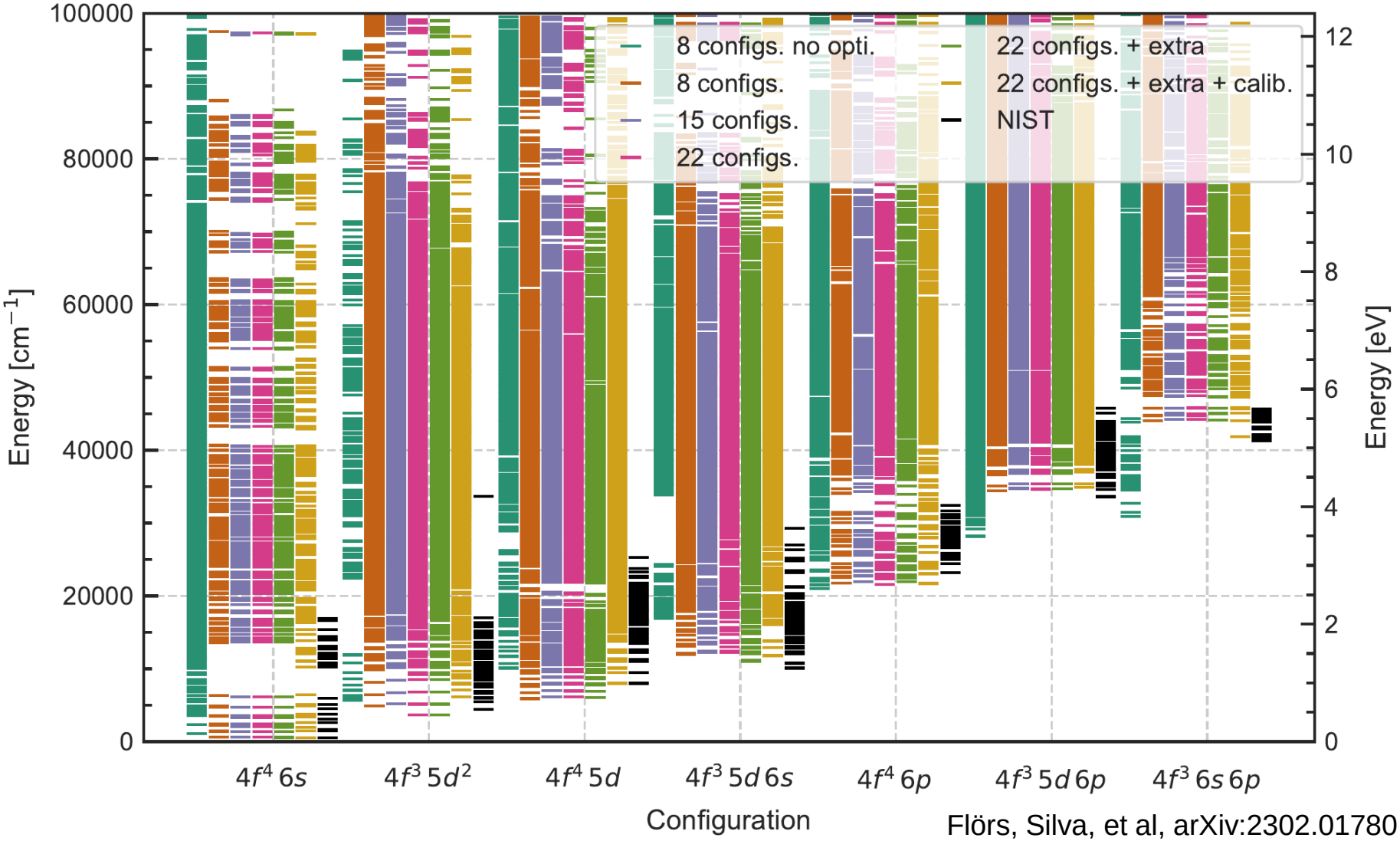

Flörs, Silva, et al, arXiv:2302.01780

Nd opacity

- Good agreement with Gaigalas+ 2019
- Differences below 2000 Å due to Nd III contribution
- Limited data Nd III, calibration difficult

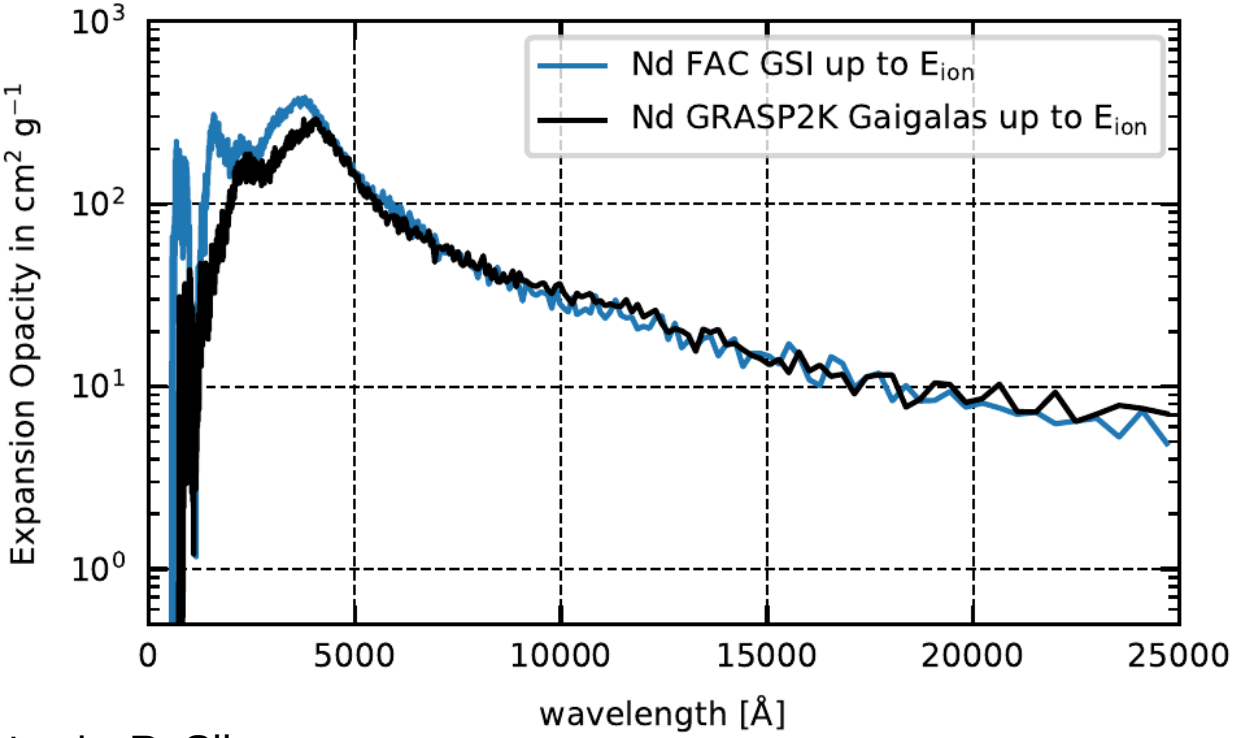

A. Flörs G. Leck R. Silva



$\rho = 10^{-13}\mathrm{g\ cm^{-3}} \quad T = 5000\ \mathrm{K}$

Actinides vs Lanthanides

- Actinides have larger opacities than Lanthanides
- Confirmed by independent calculations HFR code (U. Mons)
- Very limited data for actinides

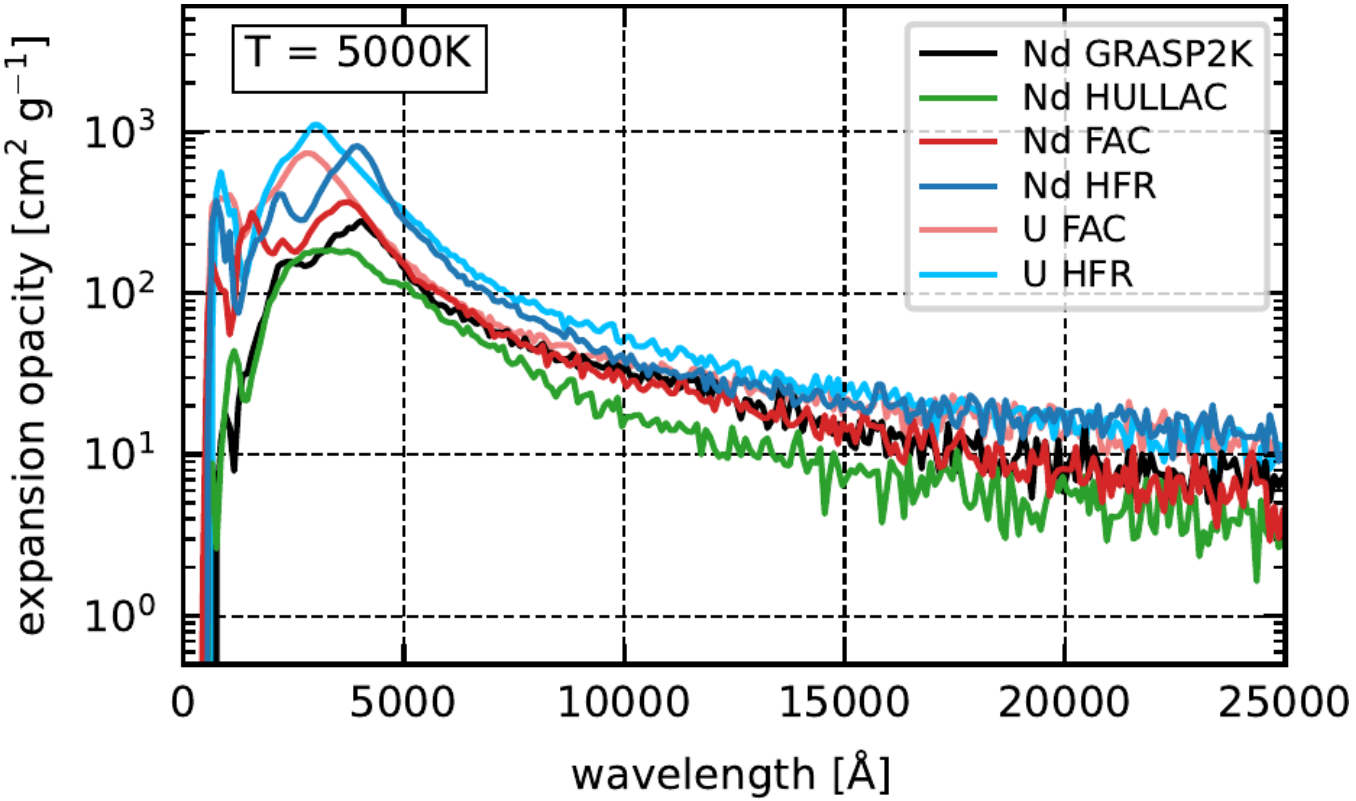

Silva et al, Atoms 10, 18 (2022); Flörs, Silva, et al, arXiv:2302.01780

Offers a method to identify presence of Actinides in spectra.

Towards fully consistent 3D models

L. Shingles

- Monte Carlo 3D radiative transfer using the ARTIS code. https://github.com/artis-mcrt/artis
- Matter distribution based on SPH Dynamical ejecta (0.005 $M_{\odot}$)
- LTE simulation: follows 2591 nuclei (283 ions with gamma-ray transport and electron thermalization, 44 millions atomic transitions lines
  AD1: Japan-Lithuania database Z=28-88, Tanaka+ 2020
  AD2: AD1 + calibrated lines for Sr, Y, and Zr, Kurucz 2018

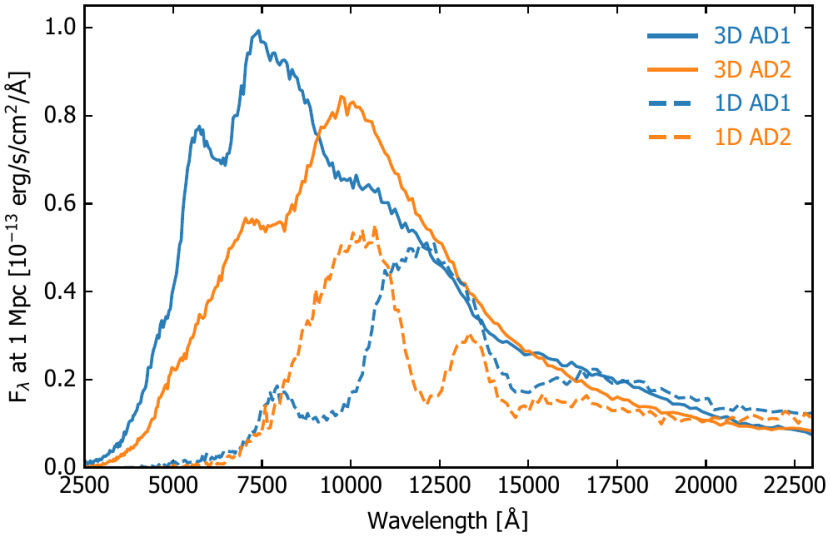

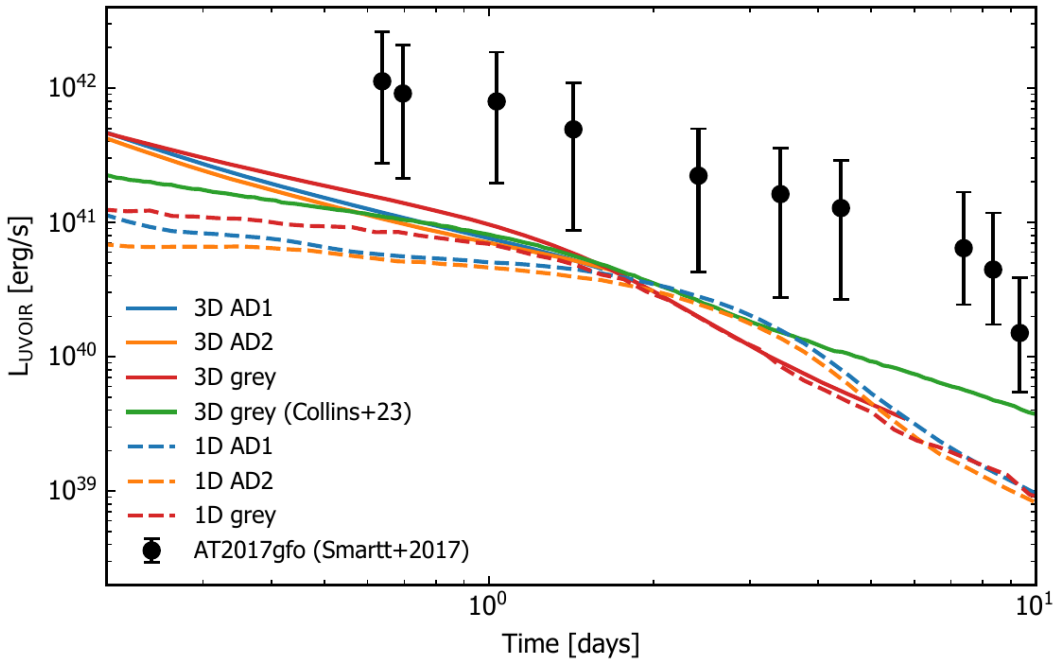

Shingles et al, in preparation

Angular dependence spectra

Polar direction

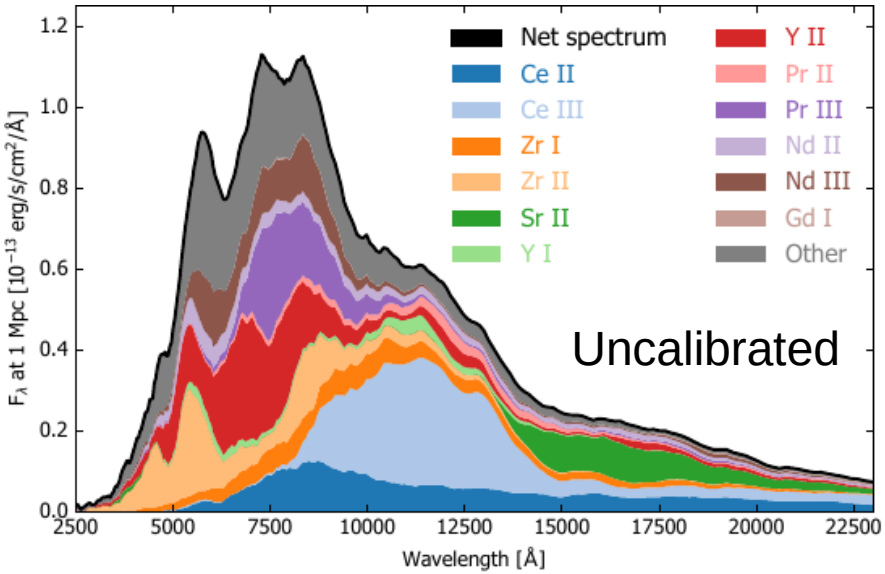

Equatorial direction

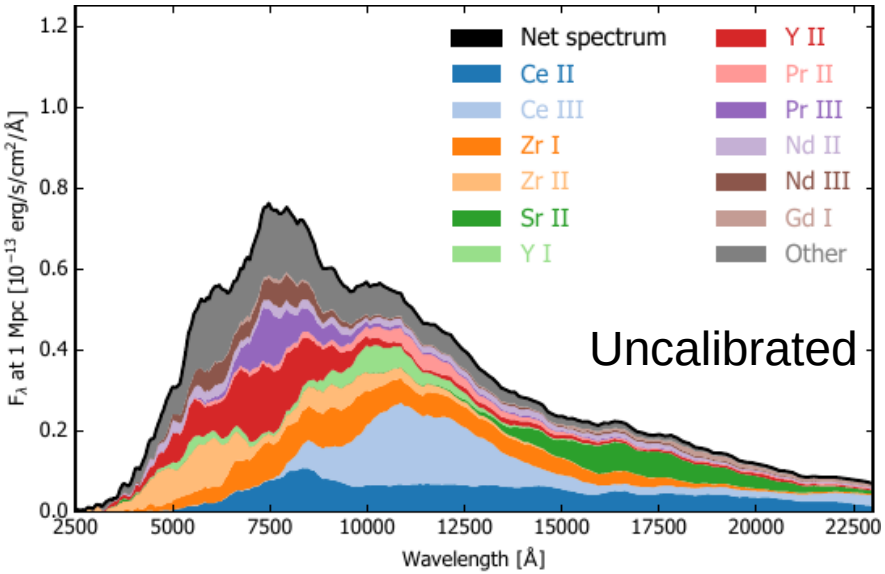

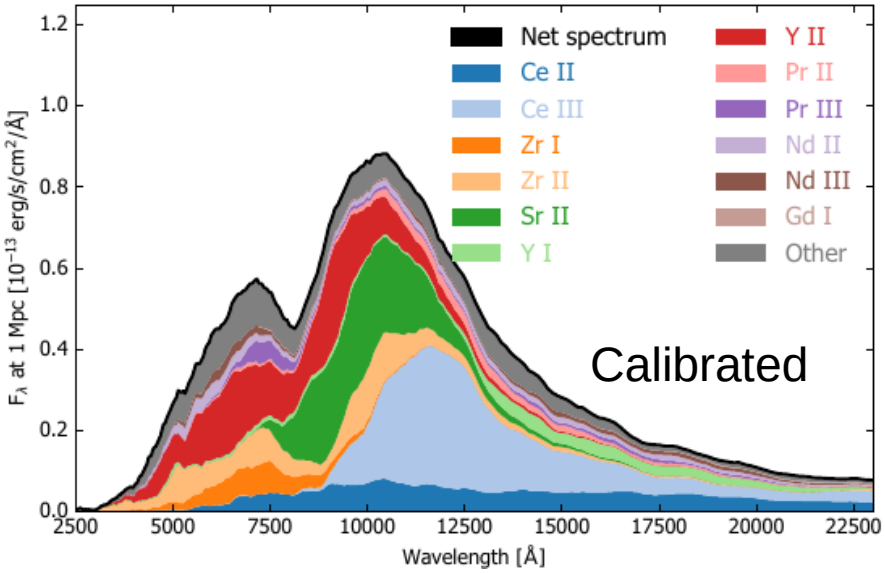

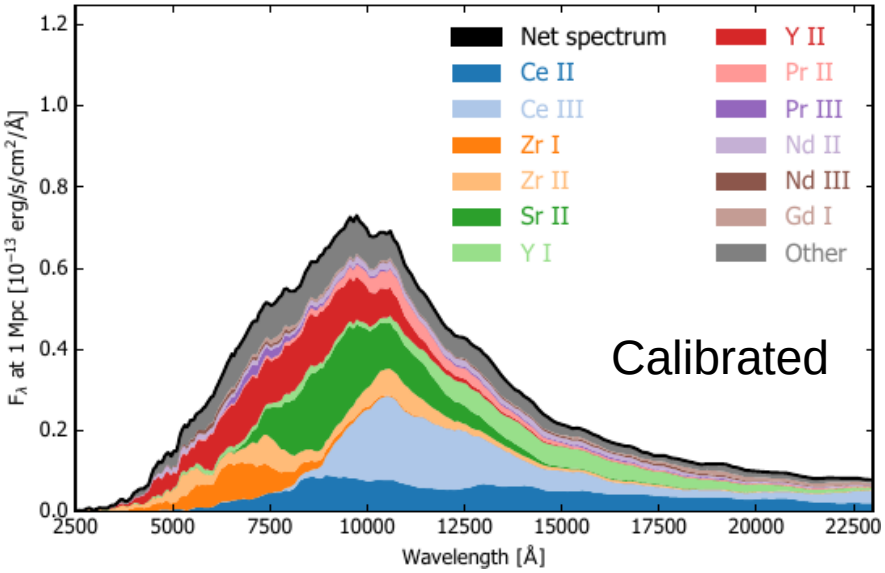

Differences reflect directional dependence of nucleosynthesis yields Shingles et al, in preparation

Comparison AT2017gfo

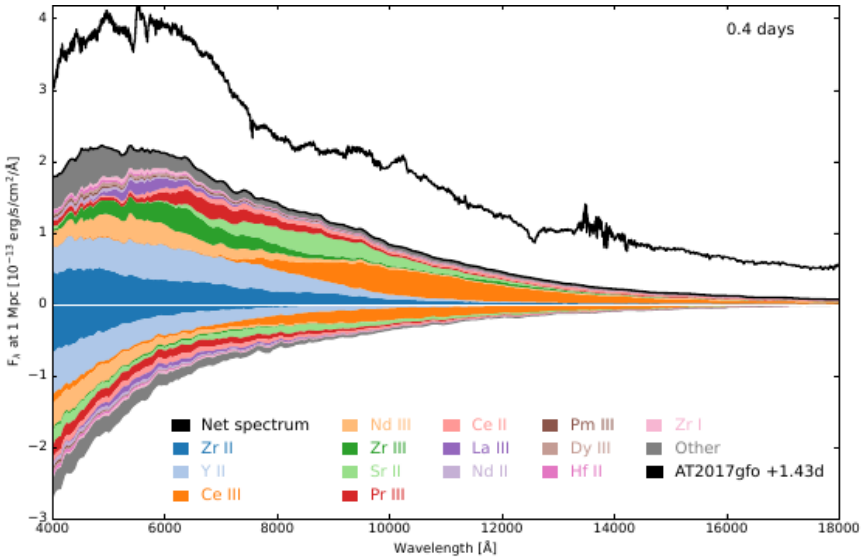

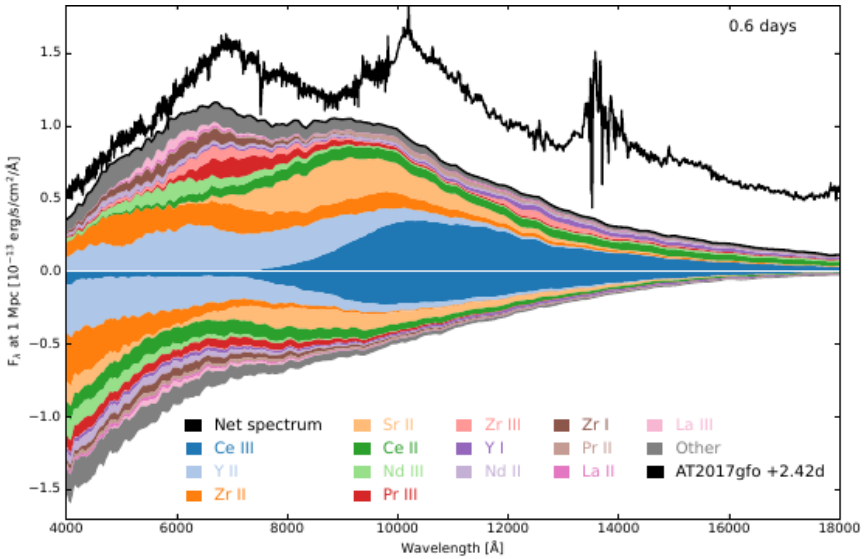

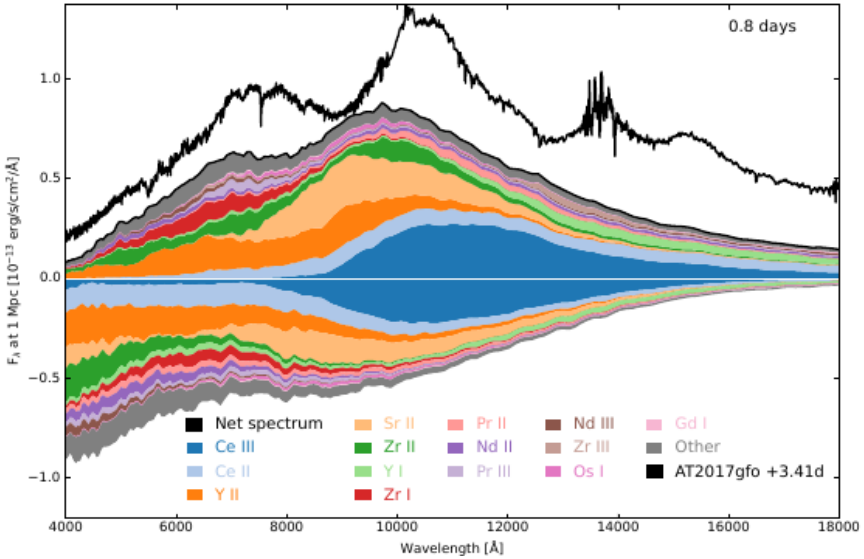

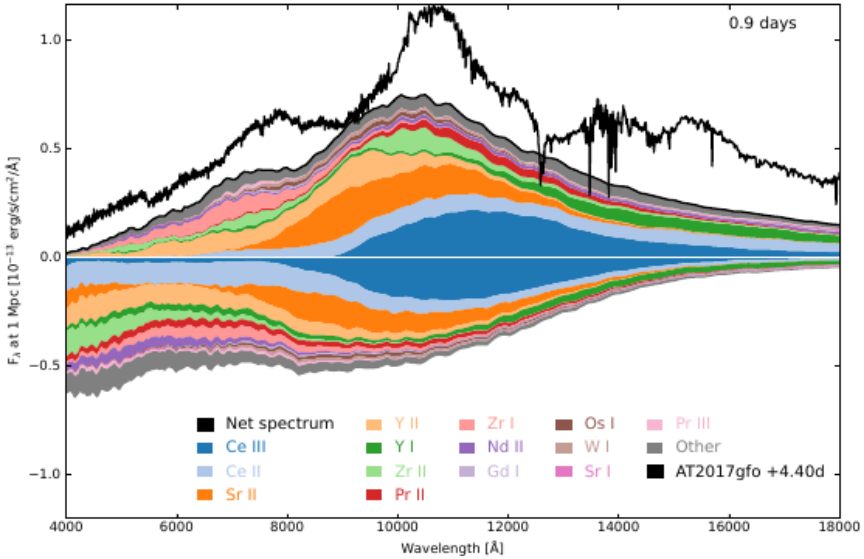

Similar spectral evolution that AT2017gfo once differences in brightness are accounted

Shingles et al, in preparation

Directional dependence

- Having 3D models allows to determine the directional dependence of all relevant quantities.

- Strong dependence both in polar and azimuthal angles

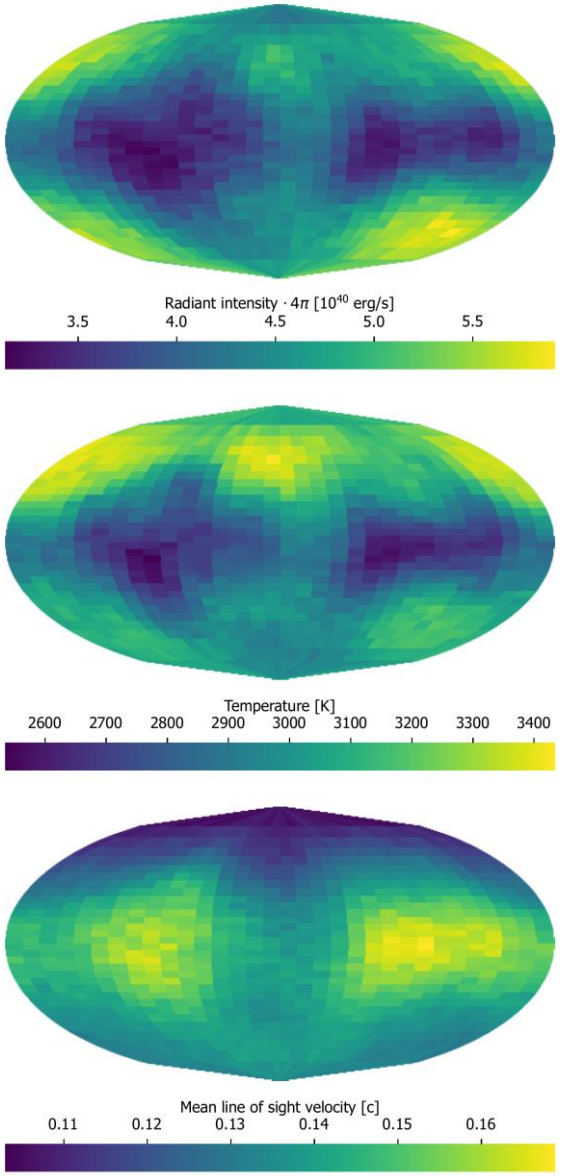

Nucleosynthesis beyond iron

Several processes contribute to the nucleosynthesis beyond Iron: s-process, r-process and p-process (γ-process)

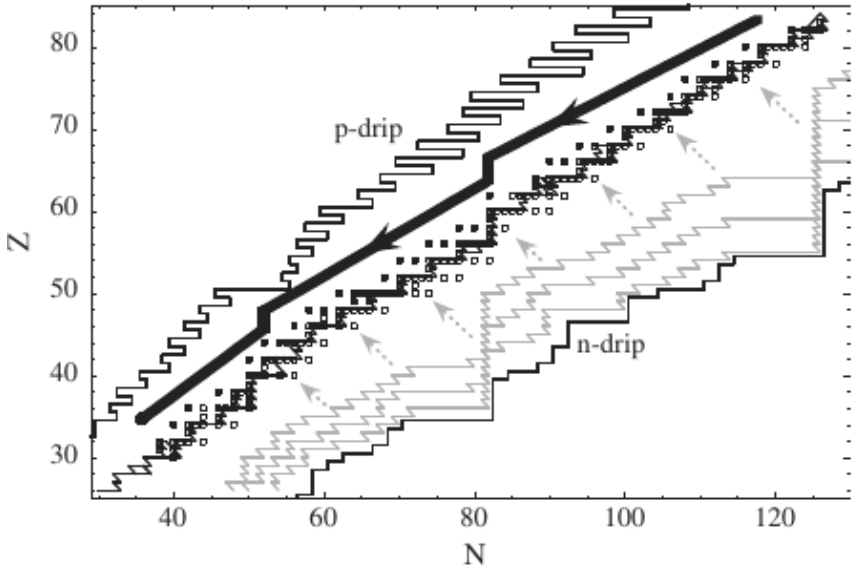

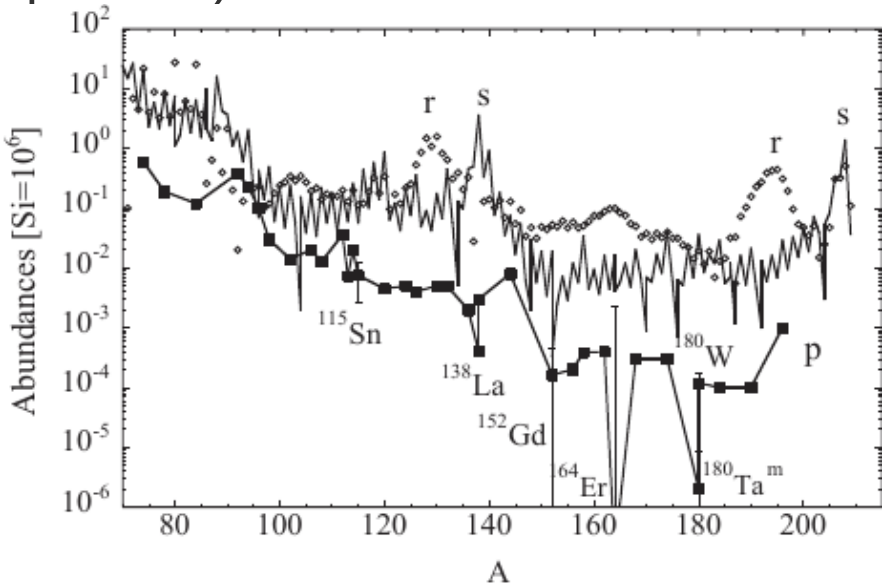

M. Arnould, S. Goriely / Physics Reports 384, 1 (2003)

- s process: low neutron densities, $n_n = 10^{10-12}$ cm^{-3}, $\tau_n > \tau_\beta$
  (site: intermediate mass stars)
- r process: large neutron densities, $n_n > 10^{20}$ cm^{-3}, $\tau_n \ll \tau_\beta$
  (site: binary neutron star mergers?)
- Additional process(es) required to produce neutron-deficient p-nuclei
  - p-process or γ-process: photodissociation material enriched by s-process
  - νp-process: (p,γ) and (n,p) reactions catalysed by $\bar{\nu}_e + p \rightarrow n + e^+$

The νr-process

arXiv:2305.11050v1 [astro-ph.HE] 18 May 2023

Production of p-nuclei from r-process seeds: the νr-process

Zewei Xiong,[1,*] Gabriel Martínez-Pinedo,[1,2] Oliver Just,[1] and Andre Sieverding[3]

[1] *GSI Helmholtzzentrum für Schwerionenforschung, Planckstraße 1, D-64291 Darmstadt, Germany*
[2] *Institut für Kernphysik (Theoriezentrum), Technische Universität Darmstadt, Schlossgartenstraße 2, D-64289 Darmstadt, Germany*
[3] *Max Planck Institute for Astrophysics, Karl-Schwarzschild-Straße 1, D-85748 Garching, Germany*

(Dated: May 19, 2023)

We present a *new* nucleosynthesis process that may take place on neutron-rich ejecta experiencing an intensive neutrino flux. The nucleosynthesis proceeds similarly to the standard r-process, a sequence of neutron-captures and beta-decays, however with charged-current neutrino absorption reactions on nuclei operating much faster than beta-decays. Once neutron capture reactions freeze-out the produced r-process neutron-rich nuclei undergo a fast conversion of neutrons into protons and are pushed even beyond the β-stability line producing the neutron-deficient p-nuclei. This scenario, which we denote as the νr-process, provides an alternative channel for the production of p-nuclei and the short-lived nucleus ^{92}Nb. We discuss the necessary conditions posed on the astrophysical site for the νr-process to be realized in nature. While these conditions are not fulfilled by current neutrino-hydrodynamic models of r-process sites, future models, including more complex physics and a larger variety of outflow conditions, may achieve the necessary conditions in some regions of the ejecta.

- A new nucleosynthesis process that may operate in binary neutron star mergers under strong neutrino fluxes when nuclei are present: charged-current neutrino-nucleus reactions faster than β^- decays.
- Novel mechanism for production of p-nuclei from neutron-rich nuclei.

Role of neutrinos in r-process

- Large (anti)neutrino fluxes drive composition to $Y_e \sim 0.5$ during alpha-particle formation (Meyer et al, 1995)
- large neutrino fluxes during the phase of neutron captures erode r-process peaks related to long beta-decays (Langanke, GMP, 2003)
- ν_e absorption cross sections $\sim (N - Z)$
- What will be the resulting nucleosynthesis?

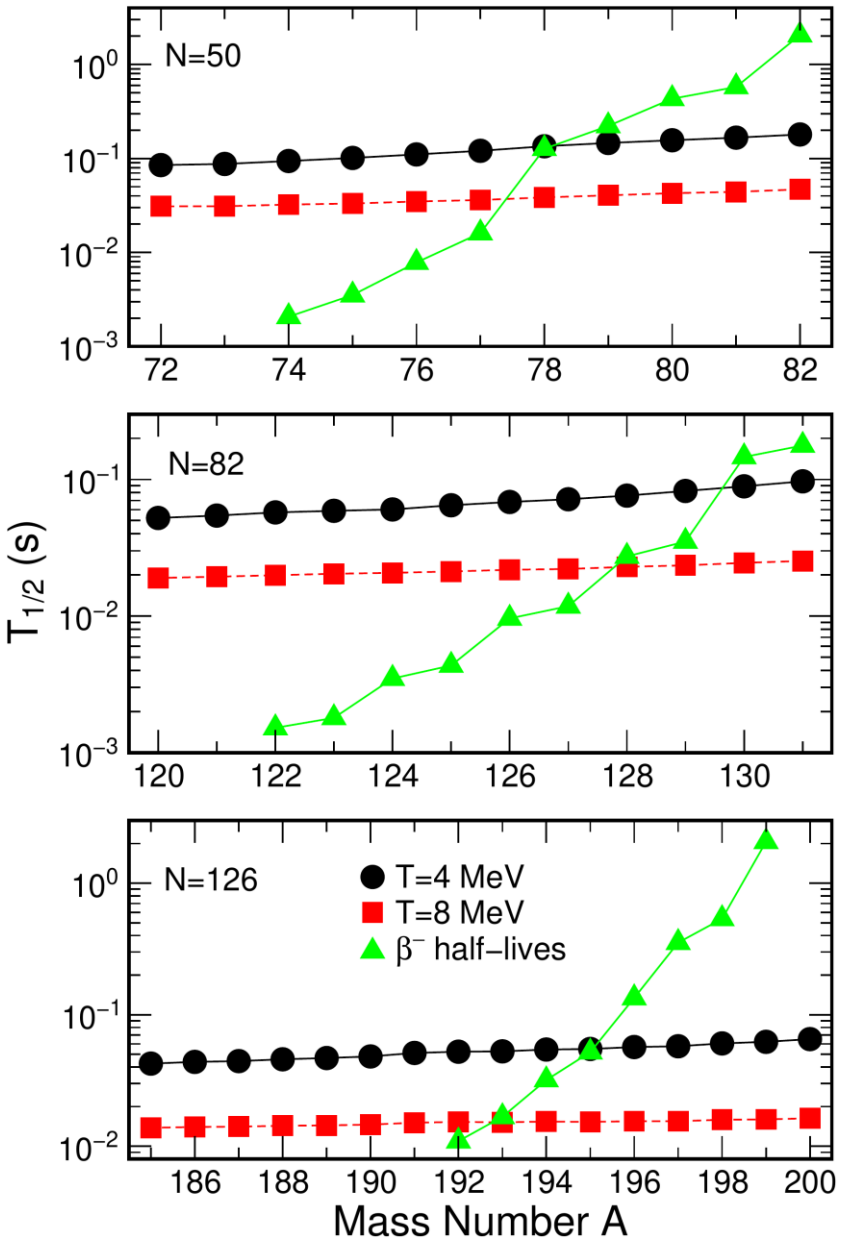

Possible source of light p-nuclei and ^{92}Nb

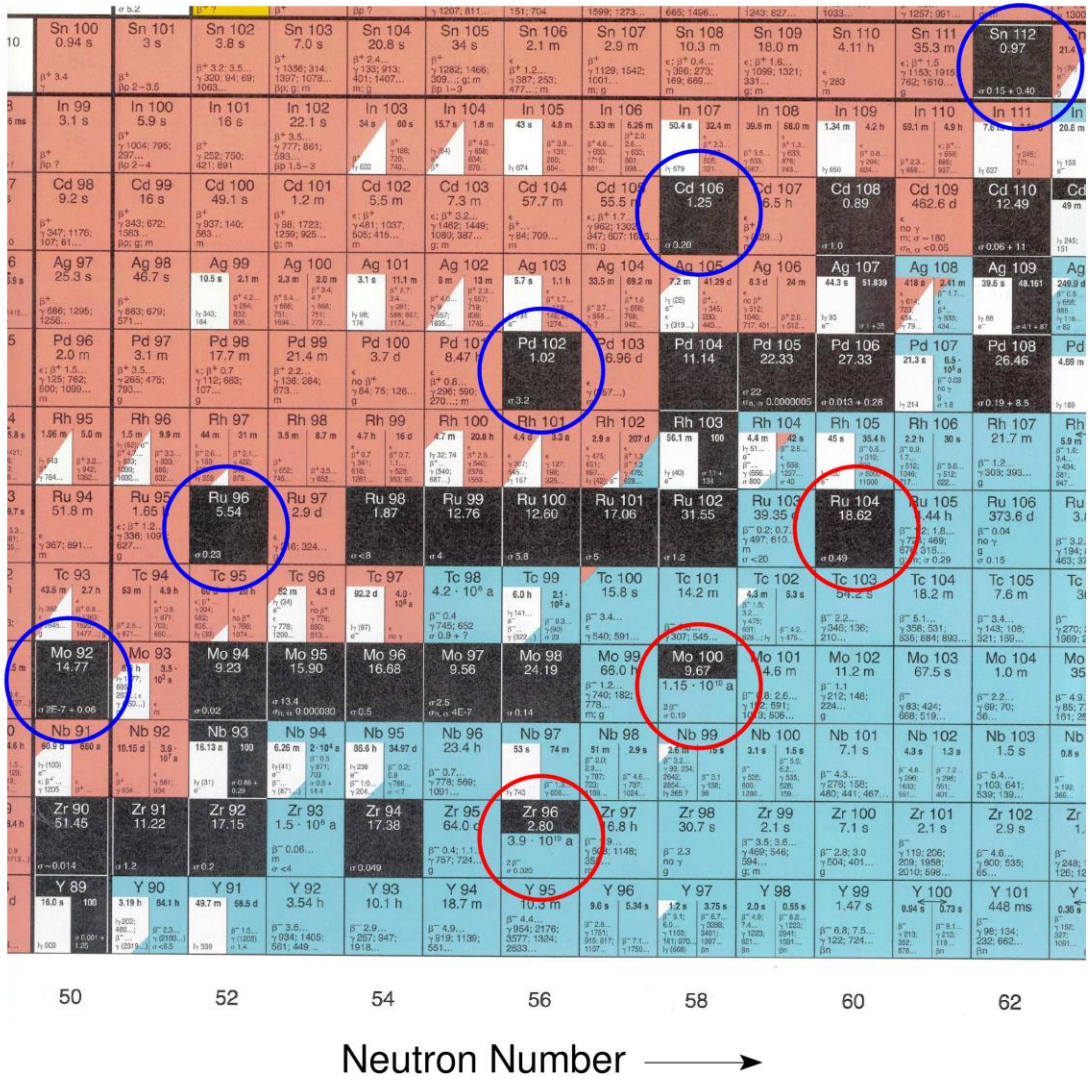

γ-process fails to produce light p-nuclei ^{92,94}Mo and ^{96,98}Ru in solar proportions

Supernova neutrino winds:

- Ejecta with $Y_e \sim 0.48$ produce ^{92}Mo
- νp-process ($Y_e \gtrsim 0.55$) produces ^{94}Mo, ^{96,98}Ru.

Long-lived ^{92}Nb present in early solar system. Cannot be produced by the νp-process

Can we produce all those nuclei in the same environment including heavier p-nuclei?

Phases during the operation of the vr-process

- **Seed production:** Strong neutrino fluxes drive material to $Y_e \sim 0.5$
- **Neutron-capture phase:** neutrons are used relatively fast by two competing mechanisms:
  - $n(\nu_e, e^-)p$ converts neutrons into protons that are captures in medium mass nuclei
  - $A(\nu_e, e^- X)\ X = n, p, \alpha$ speeds up the decay of nuclei and the build up of heavy nuclei
- **Fast "decay" to stability and beyond:** $A(\nu_e, e^- X)$ reactions drive material to beta-stability and beyond
  - Neutrons, protons and alphas produced by both charged-current and neutral current spallation reactions.
  - Protons and alphas captured mainly in light nuclei
  - Equilibrium between $A(\nu_e, e^- X)$ and $A(n, \gamma)$ determines final abundance

Nucleosynthesis (no neutrino-nucleus)

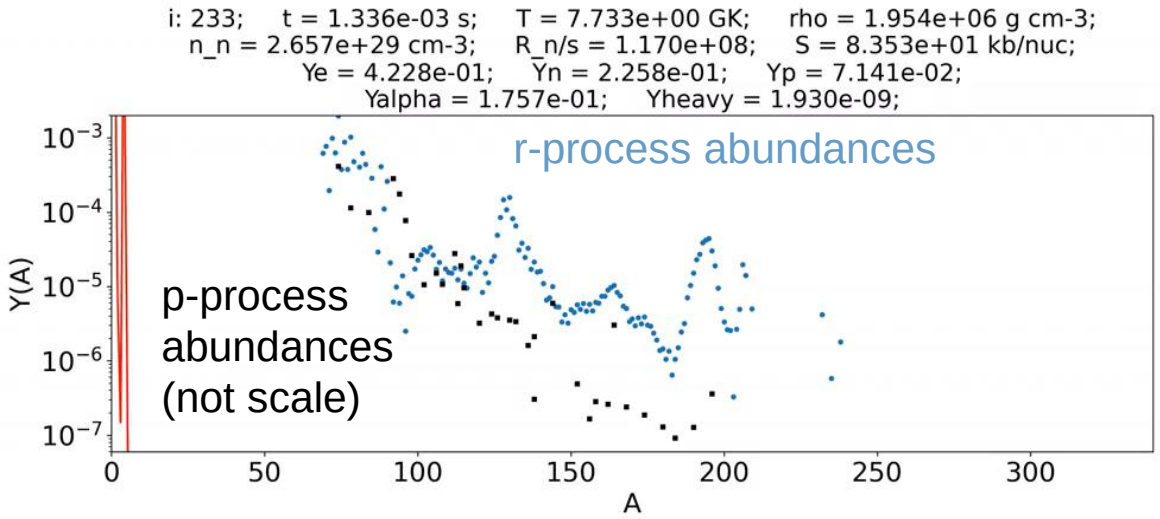

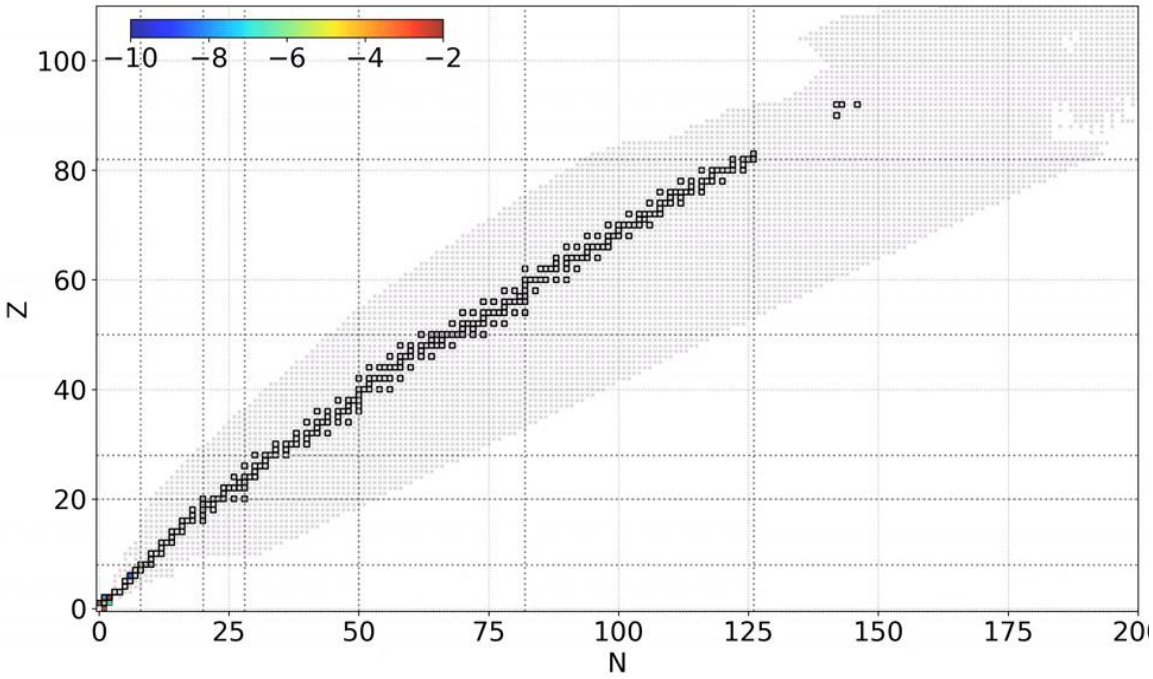

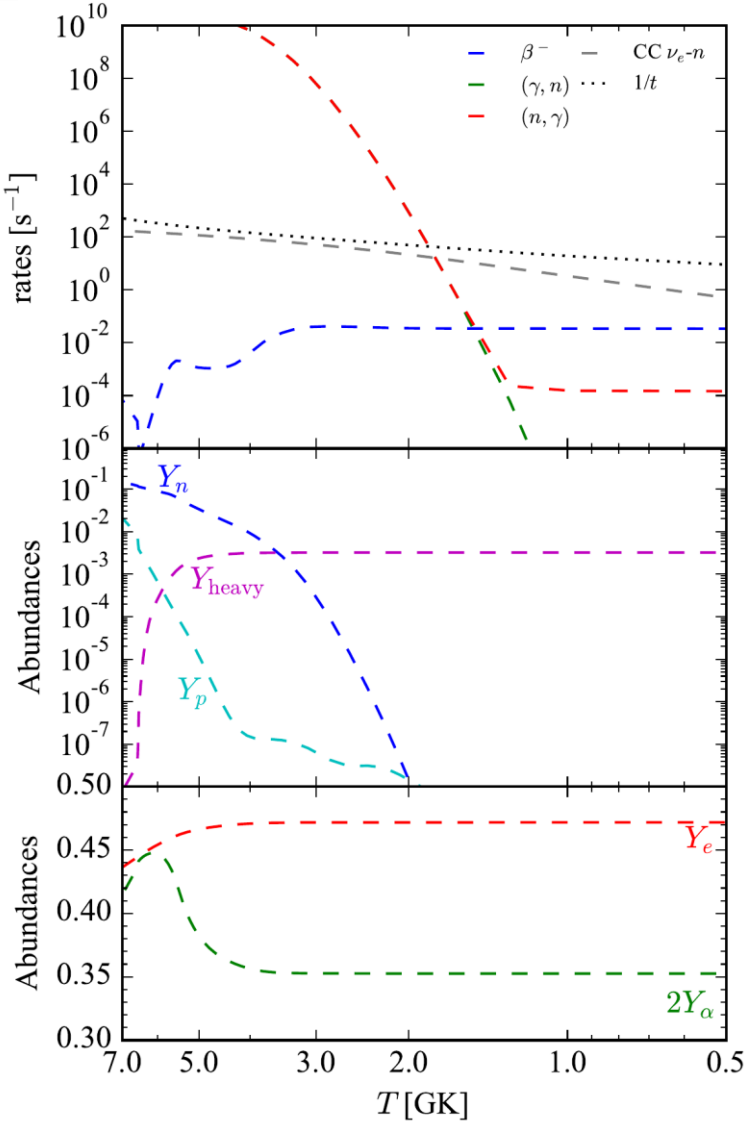

Nucleosynthesis (with neutrino-nucleus)

$\nu-A$ cross sections from Sieverding, et al, ApJ 865, 143 (2018).

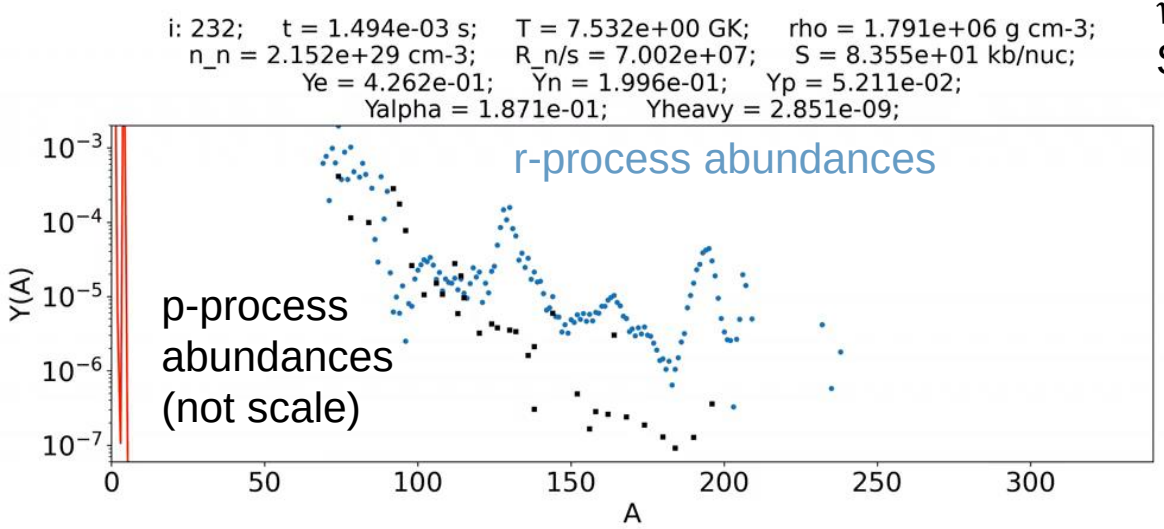

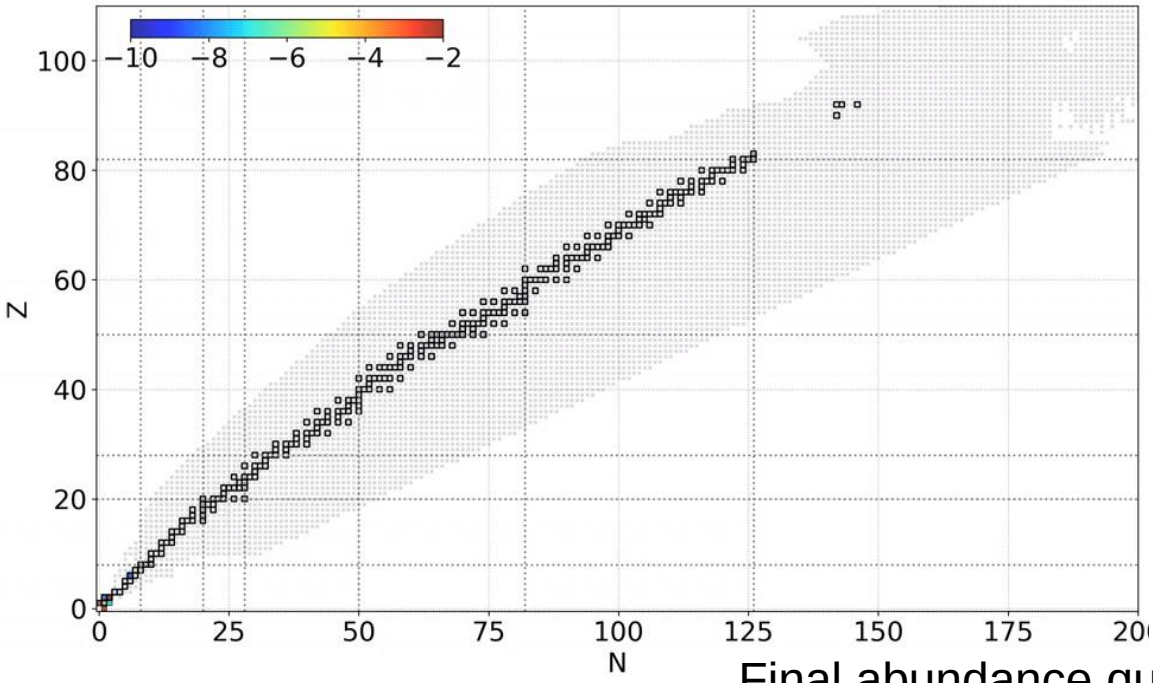

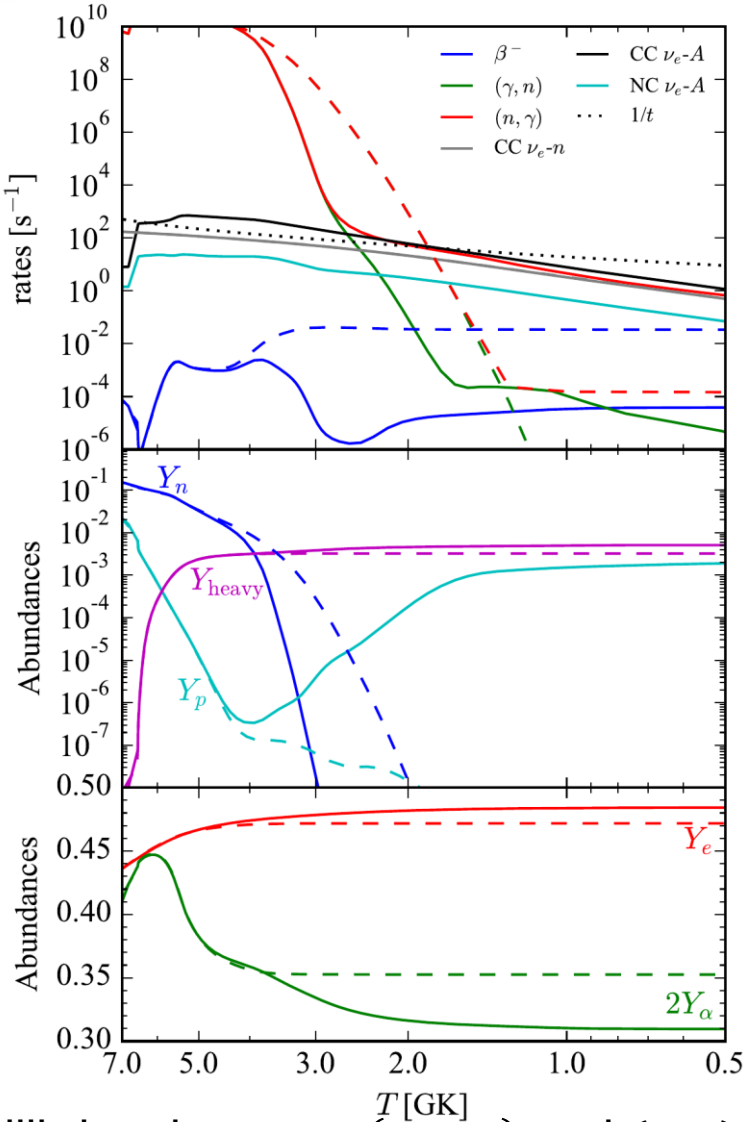

Final abundance quilibrium between (ν_e, e^-) and (n, γ)

Dependence on neutrino fluence

Increasing neutrino fluence allows to produce heavier p-nuclei

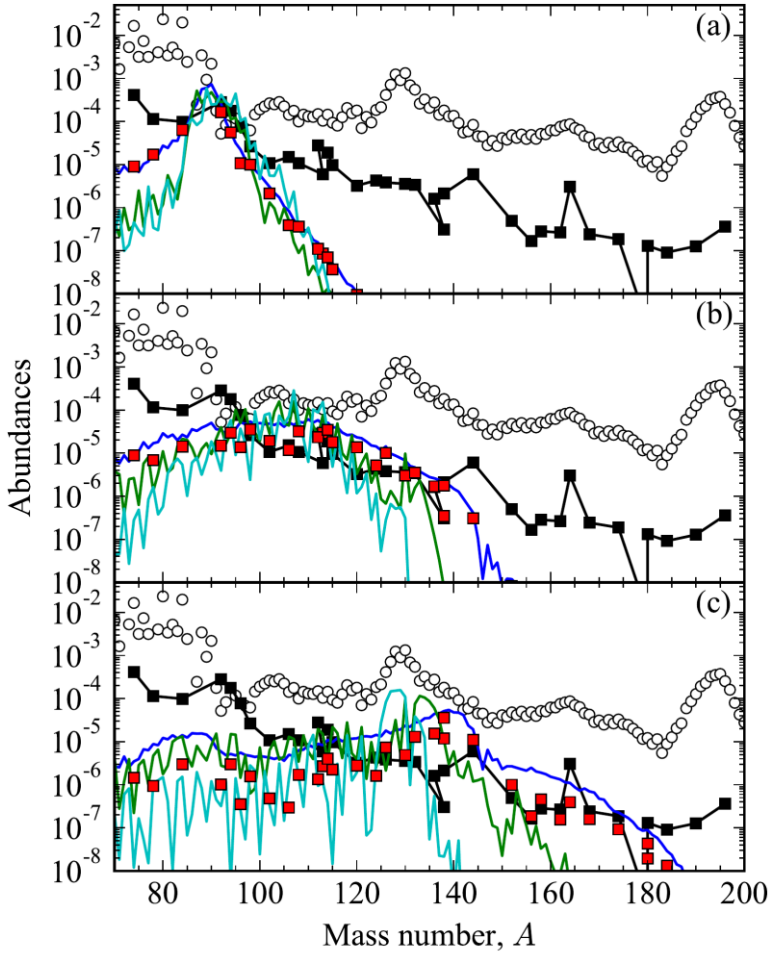

Dependence Y_e and neutrino fluence

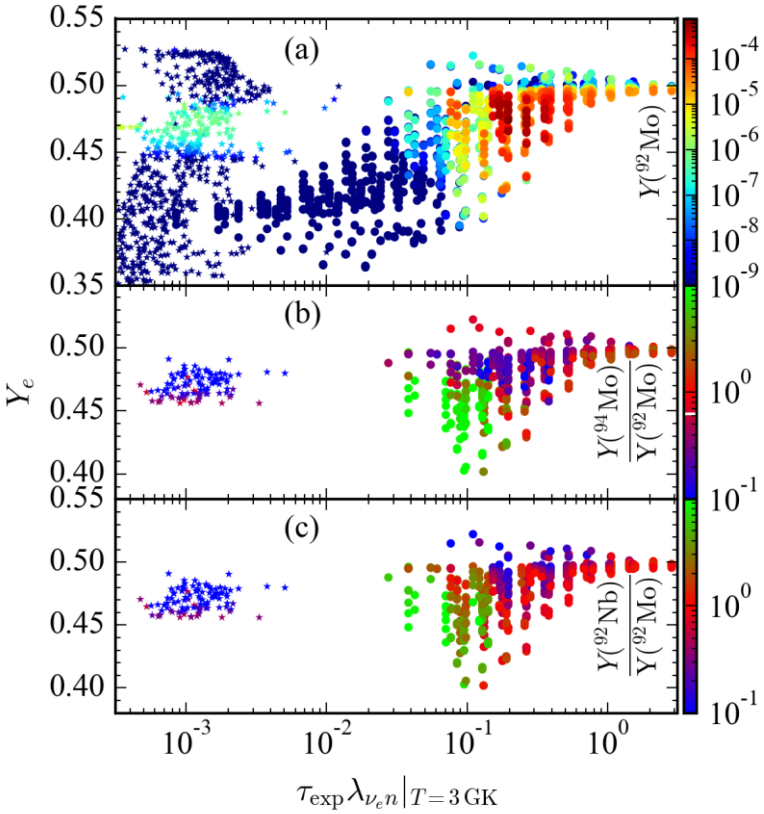

Current neutrino-hydrodynamical models far from the necessary conditions

Conditions current merger models

Dynamical, neutron-star torus, black-hole torus

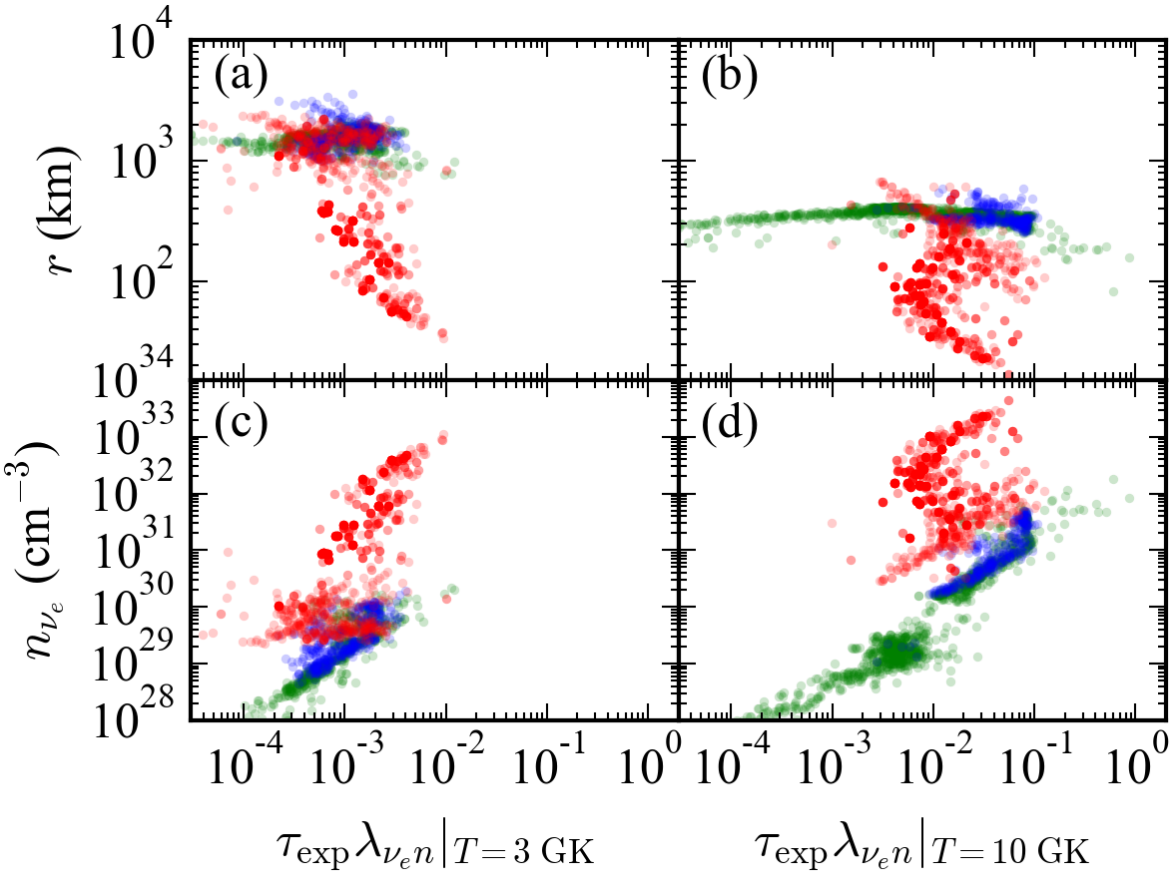

- Material reaches the necessary fluence conditions, but it is too hot form nuclei
- A non-thermal ejection mechanism is necessary (magnetic fields?)

Coproduction of all p-nuclei

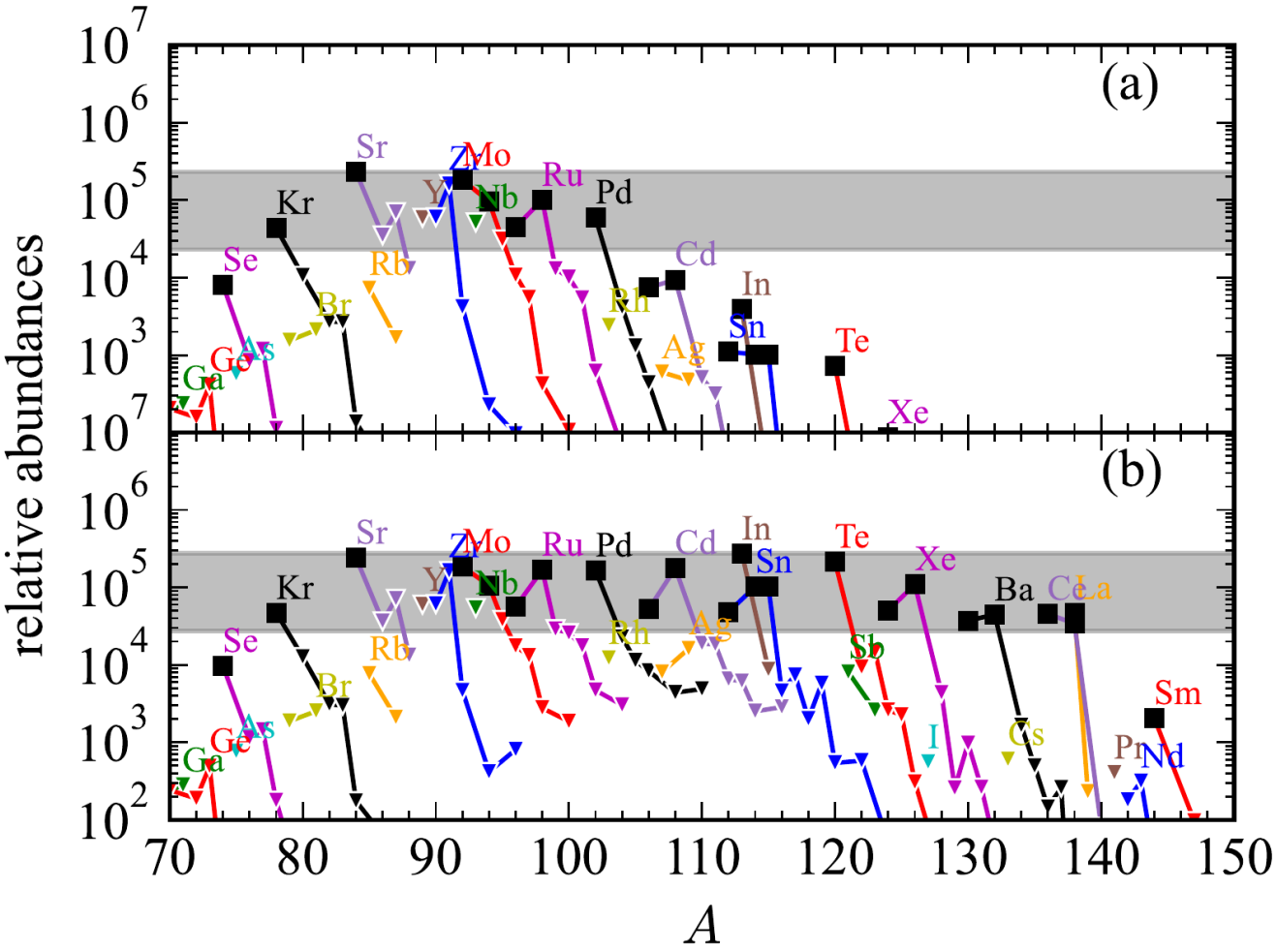

- All p-nuclei can be consistently produced
- Assuming the same astrophysical site produces both r-process and p-nuclei around 1% of the ejecta should reach vr-process conditions

Summary

- Multi-messenger observations (Gravitational and Electromagnetic waves) from binary neutron star mergers provide unique opportunities to study the production of heavy elements:
  - Neutron star mergers identified as one astrophysical site where the r-process operates
  - Kilonova observations provide direct evidence of the “in situ operation of the r-process”

- Strong synergies with laboratory experiments at future facilities.

- Challenges:
  - Impact of weak processes and EoS in the ejecta properties
  - Improved nuclear and atomic input (FAIR facility)
  - Kilonova spectral modelling

Collaborators

A. Bauswein, **C. Collins**, **A. Flörs**, O. Just, **G. Leck**, **L. Shingles**, N. Rahman, **V. Vijayan**, **Z. Xiong**
P. Amaro, J. P. Marques, J. M. Sampaio, **R. Silva**
S. Sim
J. Deprince, M. Godefroid, S. Goriely
H. Carvajal, P. Palmeri, P. Quinet
C. Robin
S. Giuliani, L. Robledo
A. Sieverding